University of São Paulo
"Luiz de Queiroz" College of Agriculture

Podzols of Ilha Comprida (SE, Brazil): organic matter chemistry and decay features

Josiane Millani Lopes

Thesis presented to obtain the degree of Doctor in Science. Area: Soil and Plant Nutrition

Piracicaba
2016

Josiane Millani Lopes
Agronomist

Podzols of Ilha Comprida (SE, Brazil): organic matter chemistry and decay features
versão revisada de acordo com a resolução CoPGr 6018 de 2011

Advisor:
Prof. Dr**. PABLO VIDAL TORRADO**

Thesis presented to obtain the degree of Doctor in Science. Area: Soil and Plant Nutrition

Piracicaba
2016

Aos meus pais **Lucinei Millani Lopes** *(in memorian)* e **João Lopes** *(in memorian)*,
pela minha vida.

Ao meu companheiro **André Mancebo Mazzetto**,
pelo amor incondicional e apoio.

DEDICO

ACKNOWLEDGMENTS

To my family: Américo, Anderson, Laís, Yasmin, Isabelly, Miguel, Aline, Cecília, Lucas, Eliza, Nilson and Daniela, for love and friendship.

Special thanks to André, for inconditional love and care and for always being by my side.

To all the people who contributed directly or indirectly to this research.

Thank you!

CONTENTS

RESUMO

Espodossolos da Ilha Comprida (SP): química da matéria orgânica e feições de degradação

Os solos mais frequentes na Planície Costeira do Estado de São Paulo são os podzóis, caracterizados por podzolização com hidromorfismo forte a moderado a bem drenado com horizontes B-podzol muito bem desenvolvidos (Bh ou Bhm). O processo de podzolização inclui os efeitos da hidrologia e do enraizamento no perfil e os efeitos subsequentes da drenagem melhorada. Uma crono-hidrosequencia de podzóis foi descrita em detalhes em um barranco na costa sul da Ilha Comprida, uma ilha barreira do Holoceno, e permitiu uma subdivisão em quatro grupos distintos: perfis mal drenados, perfis com horizonte B bem drenados, perfis fortemente enraizados e perfis superpostos. A descrição morfológica e algumas observações sobre o barranco exposto foram essenciais para o agrupamento e diferenciar os perfis de podzóis. Alguns desses podzóis bem drenados possuem manchas esbranquiçadas que estão relacionadas com a seletiva decomposição da matéria orgânica (MO) por microorganismos. Tais manchas são freqüentemente associadas aos canais radiculares. Foram estudados dezessete perfis, dos quais treze apresentaram manchas de esgotamento espalhadas ao longo do perfil. A maioria destas manchas são esbranquiçadas e estão localizadas preferencialmente nos horizontes de transição entre os horizontes E e B, particularmente em condições de boa drenagem. Tais manchas possuem algumas diferenças morfológicas e puderam ser agrupadas de acordo com semelhanças na sua morfologia e da sua posição no perfil. Os grupos são: (a) manchas concêntricas de depleção da MO; (b) manchas circulares/tubularess de depleção da MO (tocas); (c) manchas pontilhadas de depleção da MO; (d) manchas fantasmas de depleção da MO; (e) manchas irregulares de depleção da MO; e (f) manchas de depleção de Fe. A composição química da matéria orgânica do solo foi estudada em detalhe por pirólise em combinação com cromatografia em fase gasosa/espectrometria de massa (Py-CG/EM). Amostras de todos os horizontes dos perfis estudados foram coletadas, bem como amostras do centro das manchas (M) e do solo adjacente (S). Os processos envolvidos na gênese de podzóis da planície costeira arenosa estão diretamente relacionados com a drenagem, a contribuição de matéria orgânica dissolvida (MOD), a contribuição de matéria orgânica derivada de raízes, a composição química da matéria orgânica e sua decomposição por microorganismos, causando uma grande variação no podzóis. Os podzóis bem drenados diferem em características dos mal drenados em composição e deposição de MO, bem como a sua decomposição, que está directamente relacionada com a actividade dos grupos de microrganismos. Eles também diferem na contribuição relativa da MO derivada de raízes e MOD. Existe uma grande variação nas características da decomposição por microorganismos entre os perfis de podzóis permanentemente expostas ao ar e spray marinho (falésias) na Ilha Comprida e os do interior (trincheiras). Há, portanto, dois processos principais que alteram a morfologia de podzóis (composição da MO): (a) mudança na drenagem e enraizamento, e (b) a exposição ao ar.

Palavras-chave: Pirólise-CG/EM; Podzolização; Podzóis Tropicais; Matéria Orgânica Dissolvida; Química Molecular do Solo; Morfologia do solo; Holoceno; Planície Costeira.

ABSTRACT

Podzols of Ilha Comprida (SP, Brazil): organic matter chemistry and decay features

The most frequent soils in the São Paulo State Coastal Plain are Podzols, characterized by strong to moderate hydromorphic to well-drained podzolization with very well developed podzol-B horizons (Bh or Bhm). Podzolization processes include the effects of hydrology and rooting on profile morphology and the subsequent effects of improved drainage. A Podzol chrono-hydrosequence was described in detail on a cliff at the south coast of Ilha Comprida, a Holocene barrier island, and allowed a subdivision into four distinct groups: poorly-drained profiles, profiles with well-drained B horizons, strongly rooted profiles and superposed profiles. The morphological description and some observations about the exposure cliff were essential for grouping and differentiating the podzol profiles. Some well-drained podzols have OM-depleted mottles that are related to selective decomposition of organic matter (OM) by microorganisms. Such mottles are frequently associated to root channels. Seventeen profiles were studied, thirteen had depletion mottles scattered along the profile. Most of these mottles are whitish and are located preferentially in the horizons of transition between the E and B horizons, particularly in conditions of good drainage. Such mottles have certain morphological differences and may be grouped according to similarities in their morphology and their position in the profile. Distinct groups are: (a) concentric OM-depleted mottles; (b) circular/tubular OM-depleted mottles (burrows); (c) dotted OM-depleted mottles; (d) ghost OM-depleted mottles; (e) irregular OM-depleted mottles and (f) Fe-depleted mottles. The chemical composition of soil organic matter was studied in detail using pyrolysis in combination with gas chromatography/mass spectrometry (Py-GC/MS). Samples of all horizons of the distinct profiles studied were taken, as well as from the center of the mottle (M) and from the direct surroundings (S). The processes involved in the genesis of Podzols in the sandy coastal plain are directly related to drainage, the contribution of dissolved organic matter (DOM), the contribution of organic matter derived from roots, the chemical composition of organic matter and its decomposition by microorganisms, causing a large variation in adjacent Podzols. The well-drained Podzols differ in characteristics from the poorly drained ones in composition and deposition of OM, as well as its decomposition, which is directly related to the activity of groups of microorganisms. They also differ in the relative contribution of OM-derived from roots and DOM. There is a wide variation in the characteristics of decomposition by microorganisms between the profiles of Podzols permanently exposed to air and marine spray (the cliffs) on Ilha Comprida and those inland (pits). There are therefore two main processes that change the morphology of Podzols (OM and composition): (a) change in drainage and rooting, and (b) exposure to air.

Keywords: Py-GC/MS; Podzolization; Tropical Podzols; Spodosols; Dissolved Organic
      Matter; Soil Molecular Chemistry; Soil morphology; Holocene; Coastal Plain.

1 INTRODUCTION

The Restinga is an important ecosystem for the maintenance of marine and terrestrial life along the Brazilian coast. Although protected by law, the pressure for urban and agricultural use of this environment is felt in many Brazilian coastal municipalities. In order to maintain and manage this fragile ecosystem against increasing pressure it is necessary to better understand it.

Numerous studies of botany and floral biogeography have been carried out in the Restinga Paulista, and it is well-known that this ecosystem contains the richest coastal vegetation. However, few studies characterize the soils of the Restinga forest and especially the soil with the widest occurrence: the podzol. The process of podzol formation, generically known as podzolization, has been intensively studied since the late nineteenth century, but such studies were largely concentrated in cold and temperate zones of the Northern hemisphere. Much less abundant are investigations from equatorial areas. In Brazil, most of the studies on podzols are concentrated in the equatorial rainforest of the Rio Negro basin (Amazon region). These works emphasize the mechanisms involved in the Latosol/Podzol transition, which is the most common in that area.

Temperate, boreal and equatorial environments differ considerably from those found in the coastal plain of São Paulo. While the Rio Negro podzols and those from boreal areas are frequently found on parent materials with considerable amounts of fine material (clay and silt), those formed in the Brazilian coastal area are formed in pure sands. Therefore, the processes of formation and their expression in profile morphology are expected to be different.

Previous studies on podzols of the coastal region of the state of São Paulo (GOMES 2005, GOMES et al., 2007a, 2007b; COELHO, 2008; COELHO et al., 2010a, 2010b, 2010c, 2010d; GONZÁLEZ-PÉREZ et al., 2008, 2012, LOPES, 2011; BUURMAN; VIDAL-TORRADO; LOPES, 2013, BUURMAN; VIDAL-TORRADO, MARTINS, 2013) have focused on geomorphology, development of profile morphology in relation to age and hydrology, movement and accumulation of sesquioxides and soil organic matter (SOM). Studies on soil organic matter and its role in the podzolization process are still scarce, and the relation between SOM, spatial variation, and hydrology still poorly understood. Studies that provide a better understanding of the podzolization process may provide better tools for the conservation of podzols.

1.1 Tropical podzols

Podzols of tropical and temperate environments show morphological differences, such as the E horizon of tropical podzols, that is usually thicker and has hardly any organic matter (OM). Since the E horizon develops through degradation of the B horizon, it can be hypothesized that in a tropical environment, the decomposition of the OM is more efficient (BUURMAN; VIDAL-TORRADO; LOPES, 2013, BUURMAN; VIDAL-TORRADO, MARTINS, 2013). Under tropical conditions, plant debris accumulated on the soil surface and is subject to intense decomposition by fauna and microorganisms (KINDEL; GARAY, 2002). This decomposition is strongly influenced by prevailing hydrological conditions, fertility and soil temperature. Limited availability of oxygen during the process of decomposition of OM, combined with abundant rainfall favors the formation of water-soluble organic compounds, which may be transferred to drainage water (DAVID; ZECH, 1990).

1.1.1 Morphology of tropical podzols

In general, podzols are characterized by the succession of three main horizons: a shallow darker (A), followed by a strongly weathered grayish white eluvial E horizon, relatively enriched with quartz and, finally, a black to reddish brown B horizon, which contains, in addition to primary minerals, complexes of OM with Fe and Al, and amorphous (oxy) hydroxides of Fe and Al (LUNDSTRÖM et al., 2000a).

The podzol B horizon can be subdivided according to its combination of amorphous materials, organic matter and degree of cementation into Bs, Bhs, Bh and Bhm. The Bh horizon is characterized by a dominance of OM-Al complexes, with hardly any Fe. In the cemented Bhm horizon, which is largely restricted to poorly drained podzols, the pores are largely filled with OM coatings. In the southern coast of Ilha Comprida, podzols with giant Bhm horizons are exposed in the cliffs. Such cemented horizons slow down coastal erosion and the knowledge of how they are formed may support conservation. Bs and Bhs horizons are restricted to well-drained podzols, without cementation.

Several theories have been proposed to explain the formation of podzols (De CONINCK, 1980; ANDERSON et al., 1982; LUNDSTRÖM et al., 2000b; BUURMAN; JONGMANS, 2005). In all theories, the percolation of dissolved organic matter through the profile plays an essential role in the weathering process and in the formation of distinctive horizons. However, while formerly all organic material accumulated in B horizons was

thought to be due to precipitation of dissolved organic matter (DOM) upon saturation with metals, it is now clear that such precipitated complexes dominate in poorly drained podzols alone. Although OM-metal complexes are also found in well-drained podzol B horizons, the humus in such B horizons is largely due to decomposition of roots (BUURMAN; JONGMANS, 2005; BUURMAN et al., 2005).

1.1.2 Drainage of tropical podzols

Drainage is a factor that directly influences the formation of podzol B horizons (SCHWARTZ, 1988; KACZOREK et al., 2004; BUURMAN et al., 2005, BUURMAN; VIDAL-TORRADO; LOPES, 2013), but there are few studies of tropical environments. The change of hydrological position and improvement of drainage and aeration can result in strong changes, especially in originally very poorly drained soils. Such morphological alterations include greater friability in formerly cemented B horizons, accelerated decomposition of roots that were originally protected by the anaerobic environment, thickening of the E horizon at the expense of the B horizon; introduction of mesofauna that can rework the soil by burrowing, and accelerated microbial degradation of OM in B horizons (BUURMAN et al., 2005, BUURMAN; VIDAL-TORRADO; LOPES, 2013; BUURMAN; VIDAL-TORRADO; MARTINS, 2013).

The drainage of podzols is primarily controlled by topography in combination with level and yearly fluctuation of the water table. In sandy soils, stratification may influence both vertical and horizontal water movement. Furthermore, the development of cemented horizons may significantly change the hydrology of a profile. In this case the present drainage may not reflect the situation prior to the formation of such horizons (ANDRIESSE, 1968/1969). In sandy podzols most rainwater will rapidly percolate through the soil, while cemented horizons may both decrease the speed and change the direction of the percolation.

Andriesse (1968/1969) studied podzols in the humid tropical lowlands of Sarawak, Malaysia, over a period of seven years. In this area, the average annual rainfall is between 2,500 and 5,000 mm, fairly well distributed, with no single month in which the rainfall is less than 100 mm. He concluded that the podzols are morphologically similar to those of temperate regions, even though the conditions of development are not identical. The Sarawak podzols were developed in a relatively flat landscape, on a sandy substrate rich in quartz and under imperfect drainage, while in temperate areas many podzols are well-drained.

1.1.3 OM studies of tropical podzols

1.1.3.1 Chemical composition of OM in podzols

To understand decomposition, transport, and accumulation in podzols, it is essential to study the chemical composition of the OM. This chemical composition can be studied in detail using pyrolysis in combination with gas chromatography/mass spectrometry (Py-GC/MS) (SCHULTEN; SCHNITZER, 1997; LEINWEBER; SCHULTEN, 1999; GONZÁLEZ-PÉREZ et al., 2012; BUURMAN; VIDAL-TORRADO; LOPES, 2013). Py-GC/MS allows a very detailed chemical characterization and may be used to distinguish, for example, the contribution of compounds derived directly from plants and microorganisms (BUURMAN et al., 2005; 2007; BUURMAN; PETERSE; MARTIN; 2007). Some spectroscopic techniques including carbon 13 Nuclear Magnetic Resonance (^{13}C NMR) and Fourier Transform Infrared Spectroscopy (FTIR).

Wilcken et al. (1997) published evidence provided by ^{13}C NMR spectroscopy on the translocation of the OM complexes along the profile. In this study the authors demonstrated that the OM of the Bh horizon was mainly composed of alkyl-aromatic groups and O-alkyl (C lignins and carbohydrates) from lignin (intact and degraded via microbial) from the A horizon. In another study, González-Pérez et al. (2008) used spectroscopic techniques such as ^{13}C NMR and FTIR to characterize the humic acids of podzols from the coast of São Paulo, and concluded that the similarity in the OM composition over the profiles may be evidence of vertical translocation throughout the soil.

Bravard and Righi (1991) made use of FTIR to characterize humic and fulvic acids in a toposequence of Latosols and Podzols in the Amazon region. Their results indicated differences in the characteristics of OM, depending on the horizon from which they were extracted. In the OM extracted from the A horizon of Latosols, aliphatic structures were more abundant than that extracted from podzols, which contained more condensed aromatic molecules. Mafra et al. (2007) used FTIR to characterize humic acids present in three podzols of the Amazon region, and concluded that they showed similarity in the chemical composition of OM, although the profiles present minor differences in their morphology. These results indicate that the dynamics of OM in the three profiles was similar.

González-Pérez et al. (2012) conducted one study of OM with Py-GC/MS in podzols located in Ilha do Cardoso, on the coast of São Paulo state. The authors showed that the chemical composition of OM in B horizons was influenced by DOM and carbon from in situ decaying roots in two out of three studied profiles.

DOM is a mobile form of OM and exerts an important influence on the biotic and abiotic processes in the soil (ZECH et al., 1997). In podzols, the O horizon is the main source of DOM (DAVID; ZECH, 1990) and its chemical composition is mainly formed by fragmentation of plant-derived OM and microbial products (GUGGENBERGER et al., 1994). In coastal plain podzols, usually areas with high rainfall and high rates of litter deposition, drainage water can form streams ("rivers") of black water, with important concentration of dissolved organic compounds. In temperate areas, the chemical composition of DOM is influenced by the season (KAISER et al., 2002), but such information is not still available for tropical or subtropical areas.

1.1.3.2 Microorganisms

Pagé and Guillet (1991) conducted a study of podzols in Canada in order to evaluate the role of biological activity on the formation of cemented and loose subsurface horizons with varying drainage along a toposequence. Techniques used were micromorphology combined with Mean Residence Time (MRT) of OM obtained by ^{14}C dating. They concluded that the horizons with a loose consistence are more exploited by roots and are characterized by a higher biological activity than in cemented horizons, where cycling of OM appears to be slower. Studies using Py-GC/MS show the dominance of lignin moieties and polysaccharides–with an important presence of levoglucosan from relatively intact polysaccharides and a low contribution of microbial carbohydrate products in surface horizons of Dutch podzols (BUURMAN et al., 2005).

Microorganisms determine the balance of biogeochemical cycles, gas fluxes and other processes. Although the importance of soil organisms is widely recognized, studies on the variation in microbial communities are still rare, especially when it comes to Podzols (CABELLO; ARAMBARRI, 2002; SILVA et al., 2014; MUMMEY et al., 2010).

Some podzols have organic matter-depleted light-colored spots in various horizons. Such spots are evidence of microbial activity. They are especially conspicuous in podzol-B horizons. The lighter spots are individualized, poor in OM and separated by an adjacent area of higher OM content (BUURMAN et al., 2007, BUURMAN; VIDAL-TORRADO; LOPES, 2013).

A previous joint research by Silva et al. (2014) evaluated the community structure and diversity of *Bacteria* and *Archaea* in well-drained Podzols and OM-depleted mottles from Bertioga and Ilha Comprida, State of São Paulo. Significant differences were observed in the

community structures of *Bacteria* and *Archaea* between depleted mottles and the adjacent soil. There was less diversity in bacterial groups in the depleted mottles than in the adjacent soil, suggesting that a special community is responsible for the depletion. In the podzols of Bertioga, *Pseudomonas* strains were prevalent, whereas in depleted patches of the Ilha Comprida profiles, *Acidobacteria* were dominant, suggesting the involvement of these groups in the selective degradation of OM in these spots.

According Buurman et al. (2007), some well-drained podzols have OM-depleted mottles mainly associated with root channels that are related to selective decomposition of OM by microorganisms. The phenomenon is widespread in the Netherlands, Belgium and Germany, and such depletion mottles have even been observed in recently exposed fossil podzols of Tertiary age.

1.2 Methodology

1.2.1 Podzol study area

In some Brazilian regions, aspects related to the genesis of podzols or soils with incipient podzolization can be found in few studies developed in highland environments of Minas Gerais (BENITES, 1998; BENITES et al., 1999; 2001; SÁ, 2000; DIAS et al., 2003) and the Amazon basin (KLINGE, 1965, 1968, 1969; LUCAS et al., 1984; BRAVARD; RIGHI, 1989, 1990, 1991; HÖRBE et al., 2004; MAFRA et al., 2007).

There are also reports and scientific articles about the genesis and evolution of landscapes and podzols in coastal regions of Brazil, mostly in the form of theses and dissertations (GOMES, 1995, 2005; ROSSI, 1999; LOPES, 2011) and papers based on these (GOMES et al., 1998a, 1998b; ROSSI; QUEIROZ NETO, 2001, 2002; GOMES et al., 2007a, 2007b; COELHO et al., 2010a, 2010b, 2010c, 2010d). These studies are usually based on various single profiles that may have been of very different age and the relation of which has not been established. Therefore, these studies did not establish clear spatio-temporal relations that allow to connect the various profiles and understand their morphology and other features in terms of the evolution of landscape and hydrology.

There are few detailed studies of the chemical composition of OM and its lateral variation in Podzols of coastal environments in the tropics. The studies of Lopes (2011), Gonzalez-Perez et al. (2012), and Buurman et al. (2013) indicated that the morphology of podzols and the chemical composition of their OM are closely related. Lopes (2011) studied

the relations between abundance of functional groups (alkyl, O-alkyl, aromatic, carbonyl, and carboxylic-C) with the drainage and age of the Bhm horizon in podzols located in the municipalities of Cananéia and Bertioga on the coast of the State of São Paulo. This study showed that podzol-B horizons vary in composition in response to local influences, such as drainage and vertical or lateral transport of OM. The latter plays a very important role in the process of Podzolization in tropical climates.

Podzols show a large morphological variation, both within and between landscapes. Ilha Comprida, on the southern coast of Brazil (SP), has a large area of such tropical podzols. The erosion cliff on the Southern coast of the island allows a thorough study of their lateral morphological variation. The profiles in the cliff are permanently exposed to air and marine spray, a characteristic that could directly influence decomposition of OM by microorganisms. Such exposure is not present further inland, where profiles may have retained their original drainage condition. At the south-western corner of the island (Ponta da Trincheira) and in the cliffs facing the Mar de Cananéia, thick cemented B horizons are found.

1.2.2 SOM chemistry (Py-GC/MS)

Several modern analytical techniques are available for the characterization of the chemical composition of SOM. Kogel-Knaber (2000) listed a number of techniques that have been developed for the analysis of SOM: solid-state cross-polarization magic angle spinning carbon-13 nuclear magnetic resonance (CP/MAS ^{13}C NMR), nitrogen 15 nuclear magnetic resonance (^{15}N NMR), infrared spectroscopy (IR), Py-GC/MS, and others.

To elucidate the OM chemical composition in the soil, refined analytical techniques are required (KOGEL-KNABER, 2000), and Py-GC/MS is a technique that allows detailed observations on the chemistry of SOM in the podzols. Py-GC/MS is a technique that enables the identification of a very large number of organic fragments that are obtained by thermal fragmentation of larger organic molecules. The amounts of the fragments can be quantified and then determinate a fingerprint of the OM. This method is highly reproducible and very useful for the comparison of samples.

The term "pyrolysis" has a Greek origin and means "heat break", i.e., it is a fragmentation reaction of a material by thermal energy. The analytical technique of pyrolysis is the breaking up – at high temperature - of an (organic) material under an inert atmosphere. This process results in a set of small molecular species, which are related to the composition of the original sample (UDEN, 1993; ROBER, 1990). These small molecules are used to

qualitatively identify the original structure of macromolecules, through adequate and proper standardization, and to provide quantitative information about its composition (IRWIN, 1979).

In this type of analysis, the reproducibility of the results is obtained when the parameters that lead to the formation of these pyrolysates are thoroughly controlled and optimized for the polymer system investigated, as these directly influence the thermal degradation mechanisms (ERICSON, 1985). In polymer samples, the mechanisms of such fragmentation can occur via elimination of small molecules, chain scission (depolymerization) or random cleavage (TSUGE; OHTANI, 2002).

As the thermal degradation of macromolecules often results in complex mixtures of smaller molecules, the associated use of other techniques such as gas chromatography is required to separate the produced species (WANG, 1999). When this association or coupling also includes mass spectrometry, the species produced may be identified.

Briefly, the technique consists of the sudden thermal degradation of (macro) organic molecules under an inert atmosphere, where the volatilized products are separated based on molecular weight into a gas chromatographic column and identified with use of mass spectrometry, by mass ratio/charge (m/z) of ions. The results (pyrograms) indicate the relative abundance of each organic component with respect to a retention time.

Pyrolysis as an analytical tool and its development are thoroughly reported in the literature for several years (MADORSKY; STRAUS, 1948). In 1948, the first work on pyrolysis coupled to spectrometric offline masses (Py-MS) polymers was published (MADORSKY; STRAUS, 1948). Bradt et al. (1953) conducted online Py-MS under vacuum of polymer samples, obtaining information about their structures.

With the development of 'on-line' systems of Py-GC, new applications in polymer analysis were proposed simultaneously by three separate work groups: Lehrle and Rob (1959), Radell and Strutz (1959) and Martin (1959), causing a significant increase in the number of publications in this area. Vallmin et al. (1966) published the first report of the fully coupled system Py-GC-MS using a Curie point pyrolyzer coupled to a gas chromatograph and a mass spectrometer.

With the technological advances of new pyrolyzers and precise control of operating conditions, it became easier to obtain reproducible data for such analysis (TSUGE, 1995). Thus, the standardization and compilation of data on a bench with several standard samples are important for inter-laboratory comparison of analytical pyrolysis data. Tsuge and Ohtani

(1989) made an attempt to standardize a database with 135 species of typical polymers analyzed using Py-GC.

A major breakthrough in the analysis of different types of molecules was achieved when the technique could be applied to volatilized samples of any kind, coupled to other techniques of separation and identification. From 1948 to today, the coupling of a thermal degradation system (pyrolysis) to a mass spectrometer and a gas chromatograph resulted, respectively, in two techniques, known as pyrolysis coupled to mass spectrometry (Py-MS) and pyrolysis coupled with gas chromatography (Py-GC). The combination of these three techniques, lead to pyrolysis coupled to gas chromatography and mass spectrometry (Py-GC/MS). Samples which cannot be analyzed by GC/MS alone, due to difficult volatilization, can be easily analyzed by analytical pyrolysis (ROBERT, 1990).

In summary, Py-GC/MS allows a very detailed chemical characterization and may be used to understand the chemical composition of OM in podzols and to elucidate the process involved in the formation, maintenance and decomposition of these soils.

1.3 General hypothesis and objectives of the present research

Based on the strong influence of drainage variation in time and space on the SOM dynamics in podzols hypothesis, the objectives of these thesis are:

i) Elucidate the mechanisms involved in the genesis of podzols in coastal environment, as the inputs, transformations, transport and deposition of OM over the profiles, and relate to its lateral variation. The specific objectives associated with this general objective are:

    a) Describe and characterize podzols profiles present in the cliff in the south side of Ilha Comprida and the transitions to adjacent profiles;

    b) Accomplish detailed morphological description of each profile, focusing on the lateral variation of the characteristics of horizons and their features along the cliff;

    c) Characterize the OM, especially from B horizons (Bh and Bhm) and transition horizons (BE, BE) by Py-GC / MS.

ii) Qualitatively characterize the OM of podzols profiles of Ilha Comprida - SP and the OM composition with the drainage characteristics. The specific objectives associated with this general objective are:

a) Characterize the OM, especially the B horizons and organic matter-depleted light-colored spots, by Py-GC / MS;

b) Relate the data obtained from the characterization of the OM with the profile drainage.

References

ANDERSON, H.A.; BERROW, M.L.; FARMER, V.C.; HEPBURN; A.; RUSSELL, J.D.; WALKER, A.D. A reassessment of podzol formation processes. **European Journal of Soil Science**, Oxford, v. 33, p. 125-136, 1982.

ANDRIESSE, J.P. A study of the environment and characteristics of tropical podzols in Sarawak (east-Malaysia). **Geoderma**, Amsterdam, v. 2, p. 201-227, 1968/1969.

BENITES, V.M. **Caracterização química e espectroscópica da matéria orgânica e suas relações com a gênese de solos da Serra do Brigadeiro, Zona da Mata mineira**. 1998. 123 p. 123 p. Dissertação (Mestrado em Agronomia) – Universidade Federal de Viçosa, Viçosa, 1998.

BENITES, V.M.; MENDONÇA, E.S.; SCHAEFER, C.E.G.R.; MANTIN-NETO, L. Caracterização dos ácidos húmicos extraídos de um Latossolo Vermelho-Amarelo e de um Podzol por análise termodiferencial e pela espectroscopia de absorção no Infravermelho. **Revista Brasileira de Ciência do Solo**, Viçosa, v. 23, p. 543-551, 1999.

BENITES, V.M.; SCHAEFER, C.E.G.R.; MENDONÇA, E.S.; MANTIN-NETO, L. Caracterização da matéria orgânica e micromorfologia de solos sob campos de altitude no Parque Estadual da Serra do Brigadeiro (MG). **Revista Brasileira de Ciência do Solo**, Viçosa, v. 25, p. 661-674, 2001.

BRADT, P.; DIBELER, V.H.; MOHLER, F.L.J. A new technique for the mass-spectrometric study of the pyrolysis products of polystyrene. **Journal of Research of Natural Bureau of Standarts**, Maryland, v. 50, p. 201-202, 1953.

BRAVARD, S.; RIGHI, D. Geochemical differences in an Oxisol-Spodosol toposequence of Amazonia (Brazil). **Geoderma,** Amsterdam, v. 44, p. 29-42, 1989.
_____. Podzols in Amazonia. **Catena**, Amsterdam, v. 17, p. 461-475, 1990.

_____. Characterization of fulvic and humic acids form an Oxisol-Spodosol toposequence of Amazonia, Brazil. **Geoderma**, Amsterdam, v. 48, p. 151-162, 1991.

BUURMAN, P.; JONGMANS, A.G. Podzolisation and soil organic matter dynamics. **Geoderma**, Amsterdam, v. 125, p. 171-183, 2005.

BUURMAN, P.; PETERSE, F.; MARTIN, G.A. Soil organic matter chemistry in allophonic soils: a pyrolysis-GC/MS study of a Costa Rican Andosol catena. **European Journal of Soil Science**, Oxford, v. 58, p. 1330-1347, 2007.

BUURMAN, P.; VIDAL-TORRADO, P.; LOPES, J.M. The podzol hydrosequence of Itaguaré, São Paulo, Brazil. 2. Soil organic matter chemistry by Pyrolysis-GC/MS. **Soil Science Society of America Journal**, Madison, v. 77, n. 4, p. 1307-1318, 2013.

BUURMAN, P.; VIDAL-TORRADO, P.; MARTINS, V.M. The podzol hydrosequence of Itaguaré (Sao Paolo, Brazil). 1. Geomorphology and interpretation of profile morphology. **Soil Science Society of America Journal, Madison**, v. 77, n. 4, p. 1294-1306, 2013.

BUURMAN, P.; NIEROP, K.G.J.; PONTEVEDRA-POMBAL, X.; MARTINEZ-CORTIZAS, A. Molecular chemistry by pyrolysis-GC/MS of selected samples of the Penido Vello peat deposit, Galicia, NW Spain. In: MARTINI, I.P.; MARTINEZ-CORTIZAS, A.; CESWORTH, W. **Peatlands:** evolution and records of environmental and climate change. Amsterdam: Elsevier, 2006. chap. 10, p. 217-240.

BUURMAN, P.; SCHELLEKENS, J.; FRITZE, H.; NIEROP, K.G.J. Selective depletion of organic matter in mottled podzol horizons. **Soil Biology and Biochemistry**, Oxford, v. 39, p. 607-621, 2007.

BUURMAN, P.; van BERGEN, P.F.; JONGMANS, A.G.; MEIJER, E.L.; DURAN, B.; van LAGEN, B. Spatial and temporal variation in podzol organic matter studied by pyrolysis-gas chromatography/mass spectrometry and micromorphology. **European Journal of Soil Science**, Oxford, v. 56, p. 253–270, 2005.

CABELLO, M.N.; ARAMBARRI, A.M. Diversity in soil fungi from undisturbed and disturbed Celtis tala and Scutia buxifolia forests in the eastern Buenos Aires province (Argentina). **Microbiological Research**, Amsterdam, v. 157, p. 115-125, 2002.

COELHO, M.R. **Caracterização e gênese de Espodossolos da planície costeira do Estado de São Paulo.** 2008. 270 p. Tese (Doutorado em Solos e Nutrição de Plantas) – Escola Superior de Agricultura "Luiz de Queiroz", Universidade de São Paulo, Piracicaba, 2008.

COELHO, M. R.; VIDAL-TORRADO, P.; MARTINS, V.M.; PEREZ, X.L.O.; MACÍAS, F. Fracionamento do alumínio por técnicas de dissoluções seletivas em Espodossolos da planície costeira do Estado de São Paulo. **Revista Brasileira de Ciência do Solo**, Viçosa, v. 34, p. 1081-1092, 2010a.

COELHO, M.R.; VIDAL-TORRADO, P.; PEREZ, X.L.O.; MARTINS, V.M.; MACÍAS, F. Química e gênese de solos desenvolvidos sob vegetação de restinga no Estado de São Paulo. **Revista Brasileira de Ciência do Solo**, Viçosa, v. 34, p. 1951-1964, 2010b.

_____. Seletividade do pirofosfato de sódio e de cloretos não tamponados ($CuCl_2$ e $LaCl_3$) como extratores de alumínio associado à matéria orgânica em solos de restinga do Estado de São Paulo. **Revista Brasileira de Ciência do Solo**, Viçosa, v. 34, p. 1561-1572, 2010c.

COELHO, M.R.; MARTINS, V.M.; VIDAL-TORRADO, P.; SOUZA, C.R.G.; PEREZ, X.L.O.; MACÍAS, F. Relação solo-relevo-substrato geológico nas restingas da planície costeira do Estado de São Paulo. **Revista Brasileira de Ciência do Solo**, Viçosa, v. 34, p. 833-846, 2010d.

DAVID, M.B.; ZECH, W. Adsorption of dissolved organic carbon and sulfate by acid forest soils in the Fichtelgebirge FRG. **Journal of Plant Nutrition and Science**, Weinheim, v. 153, p. 379-384, 1990.

DE CONINCK, F. Major mechanisms in formation of spodic horizons. **Geoderma**, Amsterdam, v. 24, p. 101-128, 1980.

DIAS, H.C.T.; SCHAEFER, C.E.G.R.; FERNANDES, E.I.; OLIVEIRA, A.P.; MICHEL, R.F.M.; LEMOS, J.B. Caracterização de solos altimontanos em dois transectos no Parque Estadual do Ibitipoca (MG). **Revista Brasileira de Ciência do Solo**, Viçosa, v. 27, p. 469-481, 2003.

ERICSON, I. Influence of pyrolysis parameters on results in pyrolysis-gas chromatography; **Journal of Analytical and Applied Pyrolisis,** Amsterdam, v. 8, p. 73-86, 1985.

GOMES, F.H. **Gênese e classificação de solos sob vegetação de restinga na Ilha do Cardoso-SP**. 2005. 107 p. Tese (Doutorado em Solos e Nutrição de Plantas) – Escola Superior de Agricultura "Luiz de Queiroz", Universidade de São Paulo, Piracicaba, 2005.

GOMES, F.H.; VIDAL-TORRADO, P.; MACÍAS, F.; GHERARDI, B.; PEREZ, X.L.O. Solos sob vegetação de restinga na Ilha do Cardoso (SP). I - Caracterização e classificação. **Revista Brasileira de Ciência do Solo**, Viçosa, v. 31, p. 1563-1580, 2007a.

GOMES, F.H.; VIDAL-TORRADO, P.; MACÍAS, F.; SOUZA JUNIOR, V.S.; PEREZ, X.L.O. Solos sob vegetação de restinga na Ilha do Cardoso (SP): II - Mineralogia das frações silte e argila. **Revista Brasileira de Ciência do Solo**, Viçosa, v. 31, p. 1581-1589, 2007b.

GOMES, J.B.V. **Caracterização, gênese e uso dos solos de três sítios de restinga sob diferentes coberturas vegetais no estado do Rio de Janeiro**. 1995. 158 p. Dissertação de (Mestrado em Agronomia)– Universidade Federal Viçosa, Viçosa, 1995.

GOMES, J.B.V.; RESENDE, M.; RESENDE, S.B. de; MENDONÇA, E.S. Solos de três áreas de restinga. I. Morfologia, caracterização e classificação. **Pesquisa Agropecuária Brasileira**, Brasília, v. 33, p. 1907-1919, 1998a.

_____. Solos de três áreas de restinga. II. Dinâmica das substâncias húmicas, ferro e alumínio. **Pesquisa Agropecuária Brasileira**, Brasília, v. 33, p. 1921-1932, 1998b.

GONZÁLEZ PÉREZ, M.; VIDAL-TORRADO, P.; COLNAGO, L.A.; MARTIN-NETO, L.; OTERO, X.L.; MILORI, D.M.B.P.; GOMES, F.H. 13C NMR and FTIR spectroscopy characterization of humic acids in spodosols under tropical rain forest in southeastern Brazil. **Geoderma**, Amsterdam, v. 146, p. 425-433, 2008.

GONZÁLEZ-PEREZ, M.; BUURMAN, P.; VIDAL-TORRADO, P.; MARTIN-NETO, L. Pyrolysis-gas chromatography/ mass spectrometry characterization of humic acids in Spodosols under Atlantic forest in Southeastern Brazil. **Soil Science Society of America Journal**, Madison, v. 76, p. 961-971. 2012.

GUGGENBERGER, G.; ZECH, W.; SCHULTEN, H.R. Formation and mobilization pathways of dissolved organic matter: Evidence from chemical structural studies of organic matter fractions in acid forest floor solutions. **Organic Geochemistry**, Oxford, v. 21, p. 51-66, 1994.

HORBE, A.M.C.; HORBE, M.A.; SUGUIO, K. Tropical Spodosols in northeastern Amazonas State, Brazil. **Geoderma**, Amsterdam, v. 119, p. 55-68, 2004.

IRWIN, W.J. Analytical pyrolysis: an overview; **Journal of Analytical and Applied Pyrolisis**, Amsterdam, v. 1, p. 3-25, 1979.

KACZOREK, D.; SOMMER, M.; ANDRUSCHKEWITSCH, L.; OKTABA, L.; CZERWINSKI, Z.; STAHR, K. A comparative micrmorphological and chemical stydy of "Raseneisenstein" (bog iron ore) and "Orstein". **Geoderma**, Amsterdam, v. 121, p. 83-94, 2004.

KAISER, K.; GUGGENBERGER, G.; HAUMAIER, L.; ZECH, W. The composition of dissolved organic matter in forest soil solutions: changes induced by season and passage through the mineral soil. **Organic Geochemistry**, Oxford, v. 33, p. 307-318, 2002.

KINDEL, A.; GARAY, I. Humus form in ecossystems of the Atlantic Forest, Brazil. **Geoderma**, Amsterdam, v. 108, p. 101-118, 2002.

KLINGE, H. Podzols soils in the Amazon Basin. **European Journal of Soil Science**, Oxford, v. 16, p. 95-103, 1965.

_____. **Report on tropical podzols.** Rome: FAO, 1968. 88 p.

_____. Climatic conditions in lowland tropical podzols areas. **Tropical Ecology**, Cambridge, v. 10, p. 222-239, 1969.

KOGEL-KNABER. I. Analytical approches for characterizing soil organic matter. **Organic Geochesmistry**, Oxford, v. 31, p. 609-625, 2000.

LEHRLE, R.S.; ROBB, J.C. Direct examination of the degradation of high polymers by gas chromatography. **Nature**, London, v. 183, p. 1671, 1959.

LEINWEBER, P.; SCHULTEN, H.R. Advances in analytical pyrolysis of soil organic matter. **Journal of Analytical and Applied Pyrolysis**, Amsterdam, v. 49, p. 359-383, 1999.
LOPES, J.M. **Caracterização e evolução das substâncias húmicas de horizontes espódicos na planície costeira do Estado de São Paulo** 2011. 108 p. Dissertação (Mestrado em Solos e Nutrição de Plantas) – Escola Superior de Agricultura "Luiz de Queiroz", Universidade de São Paulo, Piracicaba, 2011.

LUCAS, Y.; CHAUVEL, A.; BOULET, R.; RANZINI, G.; SCATOLINI, F. Transição latossolos-podzóis sobre a Formação Barreiras na região de Manaus, Amazônia. **Revista Brasileira de Ciências do Solo, Viçosa,** v. 8, p. 325-335, 1984.

LUNDSTRÖM, U.S.; van BREEMEN, N.; BAIN, D. The podzolization process. A review. **Geoderma**, Amsterdam, v. 94, p. 91-107, 2000a.

LUNDSTRÖM, U.S.; van BREEMEN, N.; BAIN, D.C.; VAN HEES, P.A.W.; GIESLER, R.; GUSTAFSSON, J.P.; ILVESNIEMI, H.; KARLTUN, E.; MELKERUD, P.A.; OLSSON, M.; RIISE, G.; WAHLBERG, O.; BERGELIN, A.; BISHOP, K.; FINLAY, R.; JONGMANS, A.G.; MAGNUSSON, T.; MANNERKOSKI, H.; NORDGREN, A.; NYBERG, L.; STARR, M.; TAU STRAND, L. Advances in understanding the podzolization process resulting from a multidisciplinary study of three coniferous forest soils in the Nordic Countries. **Geoderma**, Amsterdam, v. 94, p. 335-353, 2000b.

MADORSKY, S.L.; STRAUS, S. High vacuum pyrolytic fractionation of polystyrene. **Industrial and Engeneering Chemistry**, Washington, v. 5, p. 848-852, 1948.

MAFRA, A.L.; SENESI, N.; BRUNETTI, G; MIKLÓS, A.A.W.; MELFI, A.J. Humic acids from hydromorphic soils of upper Negro River basin Amazonas: chemical and spectroscopic characterisation. **Geoderma**, Amsterdam, v. 138, p. 170-176, 2007.

MARTIN, S.B. Gas chromatography: application to the study of rapid degradative reactions insolids. **Journal of Chromatography A**, Amsterdam, v. 2, p. 272-283, 1959.

MUMMEY, D.L.; CLARKE, J.T.; COLE, C.A.; O'CONNOR, B.G.; GANNON, J.E.; RAMSEY, P.W. Spatial analysis reveals differences in soil microbial community interactions between adjacent coniferous forest and clearcut ecosystems. **Soil Biology & Biochemistry**, Oxford, v. 42, p. 1138-1147, 2010.

PAGÉ, F.; GUILLET, B. Formation of loose and cemented B horizons in Podzolic soils: evaluation of biological actions from micromorphological features, C/N values and ^{14}C datings. **Canadian Journal of Soil Science**, Ottawa, v. 71, p. 485-494, 1991.

RADELL, E.A.; STRUTZ, H.C. Identification of acrylate and methacrylate polymers by gas chromatography. **Analytical Chemistry**, Washington, v. 31, p. 1890-1891, 1959.

ROBERT, A.W. **Mass spectrometry for chemists and biochemists.** 2th ed. Cambria: Johnstone and Malcolm E. Rose, 1990. 525 p.

ROSSI, M. **Fatores formadores da paisagem litorânea:** a bacia do Guaratuba, SP – Brasil. 1999. 162 p. Tese (Doutorado em Geografia) – Faculdade de Filosofia, Letras e Ciências Humanas, Universidade de São Paulo, São Paulo,1999.

ROSSI, M.; QUEIROZ NETO, J. P. Os solos como indicadores das relações entre sedimentos continentais e marinhos na planície costeira: Rio Guaratuba (SP). **Revista Brasileira de Ciência do Solo**, Viçosa, v. 25, p. 113-120, 2001.

_____. Evolução de esposossolo ferrocárbico em gleissolo háplico no Planalto da Serra do Mar, Rio Guaratuba (SP). **Revista Brasileira de Ciência do Solo**, Viçosa,   v. 26, p. 407-415, 2002.

SÁ, A.F.M.M. **Geoambientes e uso atual na bacia do Rio Alcobaça (MG e BA).** 2000. 185 p. Tese (Doutorado em Agronomia) - Universidade Federal de Viçosa, Viçosa, 2000.

SCHULTEN, H.R.; SCHINTZER, M. The chemistry of soil organic nitrogen: a review. **Biology and Fertility of Soils,** Berlin, v. 26, n. 1, p. 1-15, 1997.

SCHWARTZ, D. Some podzols on bateke sands and their origins, people's republic of Congo. **Geoderma**, Amsterdam, v. 43, p. 229-247, 1988.

SILVA, K.; VIDAL-TORRADO, P.; LAMBAIS, M. Bacterial and archaeal communities in bleached mottles of tropical podzols. **Microbial Ecology**, New York, v. 69, n. 2, p. 372-382, 2014.

TSUGE, S. Analytical pyrolysis: past, present and future. **Journal of Analytical and Applied Pyrolisis**, Amsterdam, v. 32, p. 1-6, 1995.

TSUGE, S.; OHTANI, H. **Pyrolysis gas chromatography of high polymers:** fundamentals and data compilation. Tokyo: Techno-Systems, 1989. 420 p.

TSUGE, S.; OHTANI, H.; Pyrolysis gas chromatography/mass spectrometry (PY-GC/MS). In: MONTAUTO, G.; LATTIMER, R.P. **Mass spectrometry of polymers**. Boca Raton: CRC Press, 2002. p. 113-145.

UDEN, P.C. Nomenclature and terminology for analytical pyrolysis. **Pure & Applied Chemistry**, Vienna, v. 65, p. 2405-2409, 1993.

VALLMIN, J.; KRIEMLER, P.; OMURA, I.; SEIBLE, J.; SIMON, W. Structural elucidation with a thermal fragmentation- gas chromatography-mass spectrometry combination. **Microchemical Journal**, New York, v. 11, p. 73-86, 1966.

WANG, F.C. Polymer analysis by pyrolysis gas chromatography. **Journal of Chromatography. Series A**, Amsterdam, v. 843, p. 413-423, 1999.

WILCKEN, H.; SORGE, C.; SCHULTEN, H.R. Molecular composition and chemometric differentiation and classification of soil organic matter in Podzol B horizons. **Geoderma,** Amsterdam, v. 76, p. 193–219, 1997.

ZECH, W.; SENESI, N.; GUGGENBERGER, G.; KAISER, K.; LEHMANN, K.; MILTNER, A.; MIANO, T.M.; SCHROTH, G. Factors controlling humification and mineralizing of soil organic matter in the tropics. **Geoderma**, Amsterdam, v. 79, p. 117-161, 1997.

2 PODZOL MORPHOLOGY IN A HOLOCENE COASTAL TROPICAL CHRONO-HYDROSEQUENCE AT ILHA COMPRIDA (SE- BRAZIL)

Abstract

The most frequent soils in the São Paulo State Coastal Plain are Podzols, characterized by strong to moderate hydromorphic to well-drained podsolization with very well developed podzol-B horizons (Bh or Bhm). To better understand podsolization processes, including effects of hydrology and rooting on profile morphology and the subsequent effects of improved drainage, a Podzol chrono-hydrosequence was described in detail on a cliff at the south coast of Ilha Comprida, a Holocene barrier island. This cliff is 1,800 m long and was caused by marine erosion. It offers a very special opportunity to describe a association of podzol profiles that vary in age and drainage conditions and their spatial relationships. To better understand the processes and lateral/vertical pedological transformations that have been occurring, and to serve as a basis for the study of organic matter (OM) of these soils, a number of profiles in the cliff were described and sampled. Additionally, some profile pits in the interior of Ilha Comprida selected on the base of morphological variations in the cliff profiles werw studied. The morphological description and analysis of the podzol sequence from Ilha Comprida allowed a subdivision into four distinct groups: poorly-drained profiles, well-drained profiles with Bh and Bhs horizons, strongly rooted profiles and superposed profiles. Some well-drained podzols have OM-depleted mottles that are related to selective decomposition of OM by microorganisms. Such mottles are frequently associated to root channels. Seventeen profiles were studied and thirteen had depletion mottles scattered along the profile. Most of these mottles are whitish and are located preferentially in the horizons of transition between the E and B horizons, particularly in conditions of good drainage. Such mottles have certain morphological differences and may be grouped according to similarities in their morphology and their position in the profile. Distinct groups are: (a) concentric OM-depleted mottles; (b) circular/tubular OM-depleted mottles (burrows); (c) dotted OM-depleted mottles; (d) ghost OM-depleted mottles; (e) irregular OM-depleted mottles and (f) Fe-depleted mottles. Almost all types of mottles described above, with the exception of ghost OM-depleted mottles, were found both in profiles in the cliff and in the inland profiles, but the inland profiles have fewer mottles than the profiles of the cliff. We concluded that there is some influence of exposure to air or marine spray (as occurs in the profiles of the cliff) on the establishment of the microorganisms that decompose the OM. In any case, the presence of mottles appears related to improvement of drainage at the top of the B horizon in the soil. The morphological description and some observations about the cliff exposure were essential for grouping and differentiating the podzol profiles.

Keywords: Drainage variation of podzols; Tropical podzolization; OM-depleted mottles; OM decomposition; B podzol horizon

2.1 Introduction

Variations in the sea level over geological time have caused advances and retreats of the shoreline in different parts of the world, transferring sediment from coastal regions towards the continent or to the inner shelf. This constant exchange of energy between the ocean and the continent results in the formation of a series of peculiar coastal environments

(PEREIRA et al., 2003). The evolution of the coastal plain of the coast of São Paulo State (SE-Brazil) is no different, being a result of alternating transgressive and regressive sequences during the Quaternary.

During the Quaternary, two transgressive and regressive cycles modeled the Brazilian coastal plains (TESSLER; GOYA, 2005). A Pleistocene transgressione (~ 120,000 years BP), reached about 8 meters above the current sea level. In the coastal area of São Paulo, this event has been termed as the Cananéia Transgression (SUGUIO; MARTIN, 1978). Around 17,000 years BP, during the late Pleistocene, the sea level dropped from this transgressive maximum to values well below the current level. Around 7,000 years BP sea level had again risen to the actual level (SUGUIO; MARTIN, 1978).

During regressions there were large depositions of sand to the shore platform next to the beaches. This material was partially or totally relocated by longshore currents and transported until it found an obstacle. The sandy beaches thus formed, consisting of a succession of ridges and swales (FLEXOR et al., 1984), generally known as "restingas" (SUGUIO; TESSLER, 1984).

According Suguio and Tessler (1984), among the different types of coastal deposits on the Brazilian coast, only the regressive ridges seem to be able to form extensive sandy plains. These plains were called plains ridges, replacing the term "restinga" plain, commonly used. In Brazilian literature, the term "restinga" is employed for sand ridges formed by coastal currents, but its meaning is quite diverse among the various branches of science (geology, geomorphology and botany; SUGUIO; TESSLER, 1984). In this thesis, the term refers to sandy coastal plains, consisting of ridges (beaches ridge), barrier islands, bars and spurs all of them under shrub, tree and herbaceous vegetation, as suggested by Suguio and Tessler (1984) and Suguio and Martin (1990).

The most frequent soils in the coastal plain of the São Paulo State (SE-Brazil) are Podzols, characterized by strong to moderate Podzolization and the consequent presence of B podzol (Bh or Bhm). The morphological study of soil is very important for a better understanding of both the processes of their formation and transformations that are still occurring. In general, the morphology of Podzols is very complex and primarily reflects the processes of transport and accumulation of OM and Fe compounds and their changes over time. Podzols may differ in their morphology at short distances, as can be seen in the cliff on the south coast of Ilha Comprida, a Holocene barrier island (GUEDES et al., 2011) with 75 km length and 2-5 km width, located on the south coast of the São Paulo State. These differences are related to variations in drainage, vegetation and porosity. Drainage can

directly influence the transport and accumulation of OM along the soil profile. A well-drained Podzol has morphologically distinct features from a poorly drained one (BUURMAN; VIDAL-TORRADO; LOPES, 2013; BUURMAN, VIDAL-TORRADO; MARTINS, 2013).

To better understand soil processes related to the SOM dynamics at the pedon scale, and its vertical and lateral variability of soil horizons, the morphology of a Podzol chrono-hydrosequence was described in detail at a cliff on the south coast of Ilha Comprida. This 1,800 m long outcrop was caused by recent marine erosion and offers a unique opportunity for this kind of research.

2.2 Materials and Methods

2.2.1 Sampling

All profiles were described and sampled according to Santos et al. (2005). Samples were taken along the south side of Ilha Comprida. Additional profile pits, 100 to 200 m removed from the coast were described and sampled, at selected points based on morphological variation of the profiles collected at the cliff. The samples collected in pits were intended to eliminate effects of wind, marine spray and tides, to which the Podzols in the cliff were exposed.

Disturbed samples were collected from the pedogenic horizons. They were analyzed in the laboratory, and some selective extractions were carried out that are described below.

2.2.2 Chemical analysis

Exchangeable cations (Ca^{2+}, Mg^{2+}, K^+ and Na^+), pH ($CaCl_2$, H_2O) and organic C (dichromate oxidation) were determined in all samples, using procedures recommended by EMBRAPA (2011). All samples were sieved through 100 mesh Al was determined by atomic absorption, following sodium poyrophosphate extraction, also according to EMBRAPA (2011).

2.3 Results and Discussion

2.3.1 Geomorphic setting and sampled profiles

The profiles were sampled according to pedogenic horizons and according to morphopedological units map of Ilha Comprida proposed by Martinez (2015) (Figure 1).

Follows the sampled profiles and respective morphopedological unit description (adapeted from MARTINEZ, 2015):

P41, P02 - Morphopedological unit I - Oldest surface and lower to surface II, with ridges and swales. Has soils with Bhm horizon greater than 200 cm and has OM bands cemented. It has small recesses with occasional occurrence of mangroves;

P04, P01, P40 - Morphopedological unit II - Longitudinal growth surface with ridges and swales well-defined converging towards Ponta da Trincheira, where there Podzols with more than 200 cm of Bhm horizon. Bhm horizon is situated above swing area of the water table. It has plane-parallel stratigraphy with trace fossils (*Callichirus major*).

P09, P10, P30 - Morphopedological unit III - Cross growth surface with flat topography, lower and more recent than the areas I and II; being confined by the adjacent surfaces has become flooded most of the year.

P11, P37, P38, P31, P32, P33 - Morphopedological unit IV - Longitudinal growth surface with ridges and swales defined by a truncation that divides two patterns of alignments.

P34, P35, P39 - Morphopedological unit V - Youngest surface with accelerated growth. Has stabilized frontal dunes and intermittent marshes.
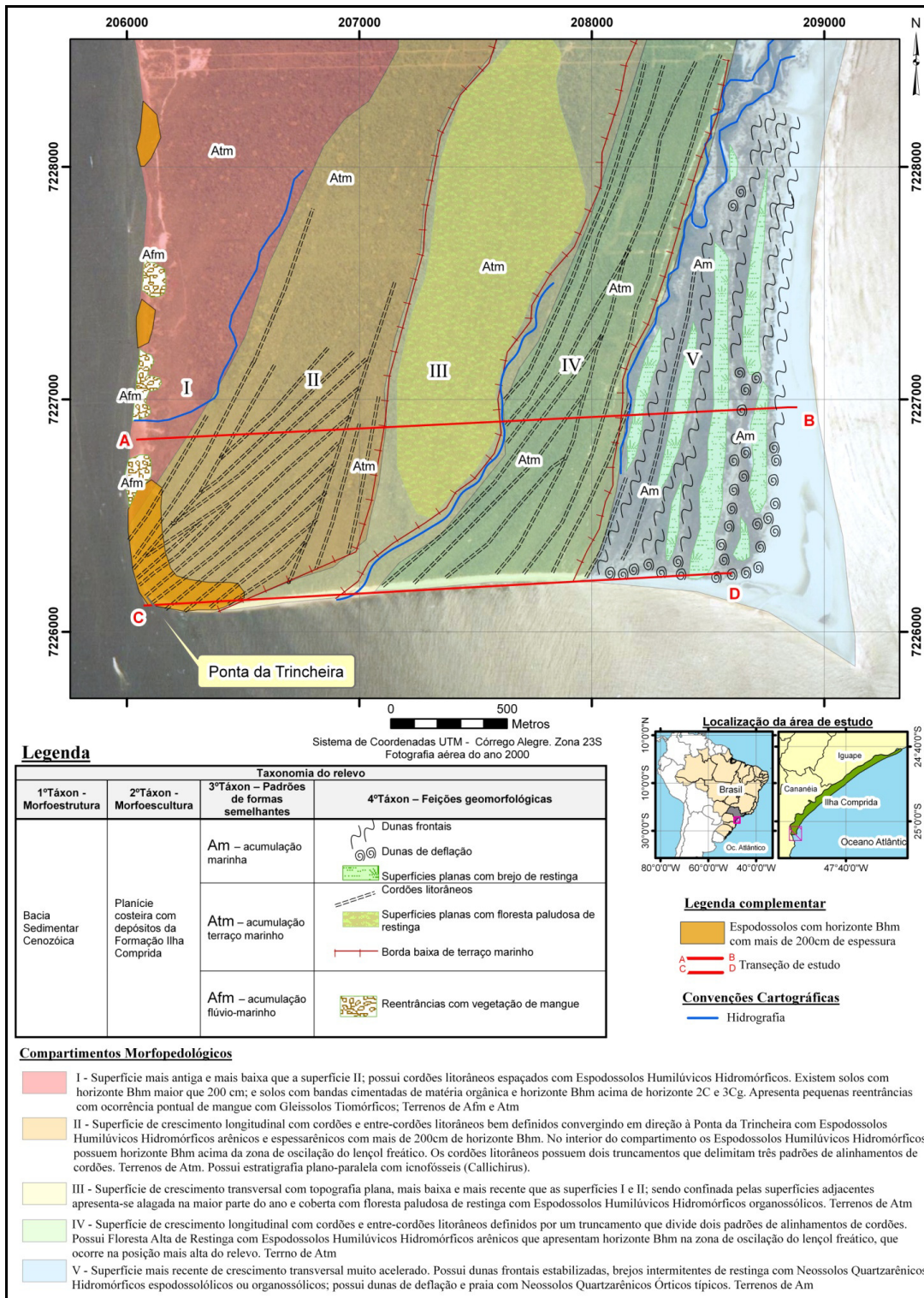
Figure 1 – Morphopedological units map of the southern part of Ilha Comprida-SP (MARTINEZ, 2015)

2.3.2 Ilha Comprida

The municipality of Ilha Comprida, which covers the total area of the island of the same name, is located on a Holocene barrier island on the south coast of São Paulo state. Its

sea coast is approximately 74 km in length, and its width varies from 625 m to 5,37 km (GERARDI; MENDES, 2001). The island is separated from the mainland by the Mar Pequeno or Iguape and the Mar de Cananéia, which is about 80 km long (Figure 2).
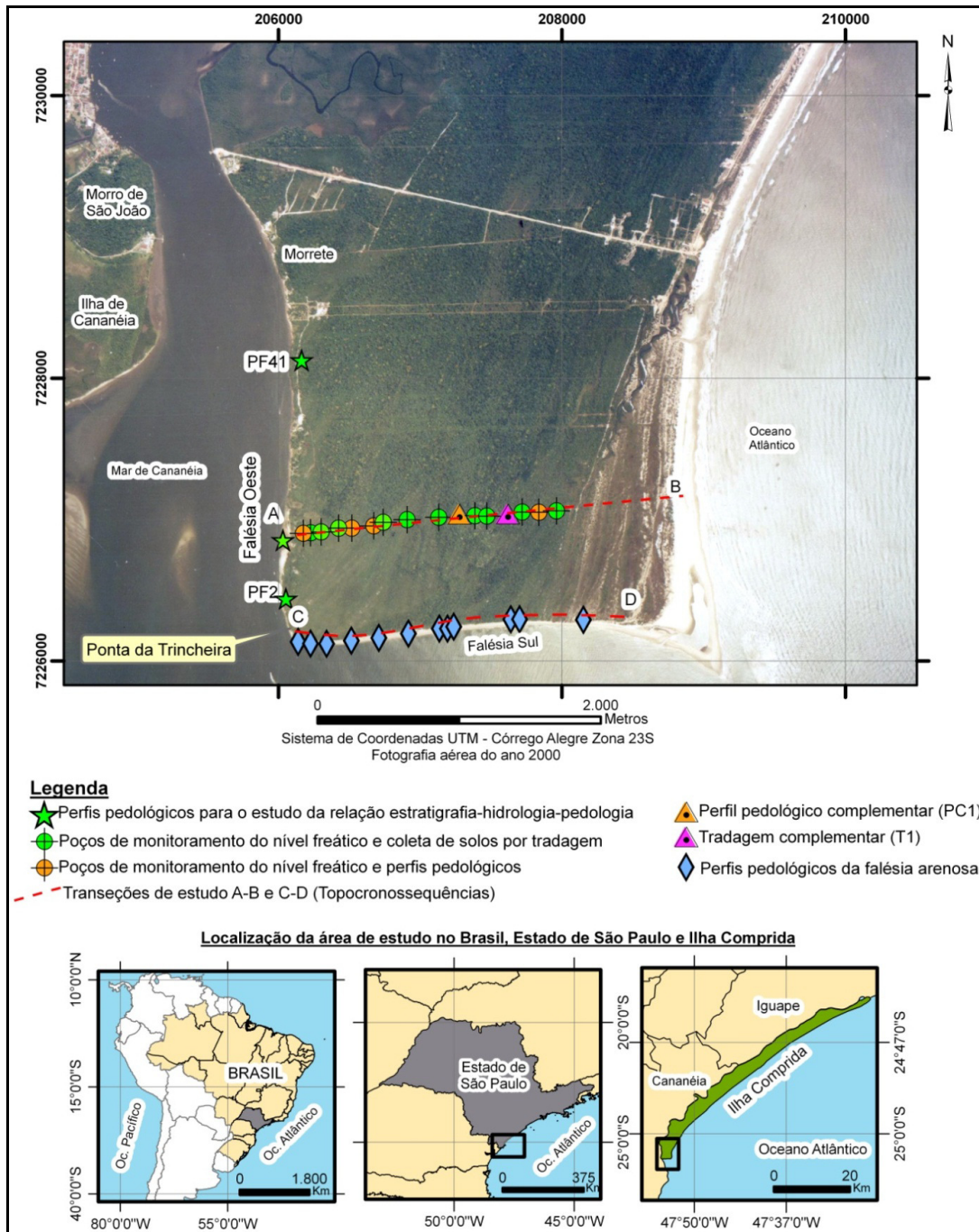
Figure 2 – Location of the Ilha Comprida section (MARTINEZ, 2015)

The southern coastal plain, according Troppmair (2004), has predominantly a humid tropical climate, with average temperature between 22° and 23°C. The average maximum temperature is around 30 °C, and the absolute maximum can reach 38 °C. According to

Koeppen's classification, the climate of the southern coastal plain is Af. Rainfall is well distributed throughout the year. In summer, rainfall is between 1,300 and 1,500 mm in 100 days, while in winter it is around 500 mm in 60 days (TROPPMAIR, 2004). These climatic conditions influence the type of vegetation in the coastal plain and in the adjacent mountainous areas. Ross and Moroz (1997) stated that the vegetation in coastal areas develops from pioneer species (grasses) to shrubs and trees of the Restinga forests.

Ilha Comprida consists predominantly of sandy sediments in the form of ridges, which are geomorphic expression of a prograding barrier. The diversity of sediments that make up the coastal plain is the result of interaction between ocean and continent. The Quaternary geological formations in the coastal zone of São Paulo consist of sedimentary deposits, and. according to the Instituto de Pesquisas Tecnológicas - IPT (1989), apart from differences in thickness; follow the same distribution pattern along the São Paulo coast. The sediments in the study area belong to the Ilha Comprida Formation, which is part of the Mar Pequeno Group (IPT, 1989).

According to Tessler (1988), Praia de Fora, which is the outer beach of Ilha Comprida, currently shows a retreat toward the mainland, and this process is responsible for the narrowing of this sector of the island. The beach is not being reduced, but is moving towards the marine terraces. Thus the width of the foreshore tends to remain stable, while the marine terrace becomes increasingly narrow. In the southern portion of Ilha Comprida there is a predominance of erosive processes, where there are the passages of cold fronts in winter, which cause strong winds from the south, which consequently accelerate and intensify the erosive processes in place. In other seasons, the erosion can be influenced by spring tides or storms. Even in recent years, an significant amount of trees have fallen on the beach at the southern coast of the island, indicates significant erosion.

2.3.3 General descriptions of profiles

Most profiles have been sampled on the south side of Ilha Comprida, where a sequence of older to younger surfaces is exposed. Additional profiles were sampled on the southwest side. Figure 3 indicates the profile locations. A morphological analysis of the podzol sequence from Ilha Comprida allowed a subdivision into four distinct groups: poorly-drained profiles, profiles with well-drained B horizons, strongly rooted profiles and superposed profiles.
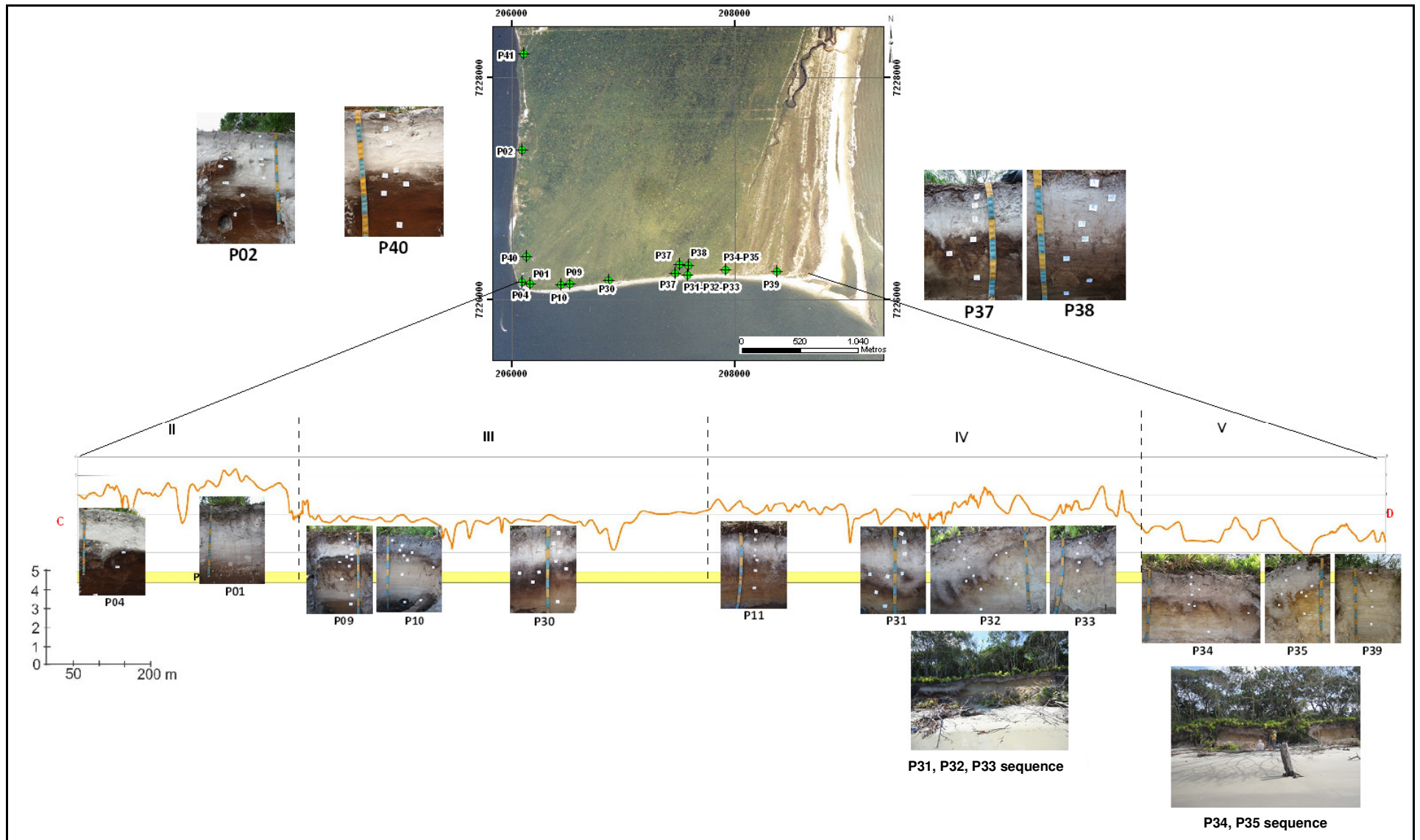
Figure 3 - Profile locations on Ilha Comprida

Poorly-drained profiles

       The profiles P01 and P04 are located in a cliff on the south side of Ilha Comprida, while profile P02 is located in a cliff on the south-west. P40, the last profile that belong this group, is a pit about 150 m from the south coast, aligned to profile P04 in the cliff. The P01, P04 and P40 profiles are located in the morphopedological compartment II and P02 on morphopedological compartment I, according to Martinez (2015).

       A special kind of burrows are found near the base of profiles P01, P02 and P04 (Figure 4a and 4b). These burrows have walls cemented with OM and are very well known in the marine ecology literature as a type of Ophiomorpha (an ichnotaxon, usually interpreted as a burrow of an organism living in the near-shore environment) attributed to *Callichirus major*, with a life cycle associated to areas close to the limit of low tide (SUGUIO; MARTIN, 1978).
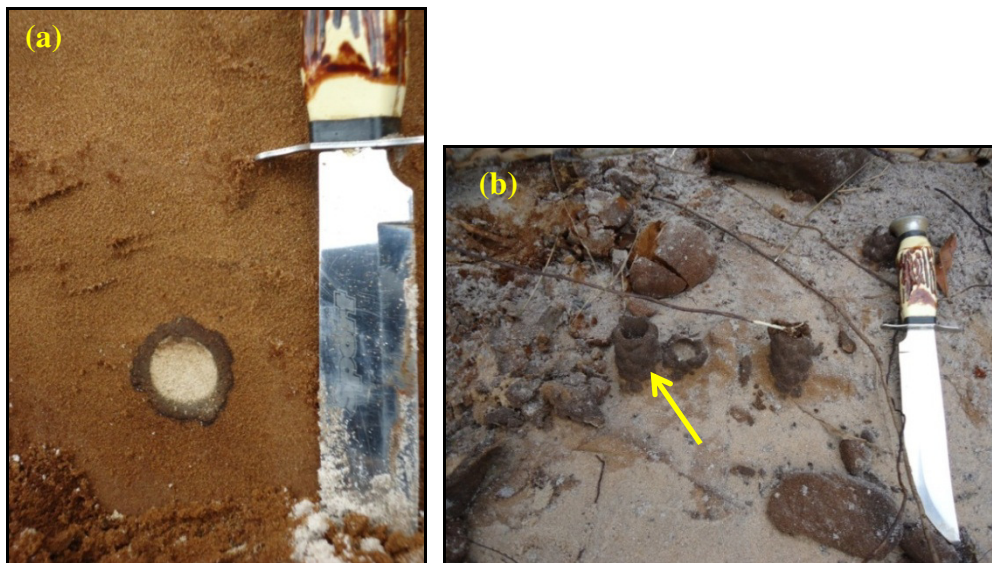
Figure 4 – Profile P02. (a) Cross section of a ghost-shrimp burrow with OM-cemented wall in the lower part of the profile; (b) Large vertical galleries of ghost-shrimp the lower part of the profile (arrow)

Profile P01

       Profile P01 (Figure 5) is an (originally) poorly drained podzol and all SOM accumulation appears to be related to lateral water flow.

Figure 5 - Profile P01, overview. Note cementation in the exposed part of the B horizon

Cementation is present in the lower part of the profile. Roots are virtually restricted to the A horizon and the top of the E horizon. The profile presents more than 3.4 m depth, and has a cemented horizon in the lower part (Bh3m) that does not appear in the picture (Figure 6).
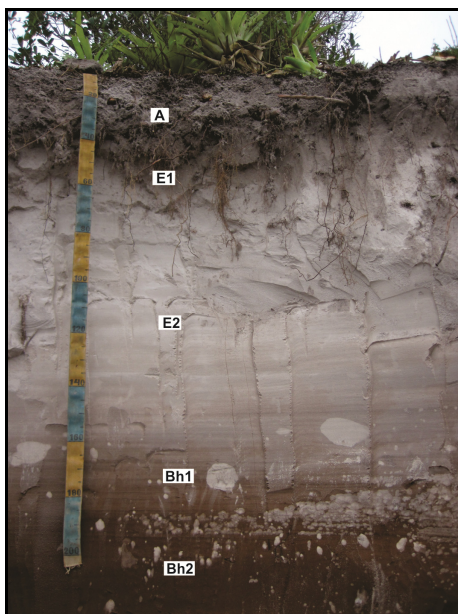
Figure 6 - Profile P01. Location of horizons in the profile. Note the abundance of OM-depleted mottles in the top of the B horizon

Concentric SOM-depleted mottles occur also lower in the profile, where they are less abundant. They clearly follow sedimentary stratification (Figure 7b). In the lower B horizon (Bh3m), colors are darker and sedimentary stratification is inclined. This part is probably influenced by flood water.

Sedimentary stratification is virtually undisturbed in the lower E horizon and below, but bleached channels with sharp boundaries that are presumably burrows are found at the top of the B horizon (arrow in Figure 7a).

In the top of the B horizon, below the larger burrows, spots with concentric structures are found, in which the SOM has been decomposed (Figure 7c). These concentric structures are concentrated in part of the B horizon. They appear to follow sedimentary stratification. The SOM depletion in the concentric structures is not complete. Under the zone of concentric SOM depletions, small SOM-depleted structures are found that might be burrows. They lack the concentric structures and have sharper boundaries (Figure 7d).
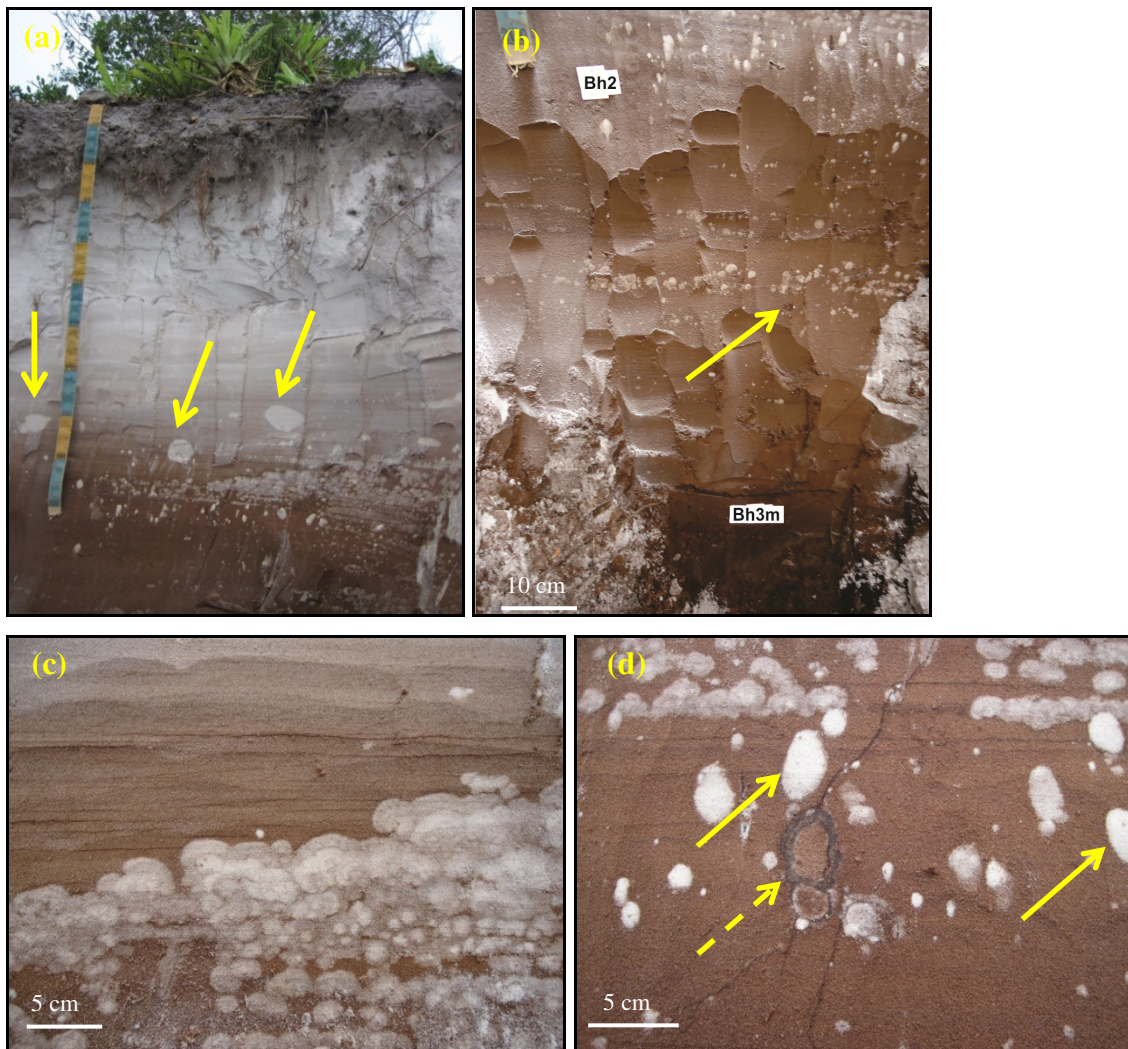
Figure 7 – Profile P01. (a) Burrow-like structures (arrows) in the stratified upper part of the B horizon. Note scarcity of roots in the upper E horizon; (b) Concentric SOM-depleted mottles lower in the profile (arrow). Note the very dark colors of the Bh3m; (c) Concentric SOM depletion structures in the top of the B horizon; (d) Small burrows (arrows) below the layer of concentric SOM depletions. The dashed arrow indicates a structure that is probably a ghost-shrimp burrow that is lined with organic matter

Profile P02

The profile shows a large lateral variation. Part of the profile was developed under hydromorphic circumstances and shows a lateral and horizontal accumulation of SOM (Figure 8, arrow). After its initial development, drainage of the profile was improved, which led to partial decomposition of the top of the B horizon (Figure 8b). This improved drainage is also shown by the development of bleached E horizon pockets along root channels (Figure 9b).
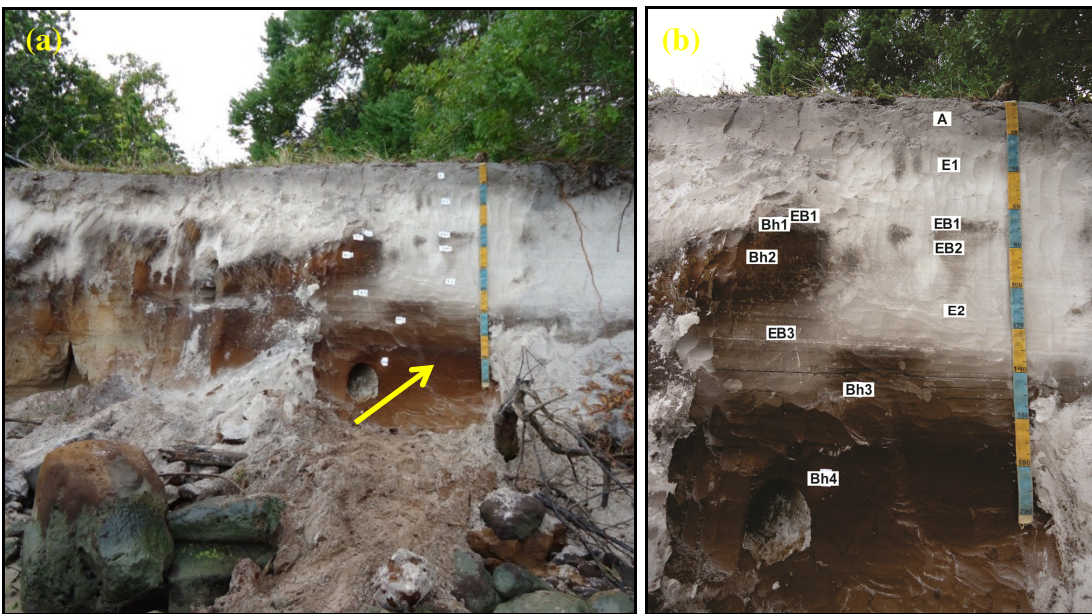
Figure 8 - Profile P02. (a) Superposition of a improved drainage on a hydromorphic podzol; (b) Location of horizons in the profile; These situation is very common in cliffs on the oldest part of the Ilha Comprida (Compartment I of MARTINEZ, 2015)

The partial decomposition of the B horizon results in a darker fringe on E horizon, which may be due either to decomposition of the original material or to addition of fresh DOM. New dark bands of precipitated DOM are found in the top of the B horizon (Figure 9a) and in bleached E horizon pockets (Figure 9b), that follow old root channels.

Different from the original, hydromorphic B horizon does not have burrows, the transition zone between the decomposing B horizon and the surrounding E horizon is strongly burrowed (Figure 9c). Small burrows also appear in the B horizon and are aligned along the sedimentary stratification (Figure 9d).
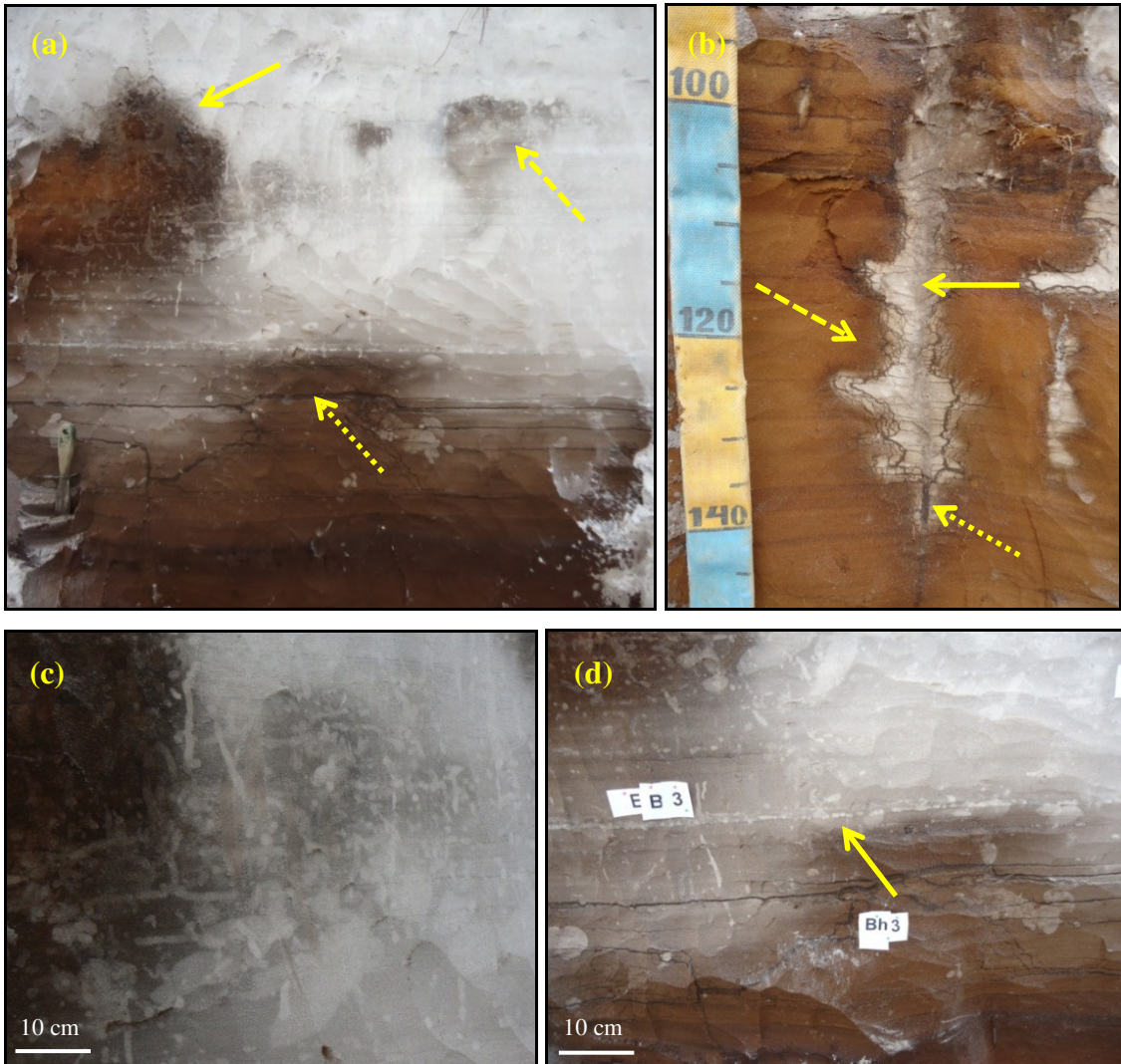
Figure 9 – Profile P02. (a) Decomposition of the –originally hydromorphic – B horizon. The horizon is still intact at the bottom of this figure. In the upper left part, the original brown B horizon is partially obliterated and surrounded by dark OM (arrow). In the upper right part, the former B horizon has all but disappeared (dashed arrow). In the top of the remaining B horizon, new dark bands have accumulated that largely follow the sedimentary stratification (dotted arrow). Roots are virtually restricted to the A horizon; (b) Bleaching along former root channels. Note the slightly dark color of the former root (arrow), the slightly darker colors at the contact with the remaining B horizon (dashed arrow), and the accumulation of DOM largely within the root channel (dotted arrow); (c) Strongly burrowed contact between decaying B horizon and EB/E horizons; (d) Rows of small burrows that follow the stratification in the EB horizon (arrow)

Profile P04

The profile (Figure 10) has a giant podzol-B horizon with strong cementation and dark colour. Currently, drainage is imperfect, but its development occurred in circumstances of strong hydromorphism.

Figure 10 - Profile P04, overview. A giant hydromorphic podzol with cemented B horizon

As profile P02, the upper part of profile P04 currently shows an improvement in drainage, which led to partial decomposition of the top of the B horizon (Figure 11a). It has many burrows in the EB horizon and in the top of the Bhm1 horizon (Figure 11b). Concentric SOM-depleted mottles are found in the middle part of the profile (between 140 and 180 cm depth), and are less abundant than the burrows. There are large concentric depletion mottles in the Bhm2 horizon (Figure 12a), and irregular SOM-depleted mottles at the top of the Bhm1 horizon (Figure 12b).
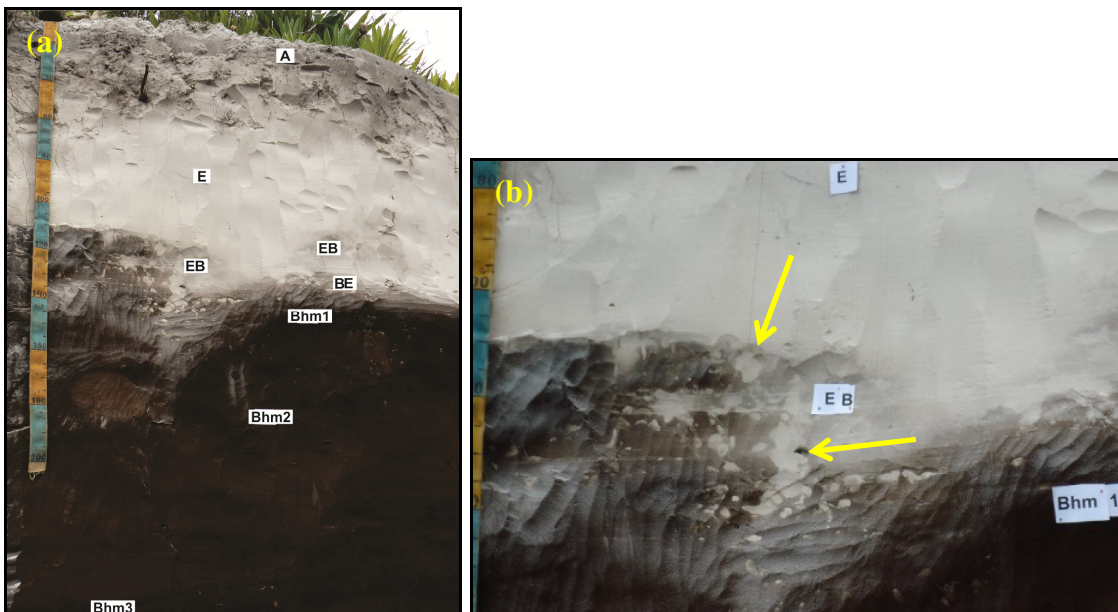
Figure 11 - Profile P04. (a) Location of horizons in the profile. Note decomposition at the top of the B horizon (EB, BE); (b) Some burrows in the EB horizon and the top of Bhm1 horizon (arrows)

This profile, as profile P02, has galleries of ghost-shrimp at its bottom, but they are more cemented than the others (Figure 12c, dashed arrow). These burrows are similar to the structure depicted in Figure 7a.

The Bhm3 horizon (Figure 12c, arrow) is a more darkened band in the middle of the profile, which may have formed by flow of the groundwater during its development, in the presence of high concentrations of DOM. At the base of the profile, in the Bhm5 horizon, there is a hard and extremely dark band with platy structure (Figure 12d).

The profile is located very close to Ponta da Trincheira (Compartment II), where a thick Bhm horizon, similar to that of the present profile, is exposed.
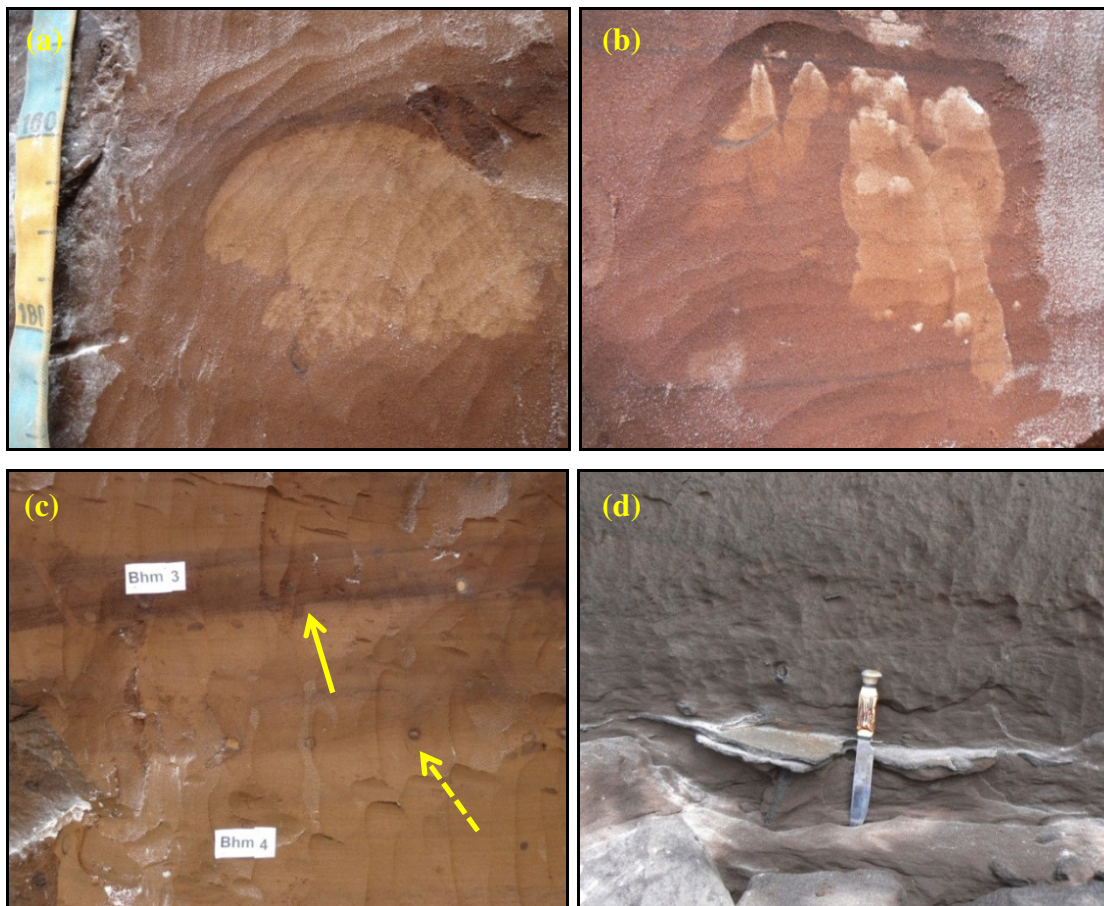
Figure 12 - Profile P04. (a) Concentric SOM-depleted mottles in the Bhm2 horizon; (b) SOM-depleted (ghost type) mottles in the Bhm1 horizon; (c) The Bhm3 horizon is a band with dark color by OM accumulation (arrow). Note some galleries of ghost-shrimp on the top of Bhm4 horizon (dashed arrow); (d) In the Bhm5 horizon is a platy band with dark coloration and very strong cementation by OM

Profile P40

It has many bands of OM deposition and some SOM-depleted mottles and burrows at the top of the B podzol horizon (Figure 13a, arrow). Currently, it has good drainage, but its development took place under pronounced hydromorphism, similar to profile P04 in the cliff. The E horizon is not as thick and the B horizon is not as deep as in profile P04 (Figure 13b).
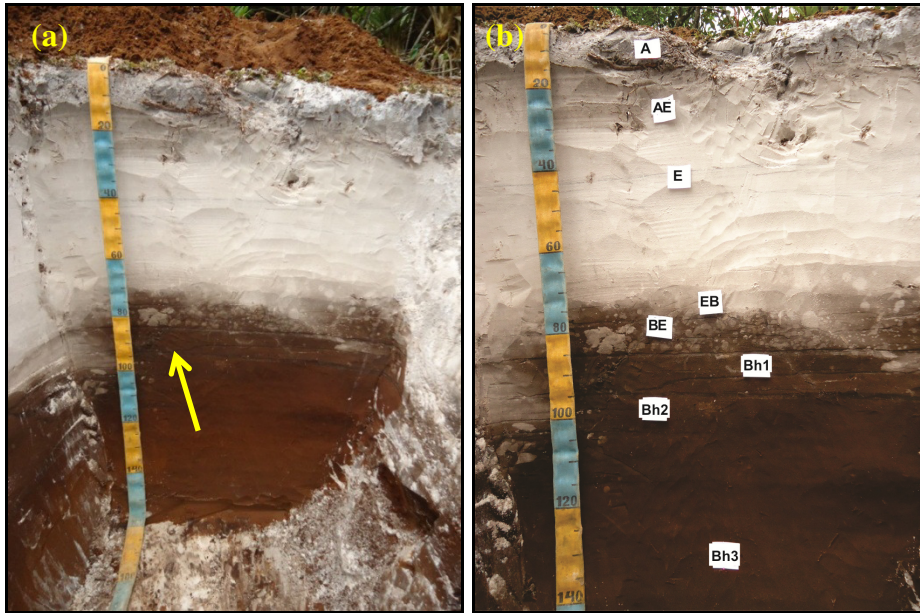
Figure 13 - Profile P40. (a) Overview. Profile pit, poorly drained podzol 150 m inland from the south coast of Ilha Comprida; (b) Location of horizons in the profile

The improved drainage is accompanied by many SOM-depleted mottles in the EB and BE transition horizons and the top of the Bh1 horizon (Figure 14a). There are some thick bands of OM deposition by stagnating vertical water flow, especially in the top of the B horizon, the Bh1 horizon (Figure 14a).

The thicker roots are concentrated in the upper portion of the profile, but some roots channels and decaying roots can be found throughout profile, especially at the top of the B horizon (Figure 14b).
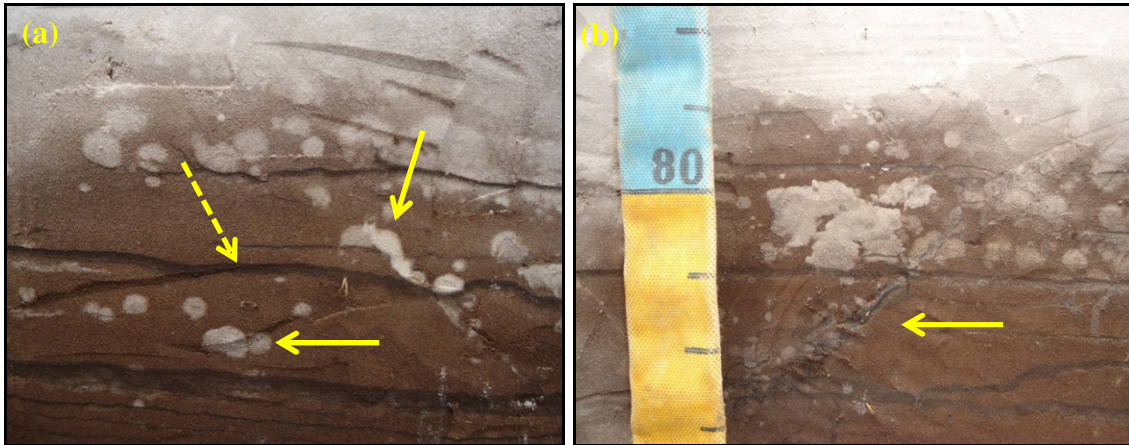
Figure 14 – Profile P40. (a) SOM-depleted mottles (arrow) and OM bands (dashed arrow); (b) Decaying root (arrow) near the bands and mottles

Profiles with well-drained B horizons

The profiles with well-drained B horizons are P30, P31, P32, P33, P34 and P35. All are located in a cliff on the south side of Ilha Comprida. Profile P30 (Figure 15) is located in the morphopedological compartment III, according Martinez (2015), while the P31, P32 and P33 are located in the morphopedological compartment IV, and finally, P34 and P35 in the morphopedological compartment V.

Profile P30

There are many SOM-depleted mottles and burrows in the top of the Bh1 horizon, especially in the EB and BE transition horizons, which are presumably related to the improved drainage as it approaches the cliffs (Figure 16a). In the Bh2 horizon, there are some concentric SOM-depleted mottles (Figure 16b).
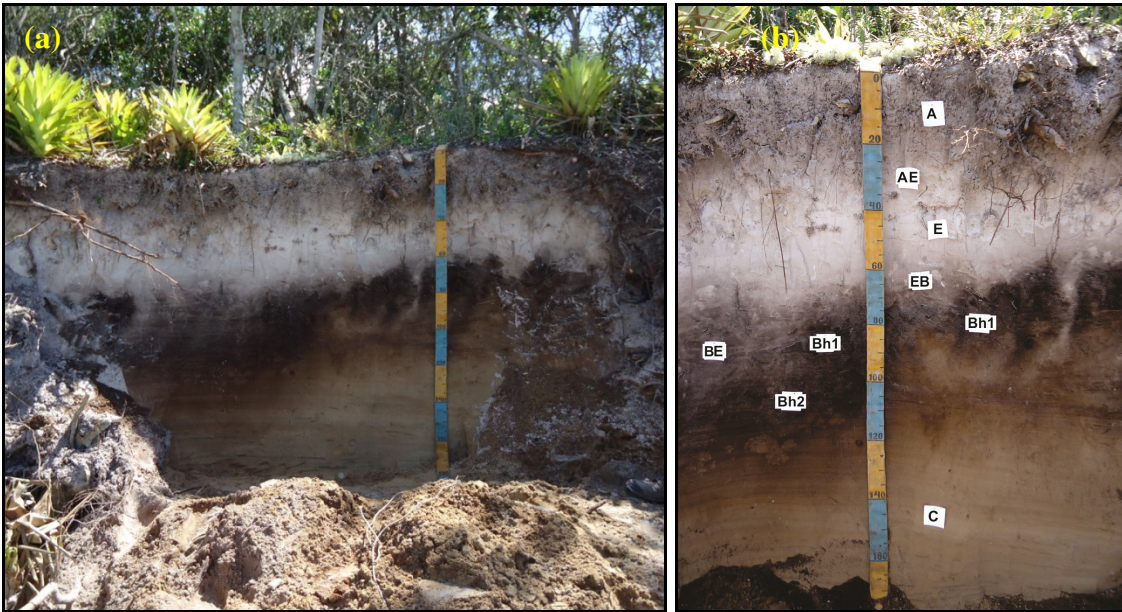
Figure 15 – Well drained podzol P30, (a) Overview. Profile located in a cliff on the south side of Ilha Comprida, close to the main drainage channel; (b) Irregular transitions and location of horizons and subhorizons in the profile.

The Bh1 horizon is a wavy band that accompanies some old root channels. In some places, there is the thickening of the E horizon in the form of tongues, accompanied by virtual disappearance of the Bh1 horizon (Figure 16c), which suggests a preferential decomposition of OM in the old root channels, where the drainage is improved an Al is removed. There are lines of dark sand at the base of the profile.
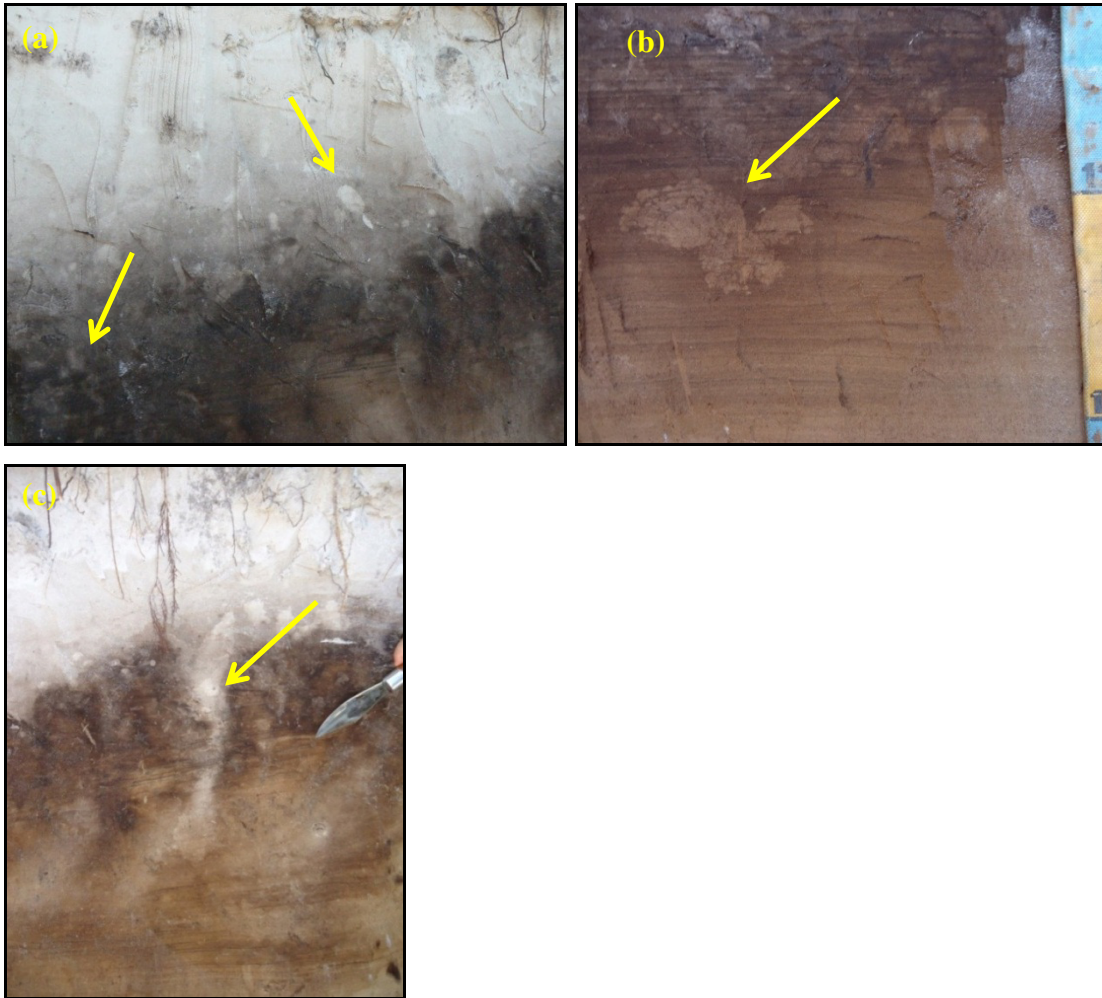
Figure 16 – Profile P30. (a) SOM-depleted mottles and burrows at the top of the Bh1 horizon and especially in EB and BE transition horizons; (b) Concentric SOM-depleted mottles in the Bh2 horizon; (c) Bh1 horizon with E horizon tongue

Profiles P31, P32 and P33

This is a section through beach ridge and swale. Both ridge and swale are sandy and show two types of Podzols, both well-drained, but with different morphology (Figure 17).
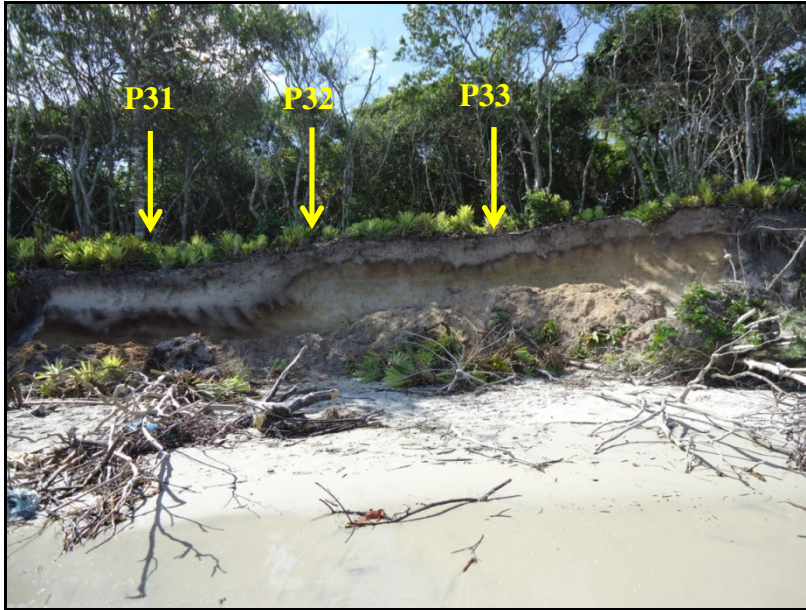
Figure 17 - Profiles P31, P32 and P33. Section about 10 m long, through beach ridge (well drained podzol) and swale (well to moderate drained podzol). Located in a cliff on the south side of Ilha Comprida

In the first stages of development, the profiles P31, P32 and P33 located in this section of beach ridge and swale probably had some Fe segregation due to groundwater fluctuations. In the higher part, this is still visible, but in the lower part it has disappeared due to later reduction and DOM percolation. In the intermediate portion, vertical transport of OM is visible, forming tongues in preferred root channels (Figure 19a).

In the higher part, the Fe-accumulations have been changed by root channels and the water passing through them. Root channels are bleached and have many remnants of small roots. Where Fe remains, roots are scarce or absent.

In the left hand part of the section (the swale) profile P31 shows a development that is related to the periodical passage of large amounts of water (due to its lower position), but not to groundwater influence (Figure 18). The passage of DOM-laden water has caused a well-developed Bh horizon, which is now being depleted (better drainage than the typical poorly drained podzols) by microbial activity (Figure 19a).
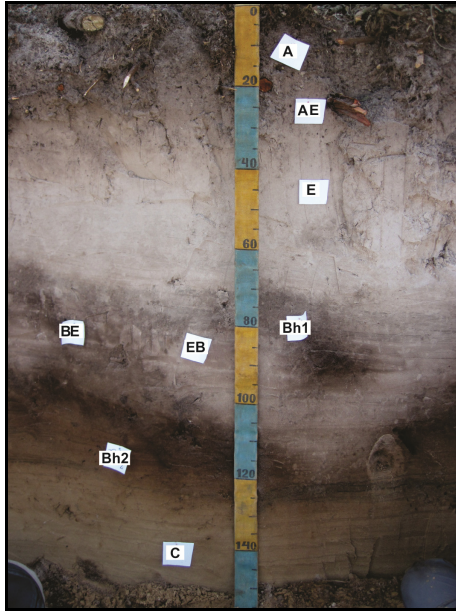
Figure 18 - Profile 31. Well to moderately drained Podzol. This profile is located in the swale portion of the compartment V (MARTINEZ, 2015)

There is an "island" of the darkened Bh horizon, the Bh1 horizon, surrounded by bleached sand. In the lower portion of the profile, the sediment is stratified and bands with dark minerals are visible (Figure 19b). There are also SOM-depleted mottles, located mainly in the transition horizons, and probably due to improved drainage.
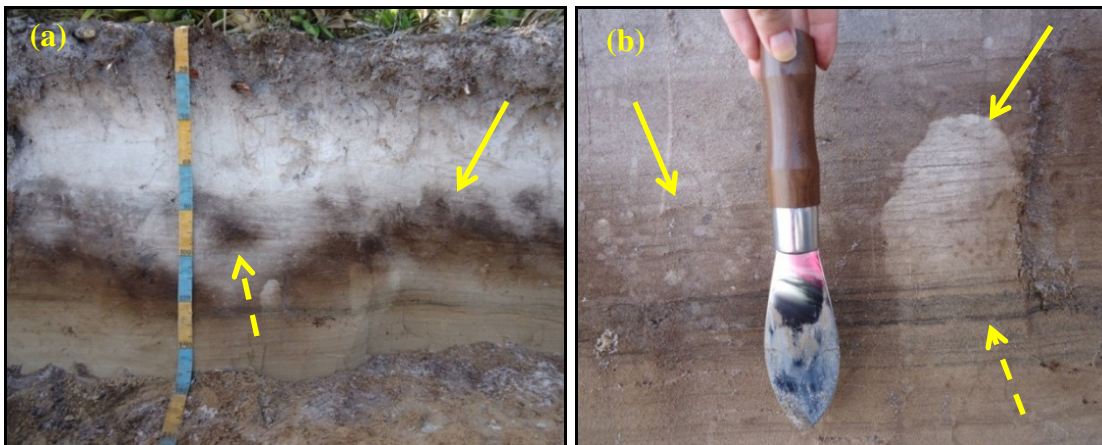
Figure 19 - Profile P31 (a) Overview. Located in the lower portion of the landscape where there is lateral flow. Note the wavy form of Bh horizon (arrow) and small islands of Bh horizon in the middle of the transition horizon (dashed arrow); (b) SOM-depleted mottles in the Bh2 horizon (arrow) and stratification with bands of dark sand (dashed arrow)

Profile P32 (Figure 20) is located in the middle portion of the transect, in the intermediate region between the beach ridge and swale (Figure 17). The profile has good

drainage and more abundant roots in the surface layers; some areas in the lower horizons have an accumulation of decomposing very fine roots.
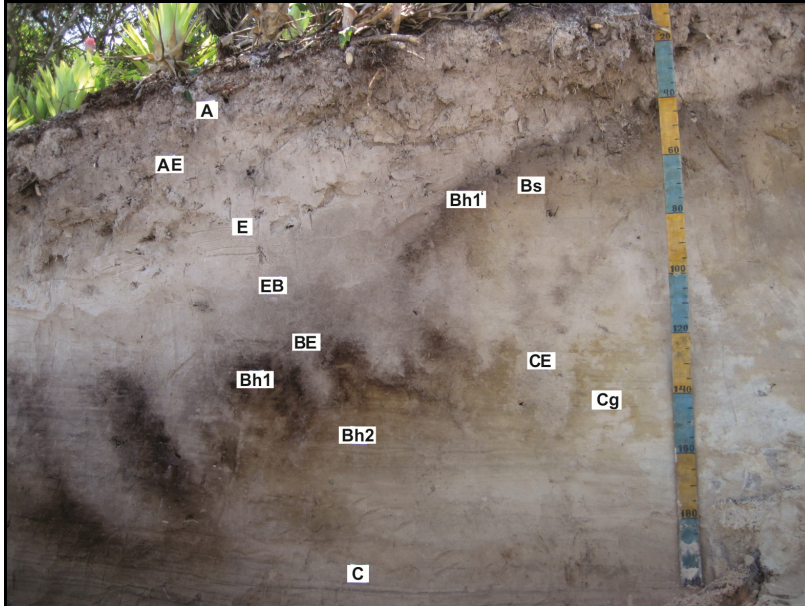
Figure 20 - Profile P32, overview. Well-drained profile located in a cliff on the south side of Ilha Comprida. Note the tonguing transition E-Bh due to root penetration

The profile has E and Bh horizons in the form of tongues, which presents a very different morphology at the transition from the lower portion to the highest of the transect. The direction of the bleached tongues of E horizon, which are inclined to the right (Figure 21a), may indicate outward flow of water from the swale (lateral pressure during high water).

The Bh1 horizon near the swale (left hand part) is deeper. Its coloration presents evidence of DOM accumulation. The Bh1' horizon, located in the right hand part of the profile, presents a discontinuous wavy line, and its OM is probably derived from roots. The Bh1' horizon can be clearly differentiated from the bottom Bh1 horizon.

There are concentrations of Fe-hydroxides in the right hand portion of the profile, nearer to the ridge. These concentrations appear as small and hardened reddish spots. In most of the profile, the accumulation of Fe was affected by root channels and water passing through them. These channels are more bleached and have a high concentration of fine root remains. Where the Fe remains, roots are rare or absent (Figure 21b).

The region below the Bh1' horizon, with yellowish coloration and evidence of higher Fe concentration than the other horizons, was designated Bs, and the lower portions of this section has a C horizon, in which thin bands of dark sand can be distinguished.

Figure 21 – Profile P32. (a) Profile P32 is located in the middle of the transect, and is intermediary between profile P31, in the lower part of the landscape (as described above) and profile P33, in the uppermost portion of the transect. Note the transition from one profile to another and the difference in B horizon morphology (arrow). (b), The CE horizon has mottles of Fe depletion, and in some of these, a high concentration of very fine roots is found (arrow). The decomposition of these roots may have triggered the reduction and removal of Fe; (c) There are many SOM-depleted mottles in the Bh1 and BE horizons, which are irregular and wavy

The profile P33 is located in the highest part of the landscape (ridge) (Figure 22a). The profile has very good drainage, with abundant roots in the surface horizon and some concentrations of fine roots in the subsurface horizons.

Figure 22 – Profile P33. Very well drained podzol, (a) Overview. Located in a cliff on the south side of Ilha Comprida corresponding to the ridge ; (b) Location of horizons and morphology of its transitions

The profile is weakly developed, with a thin and wavy Bh1' horizon (Figure 23a), at some points in the form of tongues with OM probably derived from roots (Figure 23b). This profile contains larger amounts of Fe than profiles P31 and P32, as suggested by the yellowish coloration in the subsurface horizons. There are only a few iron mottles in the left hand portion of the profile.
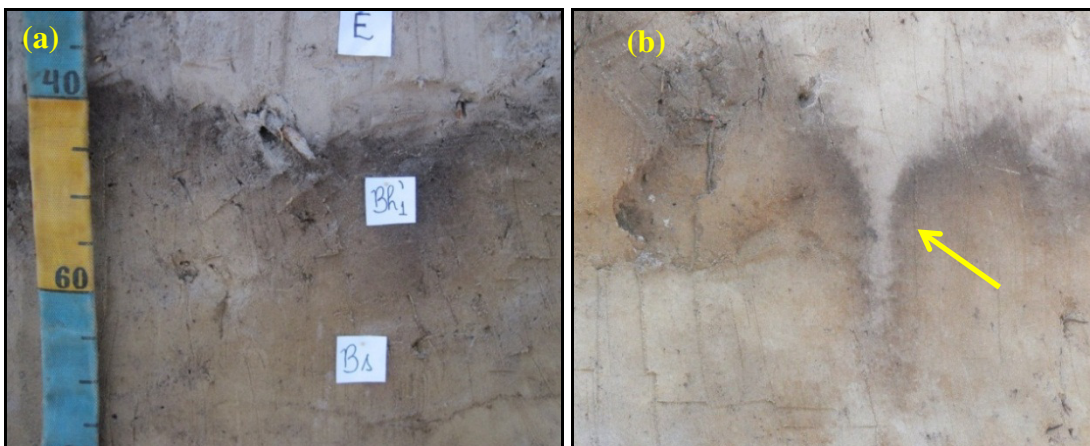
Figure 23 – Profile P33. (a) Bh1' horizon, thin and wavy, with accumulation of OM derived from roots; (b) Detail of one of the tongues of the E and Bh1' horizons, indicating a root channel (arrow)

Profile P34 and P35

This section is very similar to the previous one (profiles P31, P32 and P33), especially the lower (left-hand) part, which represents the swale (Figure 24). The swale-section is, however, more complex than the previous one, because there is a significant influence of roots in many horizons.

Figure 24 - Profiles P34 and P35. Section approximately 15 m long, through beach ridge and swale. Located in a cliff on the south side of Ilha Comprida

Profile P34 is located on the left side of the section; it has good drainage and many roots distributed throughout the profile (Figure 25a). In the upper portion there is a Bh horizon (derived from roots), up to 20 cm thick, in the form of tongues (Figure 25b). Small SOM-depleted mottles are found at the transition between BE and Bh1 horizons (Figure 25d).

Deeper in the profile, the C horizon has many large depletion mottles and some reddish iron concentration. In some areas concentrations of decaying fine roots and lines of stratification by dark sand are found (Figure 25c).
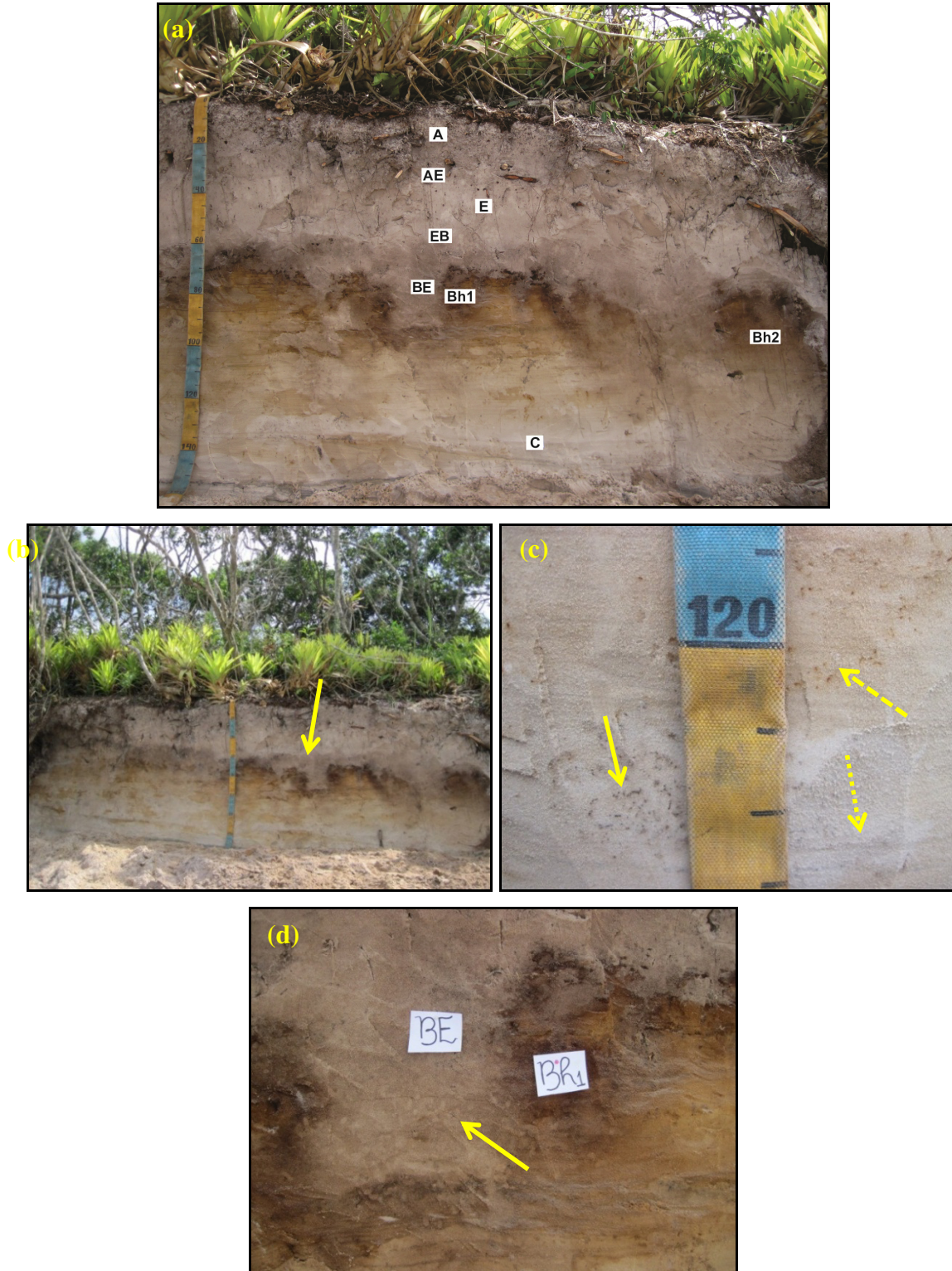
Figure 25 – Profile P34, (a). Location of horizons in the profile; (b) Well-drained profile with irregular and wavy Bh horizon with local tongues (arrow); (c) Small black spots (arrow), which are very fine decaying roots in the C horizon, and some reddish iron concentration (dashed arrow). Some lines of dark sand can be distinguished (dotted arrow); (d) Details of BE and Bh1 horizons showing small SOM-depleted mottles at the transition between these horizons (arrow)

Profile P35 is located on the right (eastern) side of the section described above. It has good drainage; thicker roots are limited to the soil surface, while the finer ones are distributed throughout the profile (Figure 26a). In the upper portion, similar to profile P34, there is a young Bh horizon (derived from roots), which is fairly thin and wavy and at some points in the form of tongues (Figure 26b). Below the Bh horizon there are many white spots, depleted of Fe (Figure 27b).
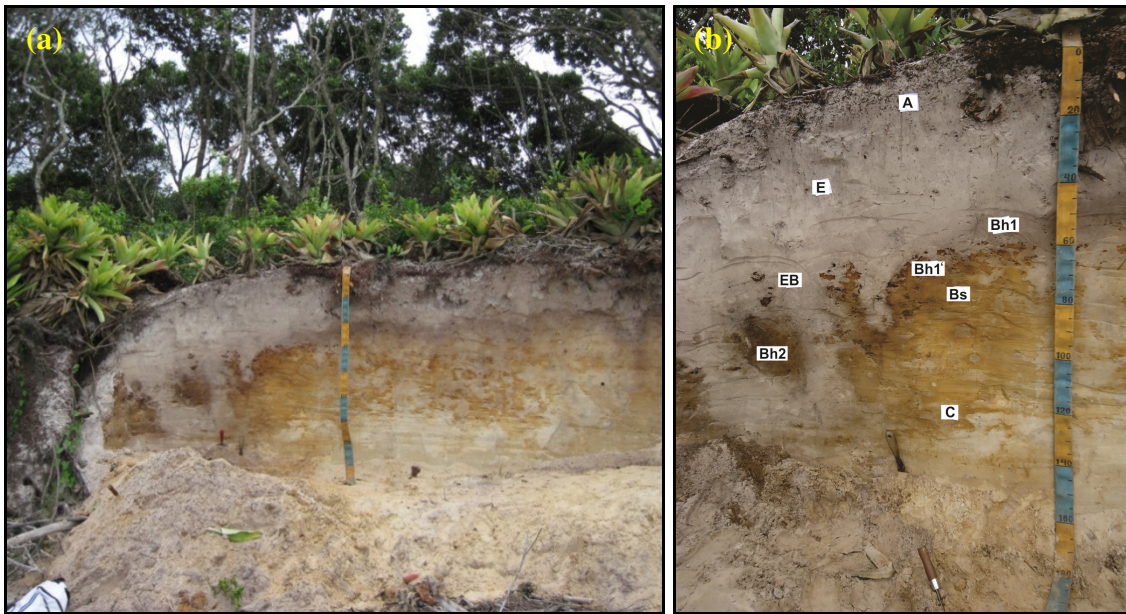
Figure 26 - Profile P35. (a) Overview. Profile located in a cliff on the south side of Ilha Comprida; (b) Location of horizons in the profile

There is a clear transitional zone where the original Fe-containing B horizon is disappearing due to penetration of roots and extension of the present E horizon. Remnants of the old B horizon are still found as islands in the E horizon (Figure 27c). Both the Bh islands in the E horizon and the top of the disappearing Bh horizon have outer rims with organic matter accumulation (presumably DOM). This organic matter accumulation is probably recent, as it is found throughout the E-Bh contact (Figure 27a).

In the upper part of the section, the young (root-derived) Bh horizon is very clear, but in the transitional zone it is difficult to identify. In the Cg horizon of the upper part, there is some clear accumulation of Fe around bleached parts, which indicates periodic saturation with water in the bleached channels while the matrix still contained oxygen (pseudo-gley).
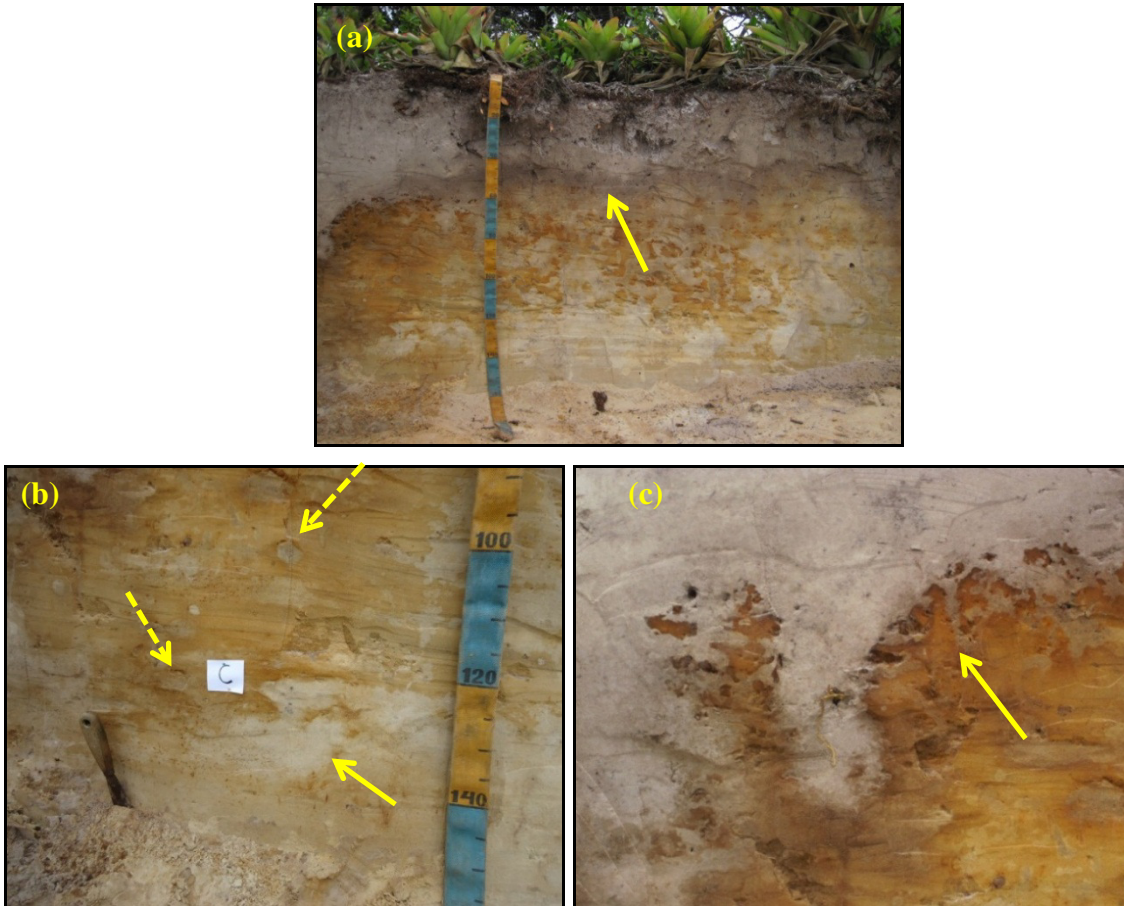
Figure 27 – Profile P35. (a)Yellowish red profile, with concentrations of Fe and many depletion mottles of Fe, and organic matter accumulation found throughout the E-Bh contact (arrow); (b) C horizon with large Fe-depleted areas (arrow) and concentrations of small red spots (dashed arrow), which are fine root channels; (c) Fe concentrations in the Bh1' horizon, yellow-reddish and strongly cemented

Rooted profiles

Profiles P11, P37 and P38 are located on the south side of Ilha Comprida, in the morphopedological compartment IV according Martinez (2015). These profiles have many roots and dark spots of decomposing roots throughout the profile. The profile P11 is located the cliff, while the others are from inland pits.

Profile P11

This profile is well-drained, but it has evidence of formation under hydromorphic conditions at the base of the profile (Figure 28a). There are many thin and thick roots in the O horizon and a few in the A horizon. The undergrowth consists of Bromeliads.
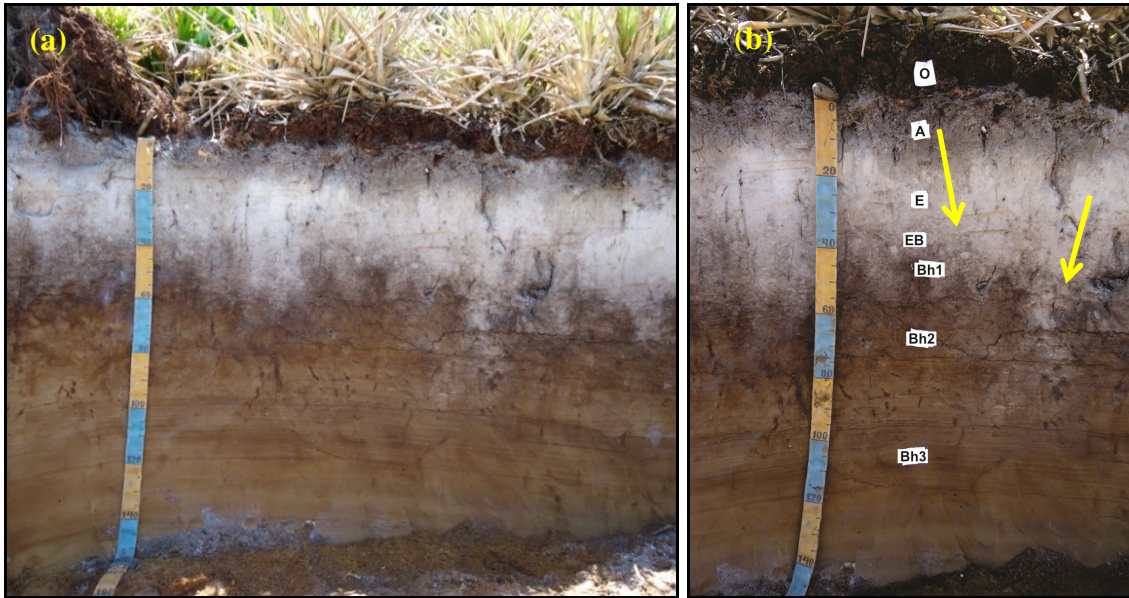
Figure 28 - Profile P11, (a) Overview. Poorly developed profile located in a cliff on the south side of Ilha Comprida; (b) Location of horizons in the profile

There are many irregular bands of OM accumulation in the Bh1 and Bh2 horizons and a few in the Bh3 horizon (Figure 28b, arrows). Many dark spots of decomposing fine roots are found mainly in the Bh1 and Bh2 horizons. The latter has larger and distinct root channels filled with decomposition products (Figure 29a).
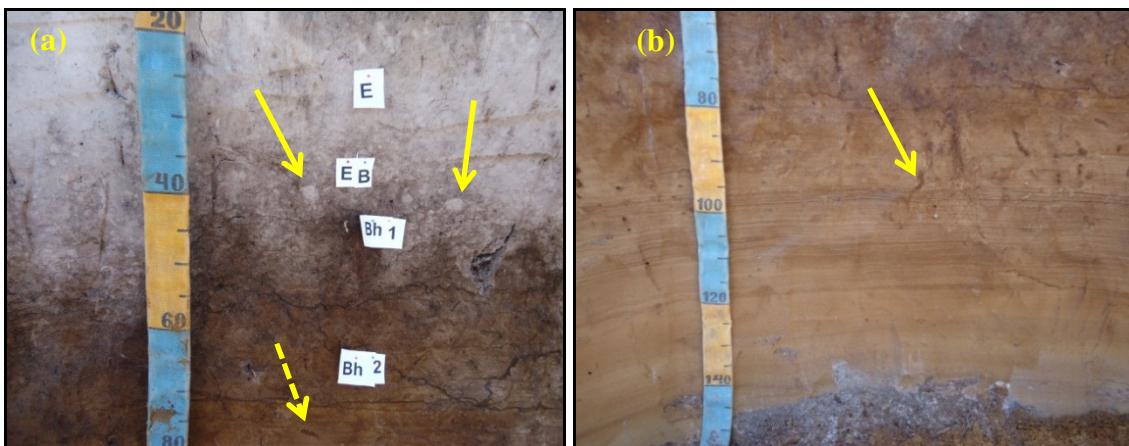
Figure 29 – Profile P11. (a) Irregular transition between EB and Bh1 horizons with many SOM-depleted mottles in the EB horizon and in the top of the Bh1 horizon (arrow) and many channels with decomposing roots in the Bh2 horizon (dashed arrow); (b) Parallel stratification in the Bh3 horizon

The transition between the E and Bh horizons is irregular and in some areas there is thickening of the E horizon in the form of tongues. The transitional EB horizon presents many small SOM-depleted mottles (Figure 29a). In the Bh3 horizon, at the base of the profile, there

is a clear parallel stratification of the sediment (Figure 29b), which is not so visible in other horizons.

Profile P37

Profile P37 is located in a profile pit 100 m inland, aligned to profiles P11 in the cliff and P38 inland. It has many bands of OM deposition and some bleached spots in the B horizon (Figure 30a).

The profile has moderate drainage (not as wet as the hydromorphic profiles previously described) without visible influence of improved drainage. OM bands that are found in part of the profile are rather irregular and probably indicate vertical rather than lateral transport (Figure 30b). This vertical transport can be seen in figure 31a, which shows a darker band at the top of the B horizon caused by the accumulation of OM around the tongues by E horizon thickening.
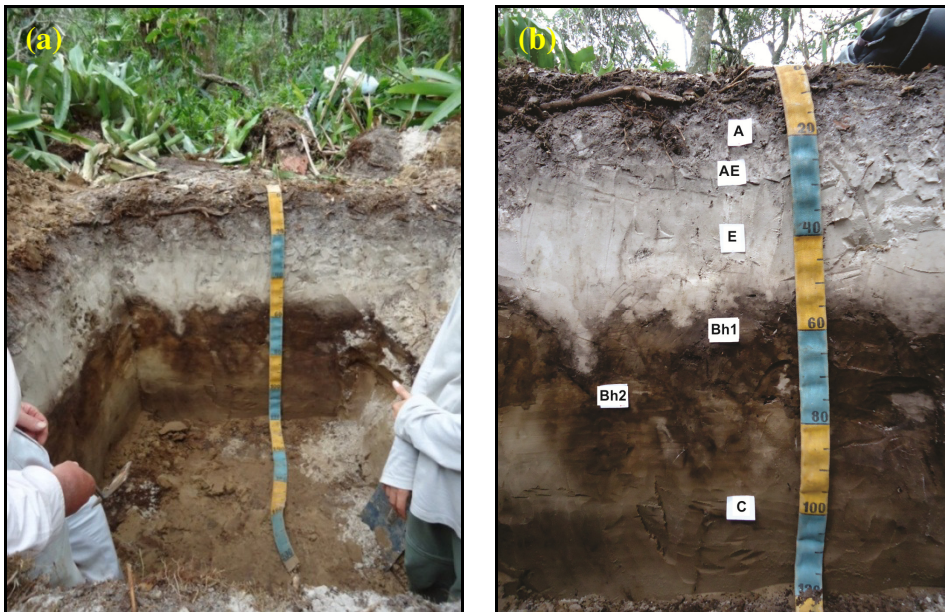
Figure 30 - Profile P37. (a) Overview. Profile with moderate drainage, a profile pit 100 m inland from the southern shore of Ilha Comprida; (b) The more darkened horizon was divided into Bh1 and Bh2. The morphology indicates vertical transport of OM without influence of lateral transport

Thicker roots are exclusive of surface horizons, while fine ones can be found throughout the profile. The vegetation that covers this area is forest with many bromeliads (Figure 31b).

Figure 31 – Profile P37. (a) Note the accumulation of organic matter in the upper portion of the B horizon (arrow) and some tongues thickening the E horizon (dashed arrow); (b) Vegetation in the area, with many bromeliads

Profile P38

This is a profile pit is located about 50 m inland from the south side of Ilha Comprida, between profiles P11 and P37. This profile presents characteristics of poor drainage at the base of the profile, but has improved drainage in its upper portion. It has many bands of OM deposition and SOM-depleted mottles along almost the full depth (Figure 32). Horizontal stratification is visible throughout the profile. The profile contains no trace of Fe.
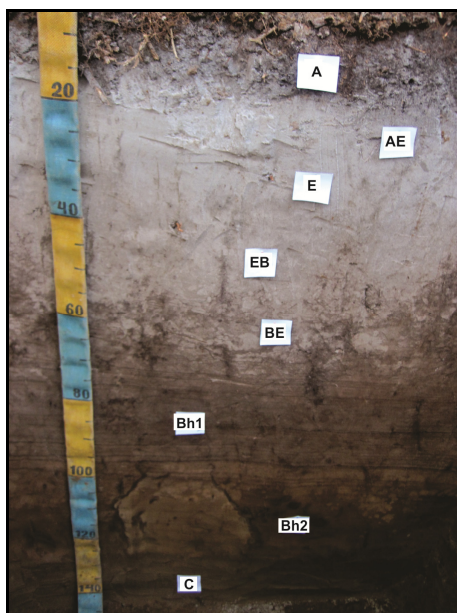
Figure 32 - Profile P38. Overview. Profile with good drainage, located in a pit about 50 m from the south side of Ilha Comprida

There are many bleached mottles throughout the profile, especially in the EB and BE transition horizons and at the top of the Bh1 horizon (Figure 33a), maybe due the improvement of drainage in the upper part of the profile.

The Bh2 horizon is darker and has few OM bands, but there are dark spots of decaying roots and a large mottle that is actually an old root channel surrounded by OM deposition. (Figure 33b). On top of the Bh2 horizon, just below the parallel lines of stratification, are many concentric SOM-depleted mottles (Figure 33c), probably different from those found at the top of the profile (EB and BE horizons and top of Bh1 horizon).

The B horizon occurs at greater depth than in profile P37. The vegetation of the site is pretty much the same as on profile P37, with many bromeliads (Figure 33d).
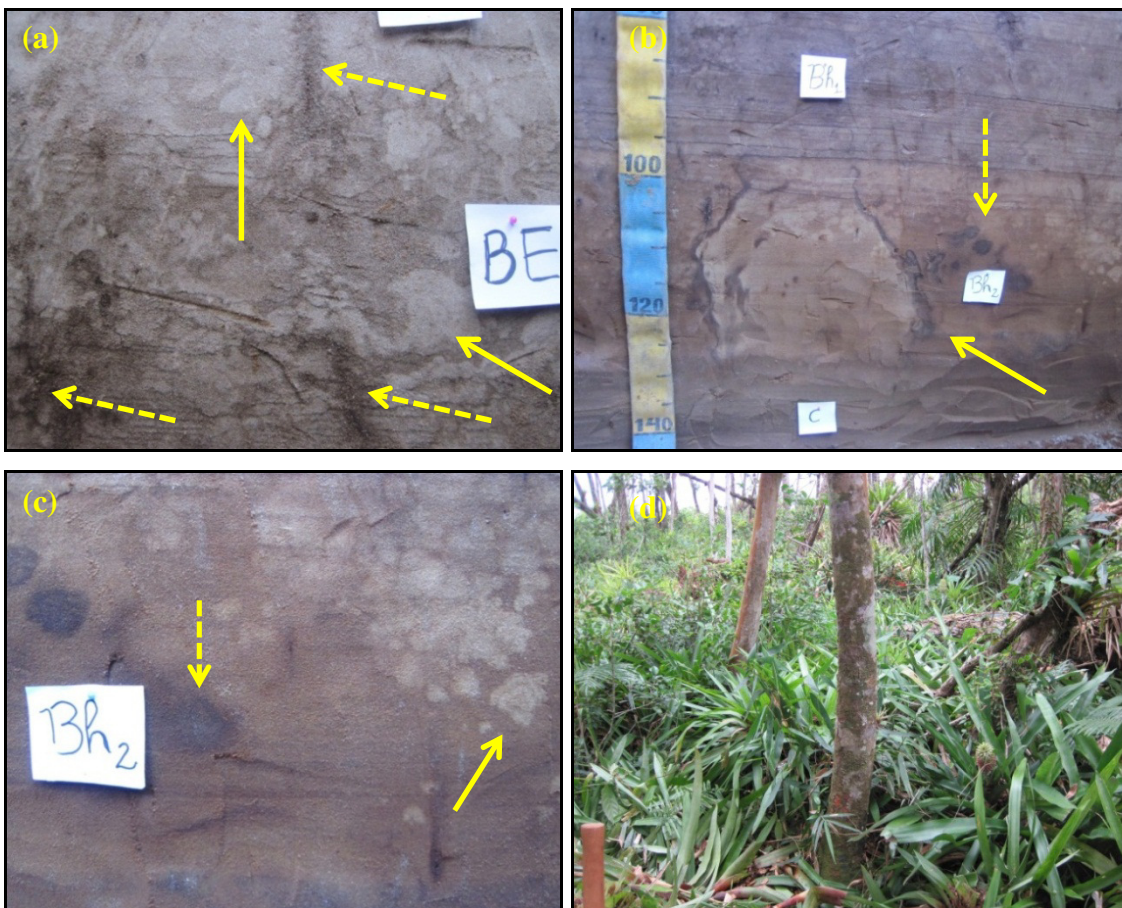
Figure 33 – Profile P38. (a) Large concentration of SOM-depleted mottles and burrows in the EB and EB horizons and the top of the Bh1 horizon (arrows) and some channels with decaying roots (dashed arrows); (b) Note the parallel stratification in the top of the Bh horizon. There is a large mottle in the Bh2 horizon (arrow), which is an old root channel that is surrounded by accumulation of OM. Small dark spots on the side (dashed arrow) are decaying roots; (c) Detail of dark spots that are decaying roots (dashed arrow) and concentric SOM-depleted mottles (arrow); (d) Bromeliad vegetation on the profile. practically the same as on profile P37

Superposed profiles

All profiles that belong to this group have buried horizons. It is possible that there has been a strong Holocene reworking of sediment in this portion of the island. This reworking may have occurred in a short period of time, under direct influence of tides.

Profiles P09 and P10 have a good drainage and are located in a cliff on the south side of Ilha Comprida, in the morphopedologic compartments III (MARTINEZ, 2015), while profile P41 is located in a cliff on the south-west side of Ilha Comprida, in the morphopedological compartments I.

Profile P09

This profile is developed in sediments overlying remnants of a strongly cemented and older B horizon (Figure 34a and b).
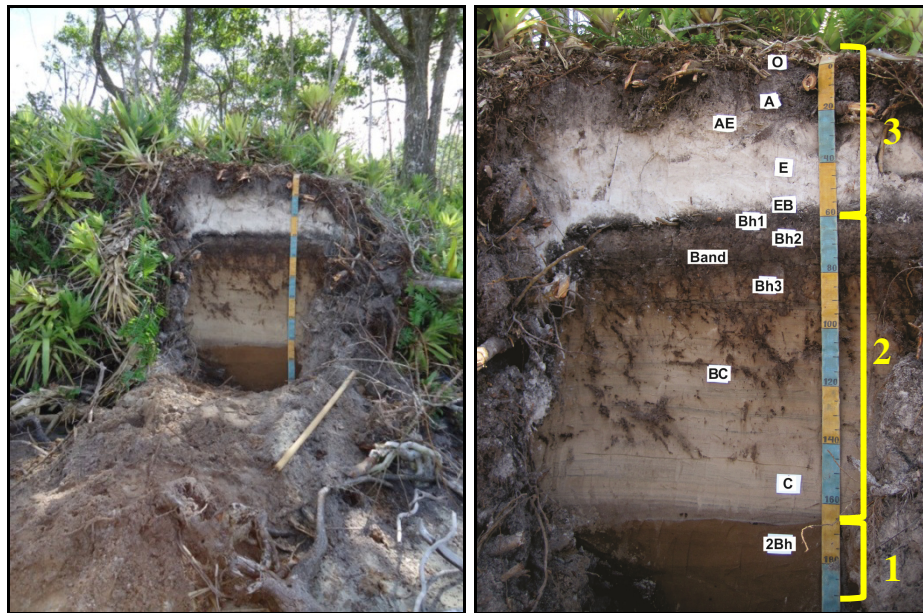
Figure 34 – Profile P09. (a) Situated in a cliff on the south side of Ilha Comprida. A rather shallow well-drained profile with a buried hydromorphic B horizon at its base; (b) Location of horizons in the profile. The yellow numbers indicate the three phases of soil formation

The designation of the B horizon in the upper profile is somewhat problematic (Figure 35a). It presents a darker band in the upper horizon (Bh1, Bh2 and Bh3), followed by a gray horizon (C) and again a darker band in the lower portion (2Bh). It is possible that the horizons Bh1, Bh2 and Bh3 represent a former surface horizon (with abundant decaying roots), which

was covered by a rapid accumulation of sand and later converted into a B horizon. The profile then shows three phases of soil formation (Figure 34b).

There are many layers of darker mineral sand in almost the entire profile, except the 2Bh horizon (Figure 35b). The latter has a high concentration of OM and is apparently without stratification. The dark color of the sand is due to an abundance of the opaque heavy minerals ilmenite and magnetite (MARTINEZ, 2015). Among the non-opaque heavy minerals that occur in the horizon are: zircon, tourmaline, staurolite, rutile and epidote. This mineralogical assemblage was identified in various parts of the island (GIANNINI et al., 2009). Such concentrations of heavy minerals are locally common on the present shore and are due to wave action.

There is no evidence of SOM-depleted mottles or burrows of ghost-shrimp in this profile. The material constituting the E horizon (Figure 35c) does not have apparent stratification.
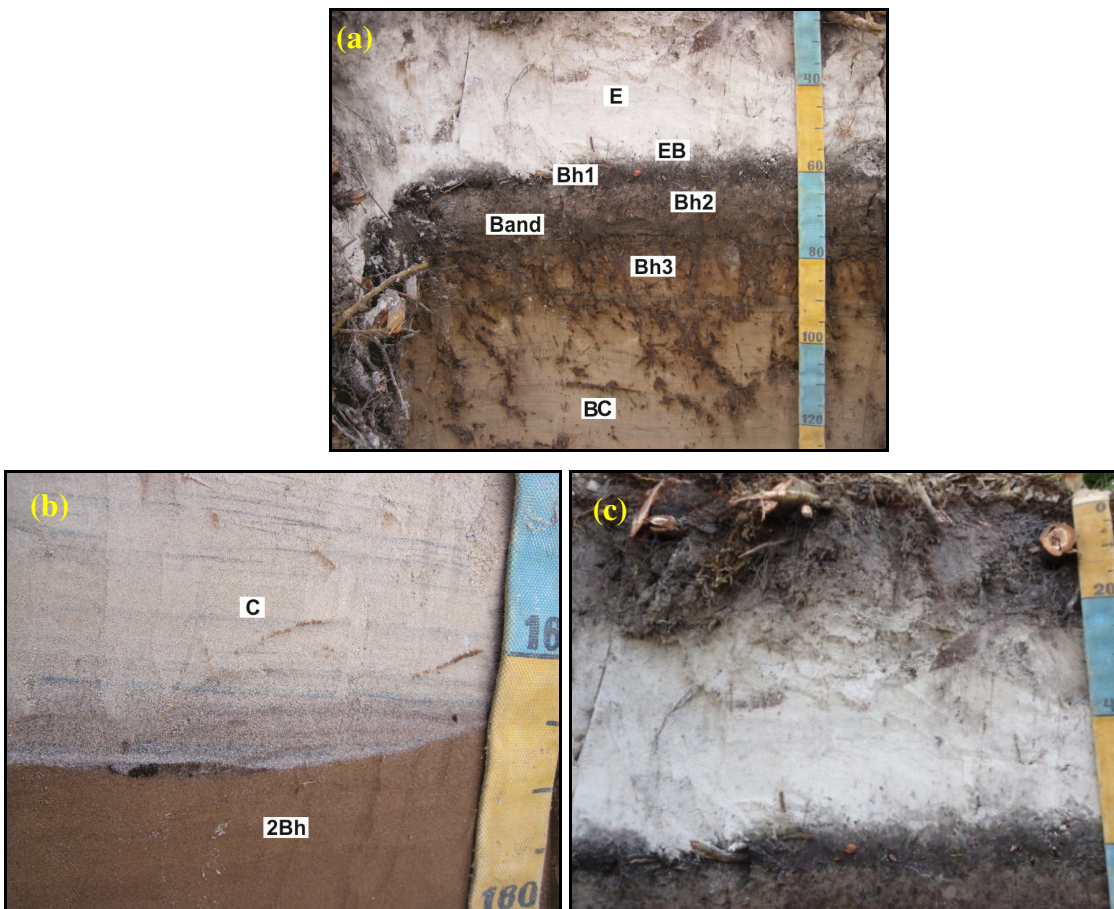
Figure 35 – Profile P09. (a) Horizons Bh1, Bh2 and Bh3, which may be remnants of buried surface horizons, as suggested by the abundance of decaying roots; (b) Contact between horizons C and 2Bh, showing the presence of parallel layering with bands of dark sand in the C horizon; (c) E horizon without apparent stratification

Profile P10

This is weakly developed profile, well-drained, with roots throughout the B and BC horizons.

This profile also shows a discontinuity at the base of the profile, different from that of Profile 09. There are small rounded blocks of eroded and cemented B horizon material above the discontinuity. The upper portion of the profile developed in sediments that overlie the eroded 2Bhm horizon (Figure 37a). Just overlying the eroded profile, there is a buried tree trunk, which clearly belongs at the contact (±1,530 years) (Figure 36). Currently, loose blocks of the cemented older B horizon are found on the adjacent beach (Figure 37b).
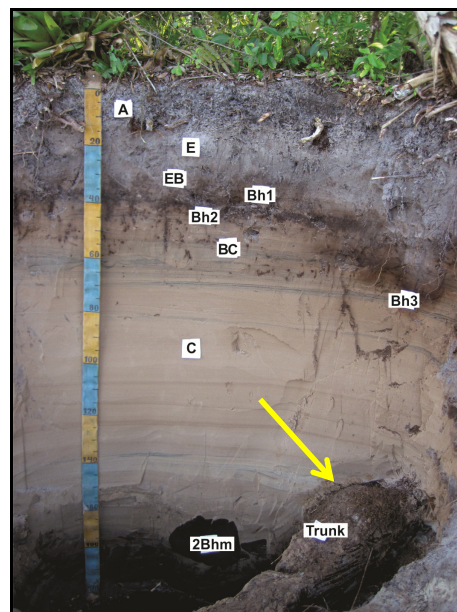
Figure 36 - Profile P10, overview. Profile located in a cliff on the south side of Ilha Comprida. The bottom layer contains rolled remnants of a cemented, earlier Bhm horizon (2Bhm). Boulders of this 2Bhm are often found at the base of actual cliffs; Buried wood trunk at its base the profile (arrow)

The top of the profile is developed in horizontally stratified sediments that contain bands with dark minerals (Figure 37c, dashed arrow). The B horizon has different sources of OM. In the Bh1 and Bh2 horizons it is presumably derived from the roots, while in the Bh3 horizon local DOM appears to be the source. The Bh1 and Bh2 horizons probably do not have illuvial OM (Figure 37d), but mainly root-derived OM. In some parts below the B horizon, there appears to be a local accumulation of recent and local DOM, probably accompanying a root channel (Figure 37c) forming the Bh3 horizon.

There is no evidence of depletion mottles, burrows, or galleries of ghost-shrimp in this profile. There is a large block of cemented Bhm material on the beach, probably the same material found in the base of the profile (Figure 37e).

Figure 37 – Profile P10. (a) Rounded blocks of eroded, cemented Bhm horizon at the base of the profile; (b) Strip of beach with some loose blocks of rounded and cemented Bhm horizon; (c) Lines of dark sand in the profile (dashed arrow) and development of a B podzol horizon with recent accumulation of local DOM in the form of a tongue accompanying a root channel (arrow); (d) Bh1 and Bh2 horizons are mainly formed by the decomposition of local roots; (e) Block of cemented 2Bhm-material on the beach

Profile P41

In this location there are two (or more) superposed profiles (Figure 38a), developed in subsequent sediments. Profile P41 is located in the upper portion of the cliff and shows a large vertical variation with distinct layers of sandy sediments. It is developed under hydromorphic circumstances and shows lateral accumulation of SOM (Figure 38b). Under the B horizon is a thick layer of black sands.
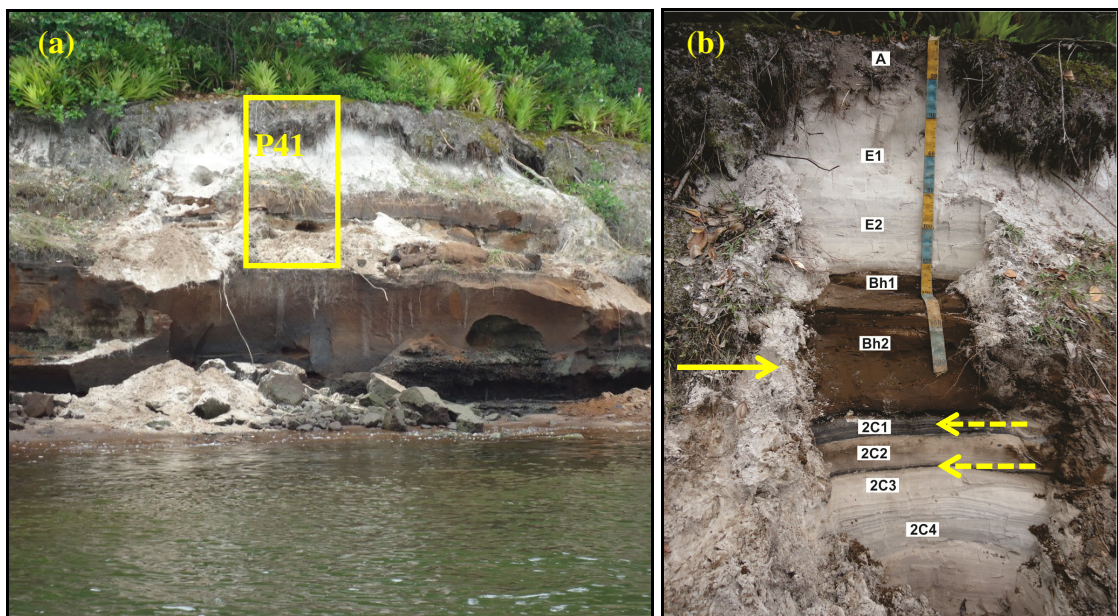
Figure 38 -Profile P41. (a) Overview. Located in a cliff on the south-west side of Ilha Comprida. The yellow rectangle delimits described profile P41; (b) Note the B horizon (arrow) and the layer of black sand (dashed arrow). The tape is two meters long.

Remnants of a - partially eroded - strongly cemented B horizon are found at the bottom of the profile. This B horizon is probably equivalent to that of profiles P01 and P04 at the south – west corner of Ilha Comprida. On this eroded B horizon, new layers of sediment have been deposited, that later developed a new B horizon.

There are abundant thin and medium roots in the A horizon, but there are no traces of roots in the other horizons. The transitions between almost all horizons are smooth, but some may be slightly inclined. The E2 and 2C4 horizons contain lines of black sand and the 2C1 horizon consists almost entirely of black sands.

Psamment

Profile 39

This profile is located in the cliff on the most recent part of the Holocene barrier island studied, on the morphopedological compartment V (MARTINEZ, 2015) very close to the the Atlantic Ocean. This profile was classified as a Psamment and was the youngest one sampled (Figure 39a). It does not have signs of podzolisation.
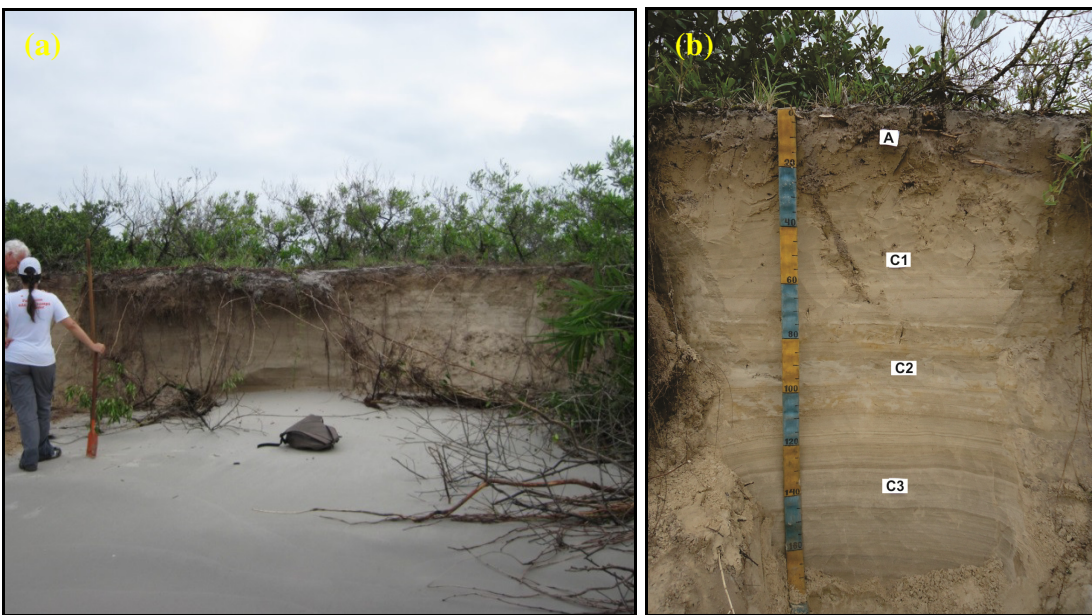
Figure 39 - Profile P39. (a) Overview. Profile very well drained, under incipient scrub vegetation and located in a cliff on the south side of Ilha Comprida, close to the Atlantic Ocean; (b) Profile showing undisturbed intense thin plane-parallel stratification

This profile has lines of parallel stratification (Figure 39b). Thick and medium roots occur exclusively in the upper portion of the profile, but traces of fine roots can be found throughout the profile. There is a layer in the middle of the profile with many spots of oxidation and depletion of Fe, indicating a higher concentration of this element and good drainage of the profile. At the basis of the profile, thick (2 to 10 cm) bands of dark sand (heavy minerals) were found.

2.3.4 Description of depletion mottles

According Buurman et al. (2007), some well-drained podzols have OM-depleted mottles that are mainly associated with root channels. The phenomenon is widespread in the

Netherlands and neighboring Belgium and Germany, and such depletion mottles have even been observed in recently exposed fossil podzols of Tertiary age (BUURMAN et al., 2007).

Of the seventeen profiles studied here, thirteen have depletion mottles scattered along the profile. Most of these mottles are whitish and are located preferentially in the horizons of transition between the E and B horizons, particularly in conditions of good drainage. These mottles have clear morphological differences. They may be grouped according to similarities in their morphology and their position in the profile, creating distinct groups of mottles.

The following item describes the differences of the mottles through purely morphological characteristics.

Concentric OM-depleted mottles

This first type of mottle shows concentric structures with an alternation of whitish and darker bands. Such mottles are sometimes fan-shaped, with the flat side at the bottom. Considering that what we see is a two-dimensional cross section, the three-dimensional shape may be mushroom-like. In some profiles (e.g. P04, Figure 40a) the concentric structures can be circular. The shape is probably influenced by sedimentary stratification.

Sometimes, these mottles are extremely whitish (e.g. P01, Figure 40b), while at other times they are just a little lighter than the soil matrix (Figure 41). Concentric mottles are identified in the upper portions of the B horizon, where there is probably a larger supply of air and OM accessible to microorganisms. The concentric OM-depleted mottles were clearly visible in the profiles that previously formed under hydromorphic conditions (P01, P04 and P38) and in the bottom of well-drained profile P30.
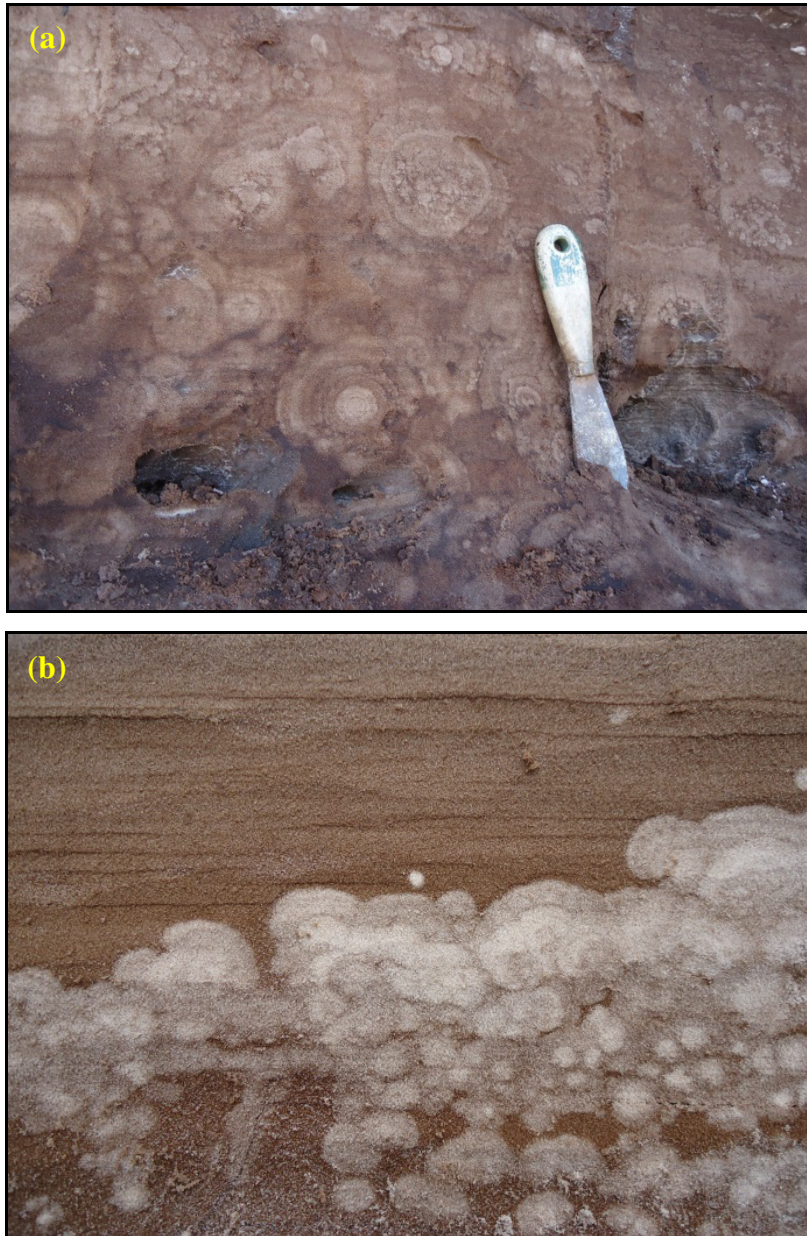
Figure 40 - (a) Profile P04. Concentric OM-depleted mottles, forming complex patterns, found at the top of the B horizon, in the cliff next to profile P04; (b) Profile P01. Cluster of concentric OM-depleted mottles with the appearance of small mushrooms, very whitish, found in Bh2 horizon (200 cm)

In profile P04, only one mottle of this type was identified; it was about 20 by 30 cm and located in the Bhm2 horizon (180 cm). Its color was just a bit lighter than the matrix (Figure 41). Already in profile P01, we found multiple mottles of this kind, but unlike the one found in profile P04, they are whitish and smaller. In profile P01 the concentric OM-depleted mottles were identified in the top of Bh2 horizon (200 cm), where they form a sort of horizontal line which appears to follow the sedimentary stratification (Figure 42a).

Figure 41 - Profile P04. Concentric OM-depleted mottles with color slightly lighter than the matrix. The concentric lines were developed mainly toward the top of the profile

In profile P30, some of concentric OM-depleted mottles were found also in the Bh2 horizon (120 cm) (Figure 42b), which are very similar to concentric OM-depleted mottle found in profile P04, but of smaller dimensions.

In profile P38, concentric OM-depleted mottles were identified in the Bh2 horizon (110 cm), but slightly less regular than those found in other profiles. Concentric lines are visible in some mottles in this profile (Figure 43).

The differences in coloration and size of concentric OM-depleted mottles may be related to the selective depletion of OM in the soil.

The concentric mottles are supposed to have formed by expansion of a bacterial colony that started at the centre.
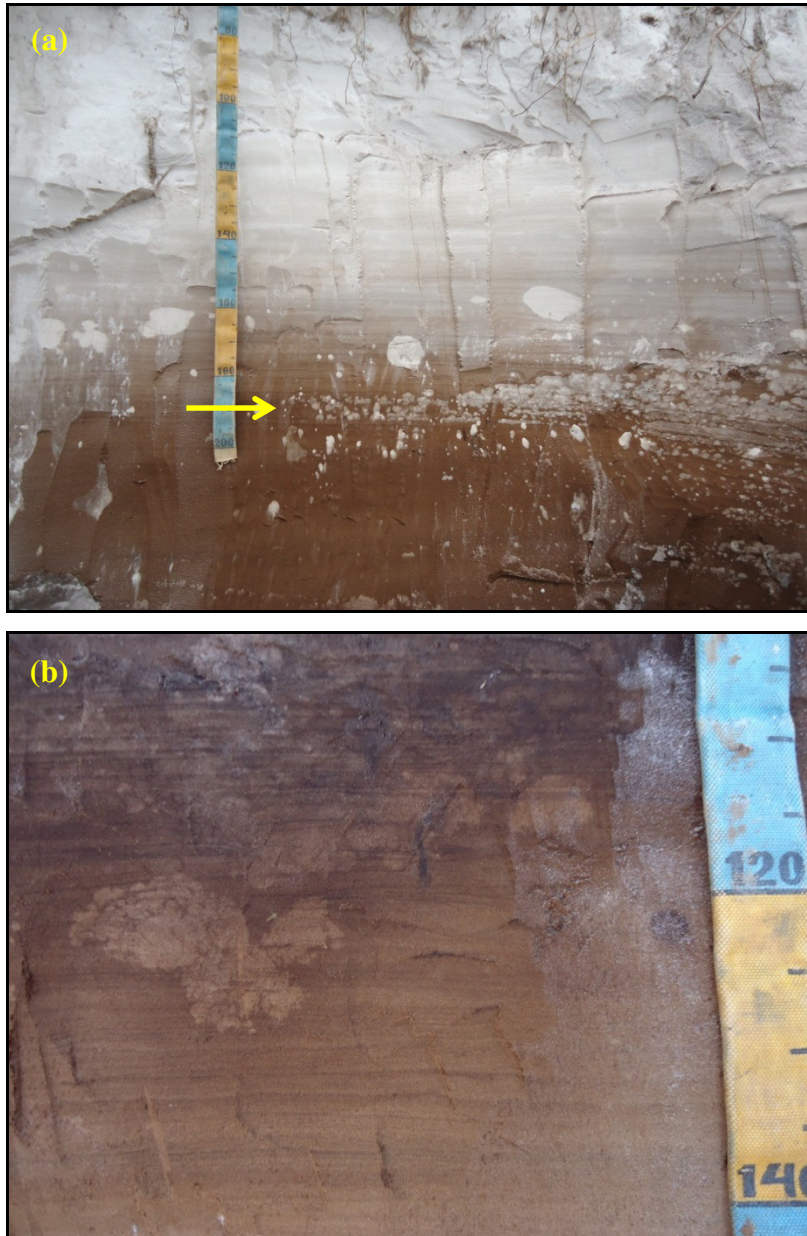
Figure 42 – (a) Profile P01. Concentric OM-depleted mottles appear to follow the sedimentary stratification (arrow); (b) Profile P30. Concentric OM depleted mottles with a color slightly lighter than the matrix, found in the Bh2 horizon
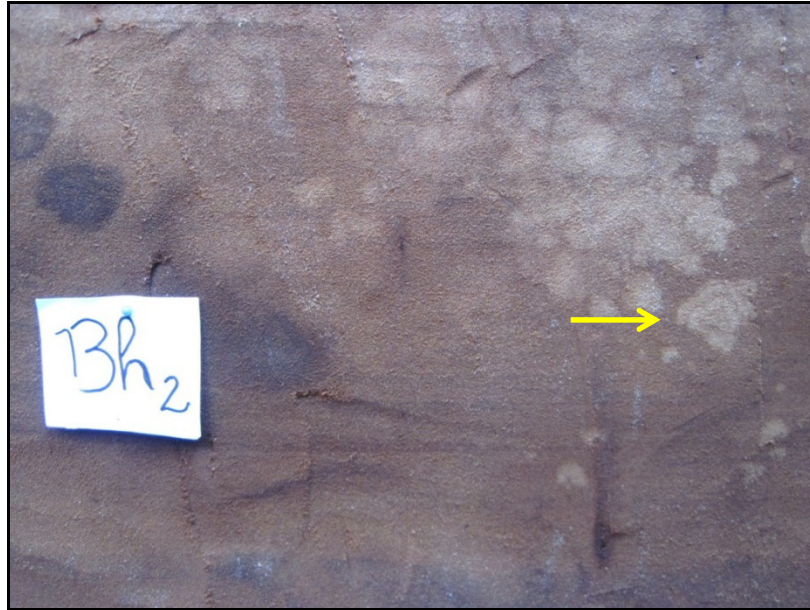
Figure 43 - Profile P38. Slightly irregular concentric OM-depleted mottles (arrow)

Circular/tubular OM-depleted mottles (burrows)

Another type of mottles that can be morphologically identified is those having a circular and / or tubular form. This type of mottles was detected in almost all profiles that have mottles. They occur preferentially in the transitional EB and BE horizons, but some were found on top of the B horizon in some profiles.

It is possible to distinguish more whitish mottles, such as those occurring in the P01 profile (Figure 44a), and some more diffuse, with color only slightly lighter than the matrix (Figure 44b). Generally, these mottles are not very large, measuring from 1 to 4 cm. They are frequently found in large concentrations, hindering the identification of their boundaries.
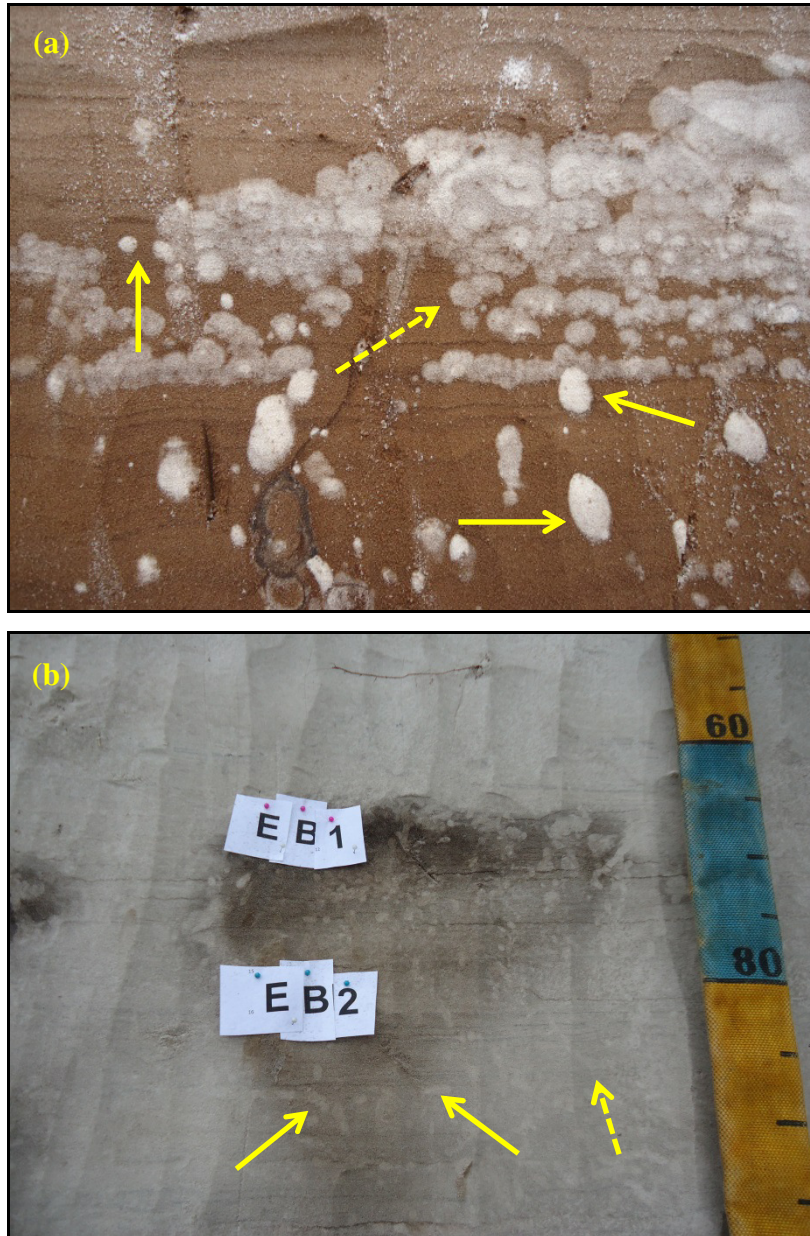
Figure 44 – (a) Profile P01.Very whitish circular and oval mottles (arrow) and concentric OM-depleted mottles (dashed arrow); (b) Profile P02. Circular/tubular OM-depleted mottles with colors only slightly lighter than the matrix (arrow). Some of these tubular mottles resemble animal burrows (dashed arrow)

The variation in the shape of these mottles (circular, oval or tubular) mainly depends on the way they are cut. The boundaries are clear. Some mottles resemble animal burrows (Figure 44b, dashed arrow). It is possible that some of these mottles have been actually burrows of animals (like the maggot of *coleoptera* insect found in the cliff located at the west side of the Ilha Comprida, Figure 46) or root channels that were subsequently colonized by microorganisms.

In some cases these mottles are found in chaotic clusters (Figure 44b) and in others they appear to follow the stratification of the sediment (Figure 45a) and/or bands of DOM accumulation (Figure 45b). It is unclear why this occurs.
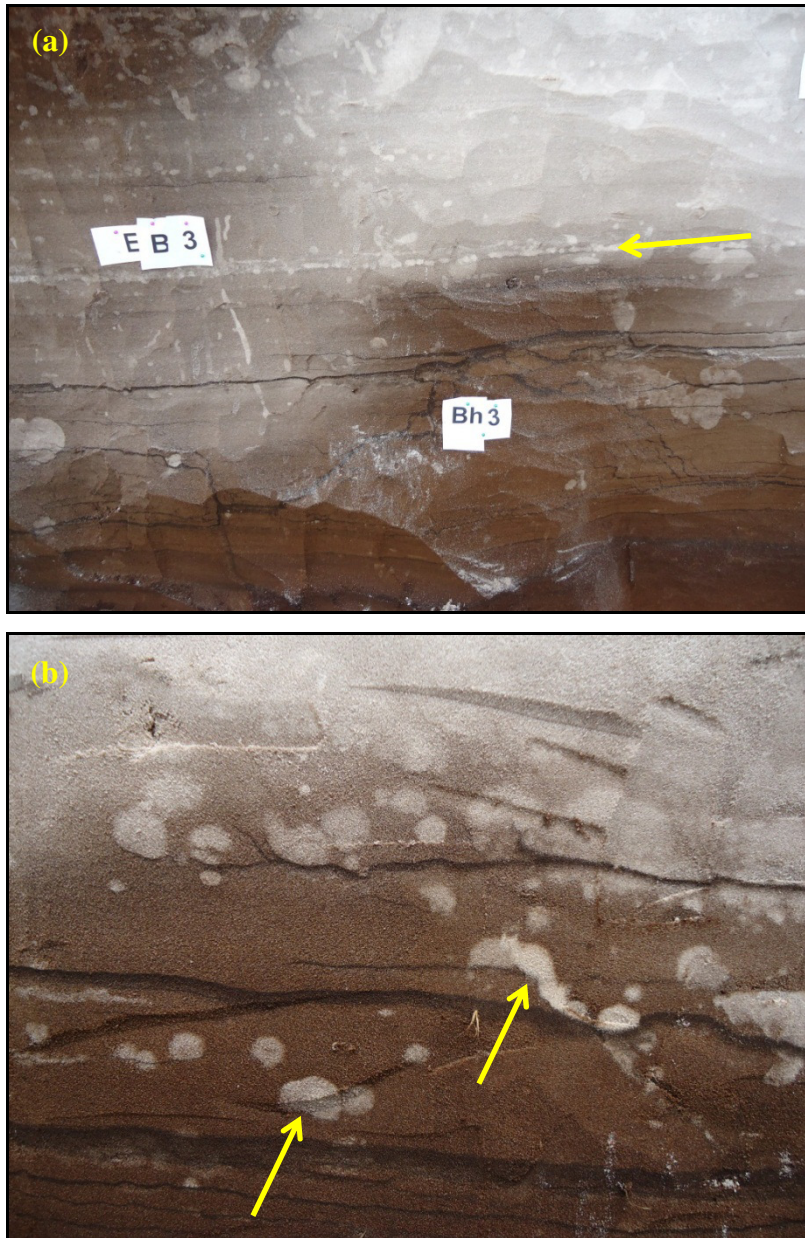
Figure 45 – (a) Profile P02. Circular / tubular mottles aligned with the sedimentary stratification (arrow); (b) Profile 40. Circular/tubular mottles (arrow) with DOM-bands

Figure 46 – (a) A maggot, probably of coleoptera, found in a cave in the cliff; (b) Note the lighter colors of the burrows (Photo: Diego L. Nascimento)

Dotted OM-depleted mottles

In some profiles large quantities of very small circular mottles have been identified. They occur very close to each other, forming a kind of dots in the soil. They were found only in hydromorphic profiles P01, P40 and P41 (Figures 47a and b).

The dotted OM-depleted mottles were identified in the Bh2 horizon (230 cm) of profile P01, the Bh3 horizon (130 cm) of profile P40 and the Bh2 horizon (160 cm) of profile

P41. Perhaps the dotted OM-depleted mottles are an early stage of development that this evolves into another type of mottle.
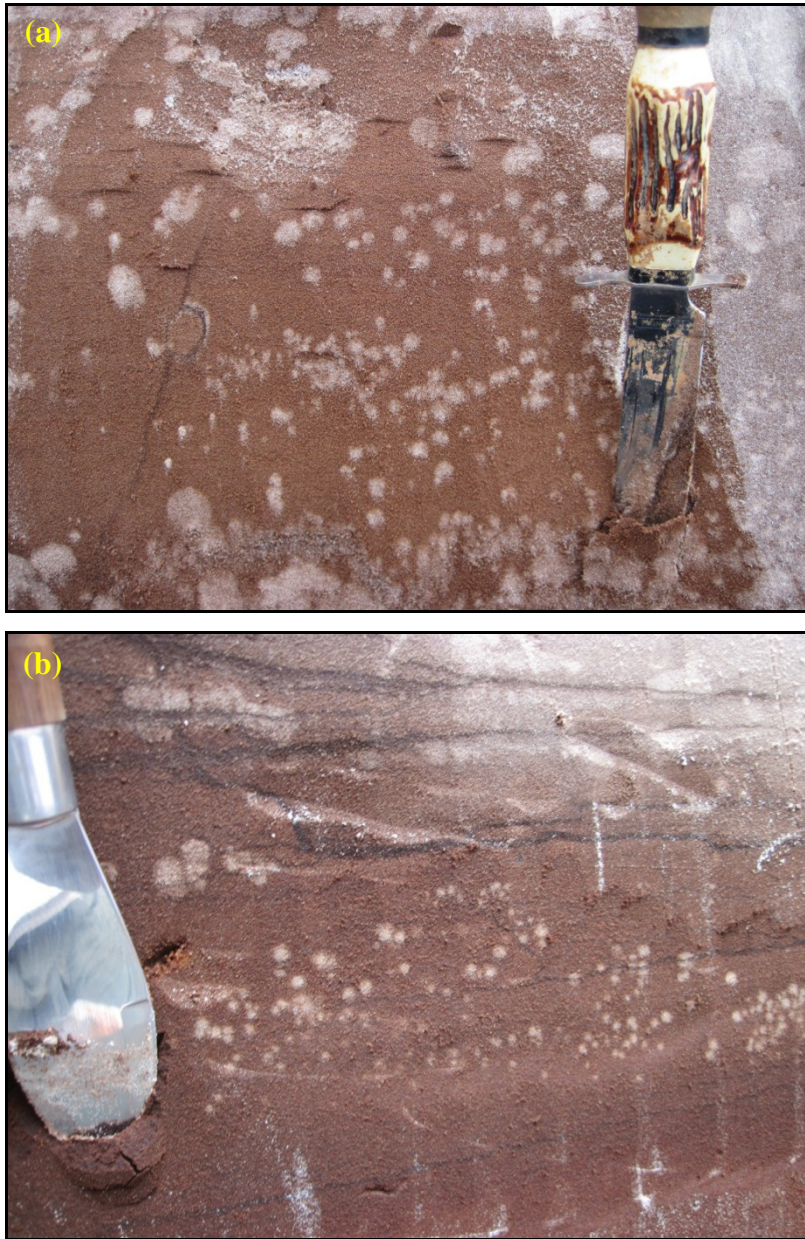
Figure 47 – (a) Profile P01. Dotted OM-depleted mottles found in the Bh2 horizon (230 cm); (b) Profile P40. Dotted OM-depleted mottles found in the Bh3 horizon (130 cm)

Ghost OM-depleted mottles

A peculiar type of mottle was identified in profiles P04 and P31 (Figures 48a and b). These mottles have a shape that resembles a viscous liquid flowing on a vertical surface. They

have a whitish coloration and are whiter at the top of the mottle, while the color contrast disappears downwards until merges with the soil matrix (Figure 48, arrow).

They may be a combination of two types of mottles, one of them lighter than the other. If we look more closely, the fading of the mottle toward its base may indicate that their formation proceeds in this direction.
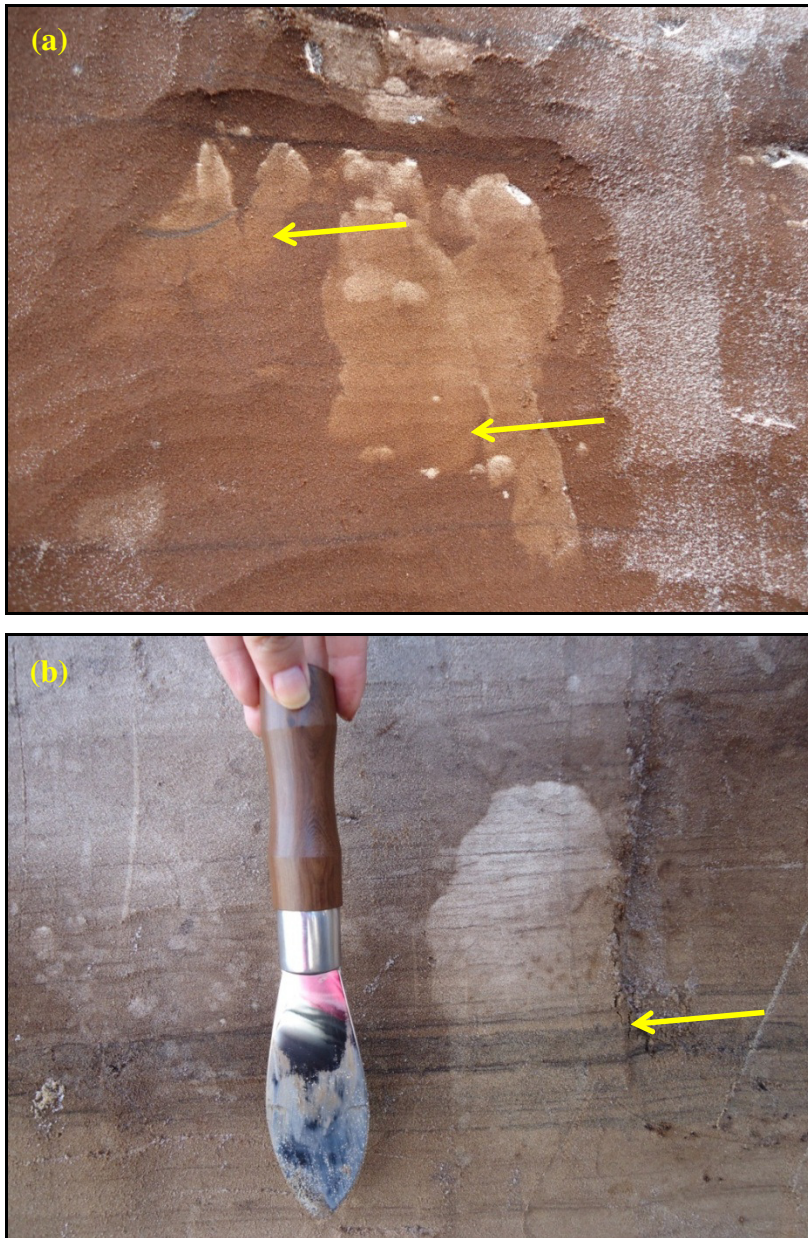
Figure 48 – (a) Profile P04. Mottle fading towards the base of the profile, found on the Bhm1 horizon (170 cm); (b) Profile P31. Ghost OM-depleted mottle in the Bh2 horizon (110 cm). Note that the sedimentary stratification does not present a barrier to the development of the mottle (arrow)

Just like the concentric OM-depleted mottles and circular/tubular OM-depleted mottles, these are linked to the top of the B horizon, where there is an improvement in drainage and consequently a larger air supply for the microbial OM-decomposers.

In profile P04 some of ghost OM-depleted mottles were identified in the Bhm1 horizon (170 cm) (Figure 49), clearly higher in the profile than the concentric OM-depleted mottles in the same profile and below the other mottles (circular / tubular and irregular). In profile P31, ghost OM-depleted mottles were identified in the Bh2 horizon (110 cm) below the other mottles (Figure 50). Concentric OM-depleted mottles were not identified in this Profile.

Apparently the development of the ghost OM-depleted mottles is not influenced by sedimentary stratification. The ghost OM-depleted mottle identified in P31 profile passes through one evident line of dark sand, which appears not to establish a barrier to its development (Figure 48b, arrow).
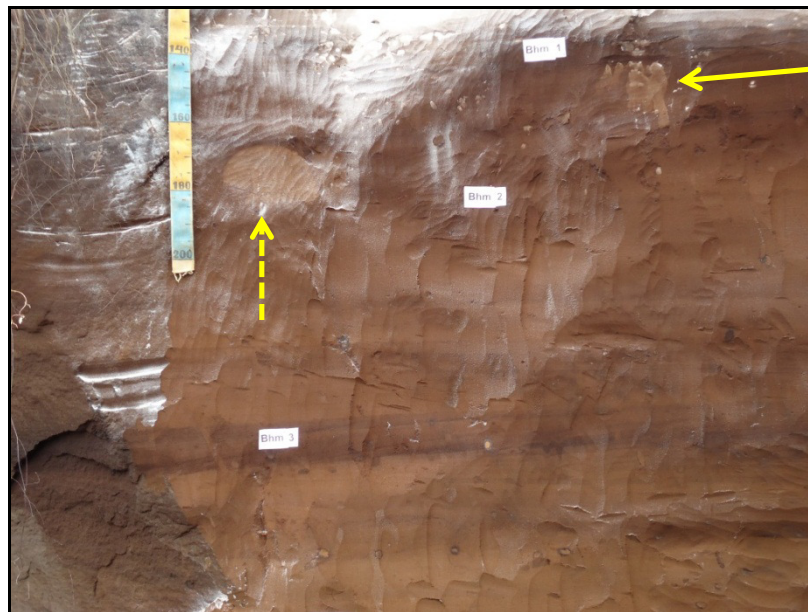
Figure 49 - Profile P04. Ghost OM-depleted mottles (arrow) higher in the profile and distant from concentric OM-depleted mottles (dashed arrow)

Figure 50 - Profile P31. Ghost OM-depleted mottles (arrows) below other mottles

Irregular OM-depleted mottles

Of all the mottles identified here, among the most common are mottles with irregular boundaries (Figure 51a). They are usually whitish and have an irregular or half rounded shape. In some cases they have very distinct boundaries with the soil matrix and in other cases they are difficult to identify (Figure 51b). They have a large variation in size and shape (Figure 52a). Some are more whitish, such as those in profile P01 (Figure 51a), and some have a color slightly lighter than the soil matrix, as in profile P40 (Figure 52b).

Sometimes, irregular mottles are related to DOM-bands and stratification of the sediment, and they may form distinct rows. In some profiles these mottles, were found on top of OM-bands, often following the irregularities of these bands (Figure 52b). It is possible that irregular mottles are due to coalescence of other types.
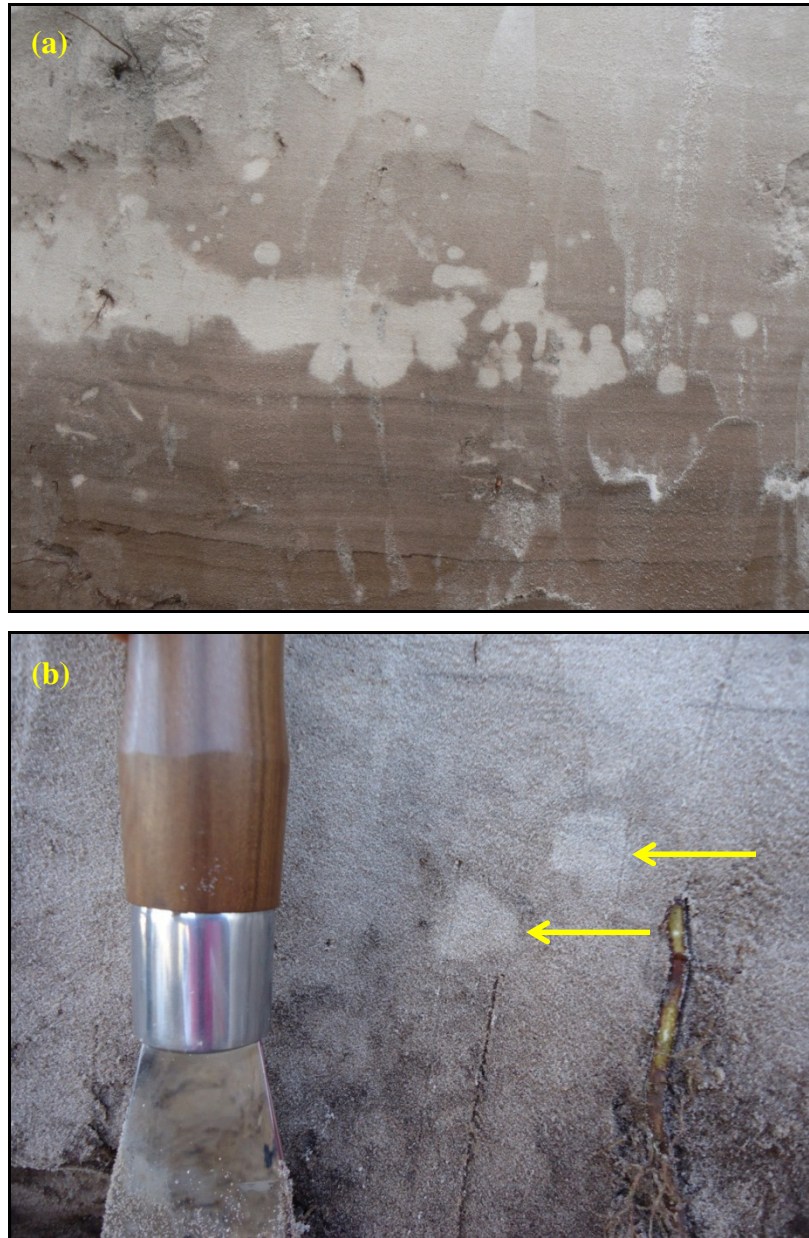
Figure 50 - (a) Profile 01. Whitish irregular mottle; (b) Profile 31. Irregular OM-depleted mottles with color slightly lighter than the soil matrix (arrow), with diffuse boundaries

These mottles are clearly associated with the circular/tubular OM-depleted mottles and, as the latter, are found in large quantities in some profiles, so that individual mottles are difficult to identify. Like the circular/tubular OM-depleted mottles, the irregular OM-depleted mottles are mainly associated with the transitional EB and BE horizons. In some profiles it is possible to distinguish this type of mottle in the E horizon. (Figure 53).
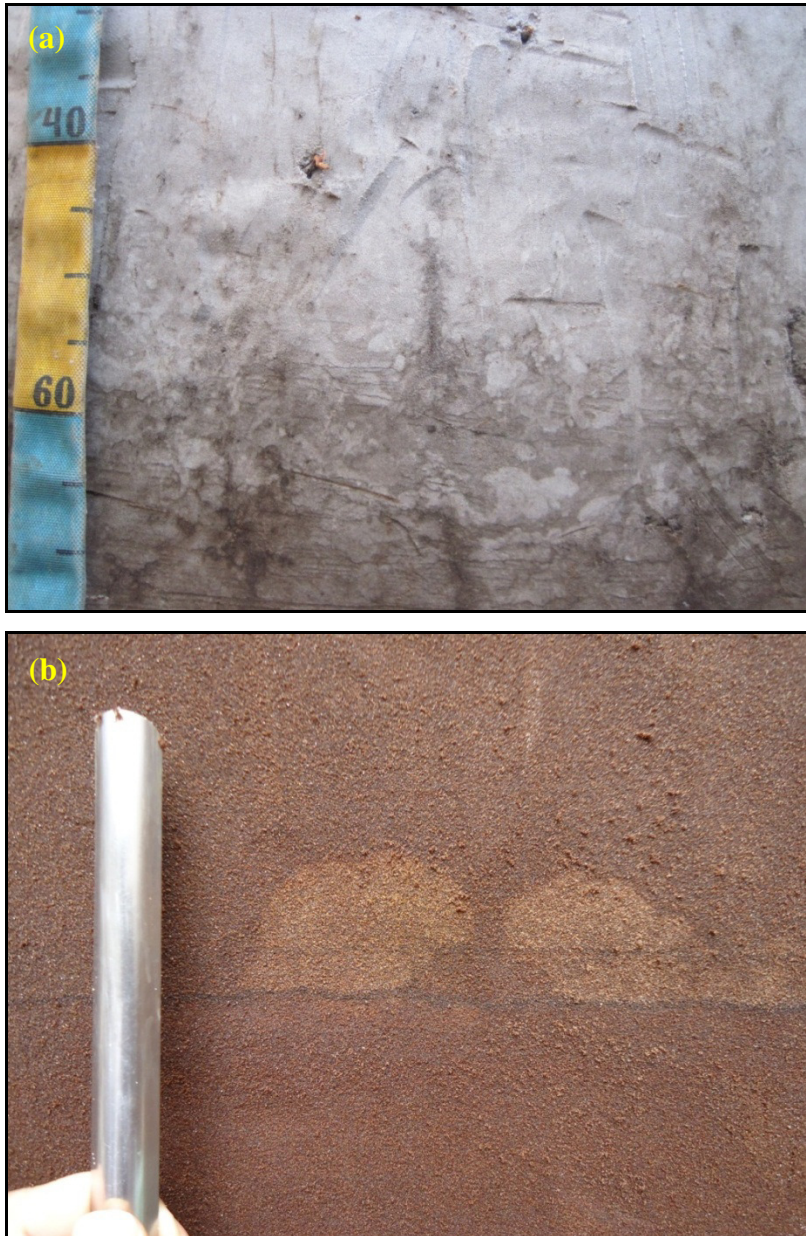
Figure 52 – (a) Profile 38. Large variety of irregular OM-depleted mottles in the EB horizon; (b) Profile 40. Irregular OM-depleted mottles on an OM-band, in the Bh2 horizon. Their coloring is just a little lighter than the soil matrix
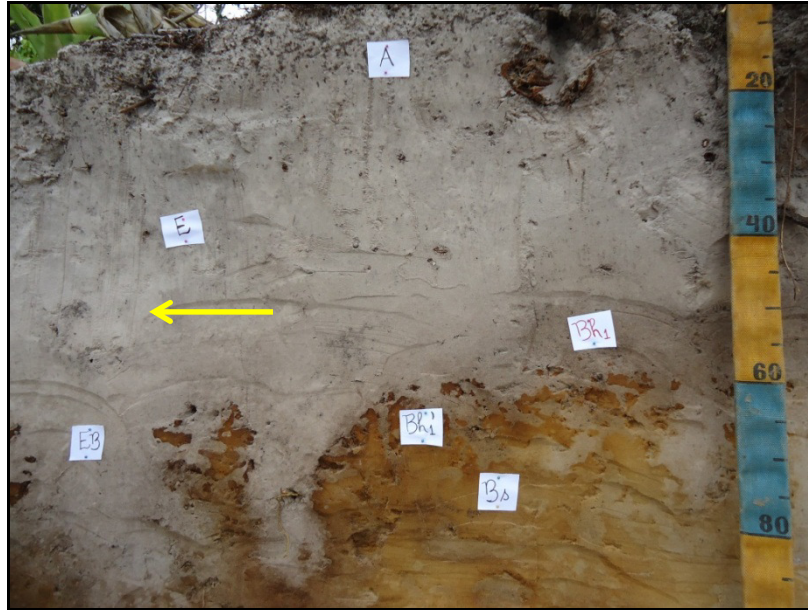
Figure 53 - Profile 35. Irregular OM-depleted mottles identified in the E horizon (arrow)

Fe-depleted mottles

In the lower part of profiles P32, P34 and P35 it is possible to distinguish a type of whitish mottle that is related to the depletion of Fe (Figure 54a).

These mottles have irregular boundaries, and occupy much of the C horizon of the profile (Figure 54b). These mottles are not related to decomposition of OM, like all other mottles that are described previously, but to removal of Fe compounds through reduction.
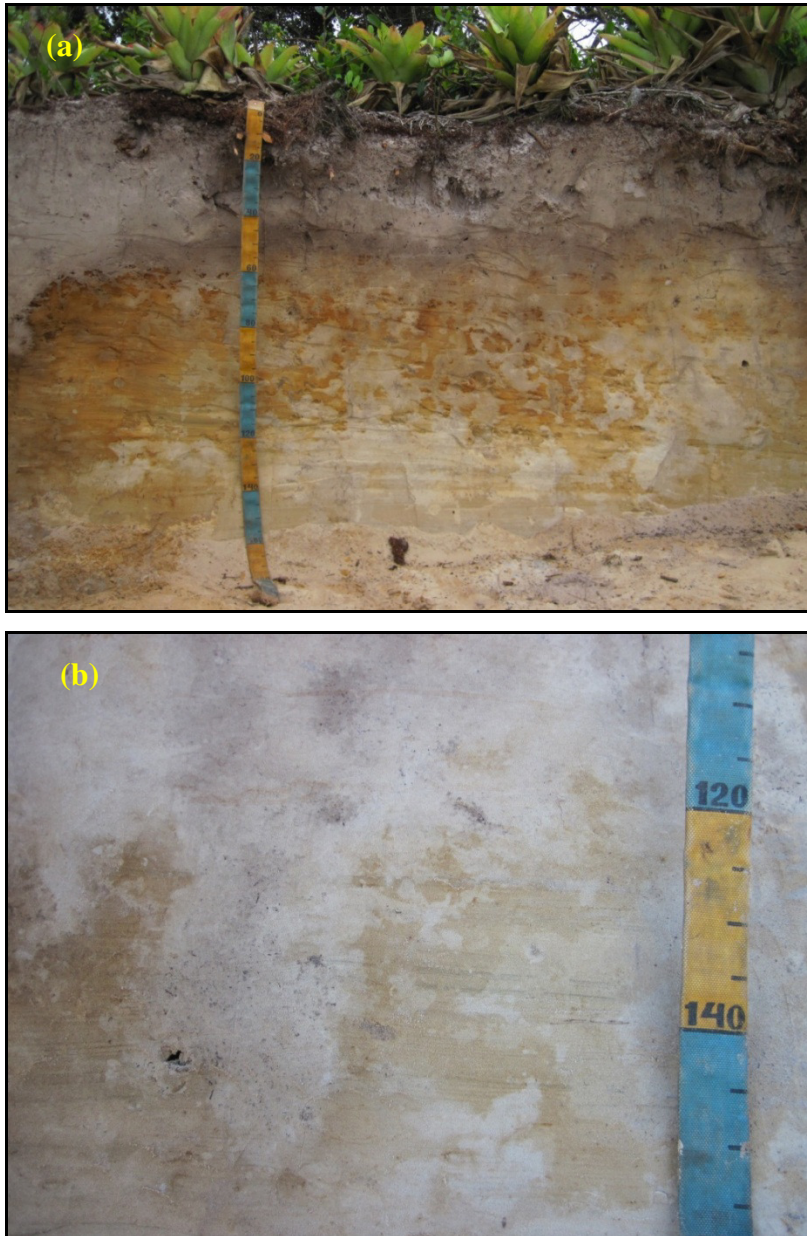
Figure 54 – (a) Profile 35. Profile with Fe-depleted mottles; (b) Profile 32. C horizon with Fe-depleted mottles

2.4 Conclusions

The poorly-drained profiles have the following similarities: (a) presence of many bleached SOM-depleted mottles at the top of the B horizon and some concentric SOM-depleted mottles in the Bh horizon; (b) *Chalicchirus major* galleries at the base of the oldest profiles P01, P02 and P40; (c) many dark SOM accumulation bands, principaly in the top of B horizon and base of the E horizon; (d) presence of cemented B horizon (Bhm) at the base of the profile; (e) strongly expressed podzol B-horizon in general. Morphology indicates that these profiles are disintegrating, with decomposition of the top B horizon and growth e of the

E horizon. Thus, the improved drainage at the top of the B-horizon and consequent influx or activation of microorganisms causes its decomposition.

Already the well-drained profiles has, in summary: (a) many SOM-depleted mottles at the top of B horizon and EB-BE horizons; (b) present a thin thickness B horizon, and especialy in wave format; (c) more roots and old roots channels than the poorly-drained profiles; (d) some Fe-depleted mottles. These profiles are more young than poorly-drained ones (MARTINEZ, 2015), and are very similar to each other.

The strongly rooted profiles has: (a) present a thin B horizon, but some influence by DOM, mainly at the base of B horizon and some old root channels; (c) many roots and channels; (d) has dark SOM accumulation bands; (e) many SOM-depleted mottles at the top of B horizon and EB-BE horizons and some at the lower part of profile. In summary, these profiles have good drainage, but are still influenced by DOM of the ground-water flow.

The superposed profiles has a special particularity: presence of two or more discontinous phases of soil formation. These profiles are developed in sediments overlying remnants of a strongly cemented and older B horizon (formerly poorly drained).

The detailed soil morphology description and analisys were essential to discriminate genetic groups of podzol profiles.

Most of the mottles described here are related to OM decomposition by microorganisms, leaving whitish (or with a color slightly lighter than the soil matrix) mottles of many different shapes and sizes. All seem to be related (mainly) to the improved drainage at the top of the profile, and occur mainly in larger quantities in transitional EB and BE horizons and in the top of the B horizon. They are virtually nonexistent in the deep horizons. This decomposition at the top of the B horizon results in thickening of the E horizon.

As already discussed, some of these mottles are related to root channels, sedimentary stratification and OM-bands found. They may form distinct horizontal bands. Almost all types of mottles described above, with the exception of ghost OM-depleted mottles, were found both in profiles in the cliff and in the inland pit profile. But the inland pit profiles have fewer mottles than the profiles of the cliff. Thus, we conclude that there is some influence of exposure to air (as occurs in the profiles of the cliff) on the establishment of the microorganisms that decompose the OM in the profile. In any case, the presence of mottles appears more related to improvement of drainage on the top of the B horizon in the soil.

References

BUURMAN, P.; VIDAL-TORRADO, P.; LOPES, J.M. The podzol hydrosequence of Itaguaré, São Paulo, Brazil. 2. Soil organic matter chemistry by Pyrolysis-GC/MS. **Soil Science Society of America Journal**, Madison, v. 77, n. 4, p. 1307-1318, 2013.

BUURMAN, P.; VIDAL-TORRADO, P.; MARTINS, V.M. The podzol hydrosequence of Itaguaré (Sao Paolo, Brazil). 1. Geomorphology and interpretation of profile morphology. **Soil Science Society of America Journal,** Madison, v. 77, n. 4, p. 1294-1306, 2013.

BUURMAN, P.; SCHELLEKENS, J.; FRITZE, H.; NIEROP, K.G.J. Selective depletion of organic matter in mottled podzol horizons. **Soil Biology and Biochemistry**, Oxford, v. 39, p. 607-621, 2007.

EMBRAPA. Centro Nacional de Pesquisa de Solos. **Manual de métodos de análise de solos**, Rio de Janeiro, 2011. 212 p.

FLEXOR, J.; MARTIN, L.; SUGUIO, K.; DOMINGUEZ, J. M. L. Gênese dos cordões litorâneos da parte central da costa brasileira. In: LACERDA, L.D.; ARAÚJO, D.S.D.; CERQUEIRA, R.; TURCO, B. (Org.). **Restingas:** origens, estrutura, processos. Niterói: CEUFF, 1984. p. 35-45.

GERARDI, L.H.O.; MENDES, I.A. **Teoria, técnicas, espaços e atividades:** temas de geografia contemporânea. Rio Claro: UNESP, Programa de Pós-Graduação em Geografia; Associação de Geografia Teorética AGETEO, 2001. 432 p.

GIANNINI, P.C.; GUEDES, C.C.; NASCIMENTO Jr., D.R. do; TANAKA, A.P.; ANGULO, R.J.; SOUZA, M.C. de; ASSINE, M.L. Sedimentology and morphological evolution of the Ilha Comprida barrier system, southern São Paulo coast. In: DILLENBURG, S.R.; HESP, P.A. (Ed.). **Geology and geomorphology of holocene coastal Barriers of Brazil**: NewYork: Springer, 2009. p. 177-224.

GUEDES, C.C.F.; GIANNINI, P.C.F.; SAWAKUCHI, A.O.; DEWITT, R.; NASCIMENTO Jr., D.R.; AGUIAR, V.A.P.; ROSSI, M.G. Determination of controls on Holocene barrier progradation through application of OSL dating: the Ilha Comprida Barrier example, Southeastern Brazil. **Marine Geology,** Amsterdam, v. 285, n. 1, p. 1-16, 2011

INSTITUTO DE PESQUISAS TECNOLÓGICAS. **Compartimentação estrutural e evolução tectônica do Estado de São Paulo**. São Paulo, 1989. 288 p.

MARTINEZ, P.H.R.M. **Relações sedimentologia-geomorfologia-hidrologia e seus efeitos na gênese de Espodossolos sob Restinga na Ilha Comprida-SP.** 2015. 157 p. Dissertação (Mestrado em Solo e Nutrição de Plantas) - Escola Superior de Agricultura "Luiz de Queiroz", Universidade de São Paulo, Piracicaba, 2015.

PEREIRA, A.J.; GAMBÔA, L.A.P.; SILVA, M.A.M. da; RODRIGUES, A.R.; COSTA, A. da. Utilização do ground penetrating radar (gpr) em estudos de estratigrafia na praia de Itaipuaçú – Maricá (RJ). **Revista Brasileira de Geofísic**a, Rio de Janeiro, v. 21, p. 163-172, 2003.

ROSS, J.L.S.; MOROZ, I.C. **Mapa geomorfológico do Estado de São Paulo.** São Paulo: IPT; FAPESP, 1997. 64 p.

SANTOS, R.D.; LEMOS, R.C.; SANTOS, H.G.; KER, J.C.; ANJOS, L.H.C. **Manual de descrição e coleta de solo no campo**. 6. ed. Viçosa: Sociedade Brasileira de Ciência do Solo, 2013. 92 p.

SUGUIO, K.; MARTIN, L. Formações quaternárias marinhas do litoral paulista e sul fluminense. In: INTERNATIONAL SYMPOSIUM ON COASTAL EVOLUTION IN THE QUATERNARY, 1., 1978. São Paulo. **The Brazilian national working group for the IGCP Project 61**. São Paulo: USP, IG; SBG, 1978. 55 p. (Special Publication, 1).

_____. Geomorfologia das restingas. **Anais da Academia Brasileira de Ciência**, São Paulo, v. 3, p. 185-206, 1990.

SUGUIO, K; TESSLER, M. Planícies de cordões litorâneos quaternários do Brasil: origem, nomenclatura. In: LACERDA, L.D.; ARAÚJO, D.S.D.; CERQUEIRA, R.; TURCO, B. (Org.). **Restingas:** origens, estrutura, processos. Niterói: CEUFF, 1984. p.15-25.

TESSLER, M.G. **Dinâmica sedimentar quaternária no litoral sul paulista**. 1988. 276 p. Tese (Doutorado em Geologia Sedimentar) - Instituto de Geociências, Universidade de São Paulo, São Paulo, 1988.

TESSLER, M.G.; GOYA, S.C. Processos costeiros condicionantes do litoral brasileiro. **Revista do Departamento de Geografia da USP,** São Paulo, v. 17, p. 11-23, 2005.

TROPPMAIR, H. **Sistemas, geossistemas, geossistemas paulistas, ecologia da paisagem.** Rio Claro: [s.n], 2004. 130 p.

3 ORGANIC MATTER MOLECULAR CHEMISTRY OF SELECTED TROPICAL COASTAL PODZOL PROFILES

Abstract

Podzols show a large morphological variation, both within a landscape and between landscapes. A morphological analysis of the podzol sequence from Ilha Comprida allowed a subdivision into four distinct groups: poorly-drained profiles, profiles with well-drained B horizons, strongly rooted profiles and superposed profiles. This suggests, among others, varying contributions of DOM and root-derived OM in relation to drainage, decay of the upper B horizon by (biological and) microbial activity, precipitation of DOM in bands within the E horizon and below the B horizon, and differentiation of OM within the B horizon. In order to understand these processes we decided to study in detail the molecular composition of OM, using pyrolysis in combination with gas chromatography/mass spectrometry (Py-GC/MS), of the OM of the podzol chrono-hydrosequence on the southern side of Ilha Comprida, a Holocene forested barrier island in SE-Brazil, and relate the results to the morphological features and their variability. Factor analysis was carried out to reveal the covariance of various (groups of) pyrolysis products. It allows the distinction of patterns of behavior in large groups of variables. A first factor analysis was applied to all quantified pyrolysis products (n=196) for litter and soil samples from a selection of profiles. A second factor analysis was applied to soil samples alone from all profiles; because litter chemistry deviates considerably from that of soil OM, the litter samples were excluded here in order not to bias the factor analysis. For the factor analysis without litter samples, all profiles were included. Four factors explained 71% of the variance. In summary, the interpretation of loadings factor analysis: (a) F1 negative – macromolecular structures; F1 positive – phenolic DOM; (b) F2 negative – fresh plant material, F2 positive – microbial / plant material; (c) F3 positive – leaf waxes; (d) F4 negative - microbial material, F4 positive – (poly)aromatic DOM. The processes involved in the genesis of Podzols in the sandy coastal plain are directly related to drainage, the contribution of DOM, the contribution of organic matter derived from roots, the chemical composition of organic matter and its decomposition by microorganisms, causing a large variation in adjacent Podzols. The well-drained Podzols differ in characteristics from the poorly drained ones in composition and deposition of OM, as well as its decomposition, which is directly related to the activity of groups of microorganisms. They also differ in the relative contribution of OM-derived from roots and DOM. There is a wide variation in the characteristics of decomposition by microorganisms between the profiles of Podzols permanently exposed to air and marine spray (the cliffs) on Ilha Comprida and those more inland. There are therefore two main processes that change the morphology of Podzols (OM and composition): (a) change in drainage and rooting, and (b) exposure to air.

Keywords: Py-GC/MS; DOM; OM molecular composition; Podzol degradation

3.1 Introduction

Drainage is a factor that can directly influence the formation of B podzol horizons (SCHWARTZ, 1988; KACZOREK et al., 2004; BUURMAN et al., 2006). Any change of

hydrological position and improvement of drainage and aeration can result in strong differences, especially in originally poorly drained soils. Such morphological alterations include greater friability in subsurface horizons, accelerated decomposition of roots present in subsurface horizons that were protected by the anaerobic environment at depth; thickening of the E horizon with consequent thinning of the B horizon; introduction of mesofauna that can rework the OM by burrowing, and microbial degradation of OM (BUURMAN et al., 2005; BUURMAN; VIDAL-TORRADO; LOPES, 2013; BUURMAN; VIDAL-TORRADO; MARTINS, 2013).

Podzols from tropical and temperate environments show morphological differences, and one of those is that the E horizon of tropical podzols is usually thicker and hardly contains OM. Because the E horizon develops through degradation of the B horizon this indicates that decomposition is more efficient in tropical environments (BUURMAN; VIDAL-TORRADO; LOPES, 2013; BUURMAN; VIDAL-TORRADO; MARTINS, 2013; KINDEL; GARAY, 2002). Decomposition is strongly influenced by prevailing hydrological conditions, nutrients, and temperature. Limited availability of oxygen during the process of decomposition of OM favors the formation of water-soluble organic compounds, which can be easily transferred to drainage water (DAVID; ZECH, 1990).

Ilha Comprida is dominated by such tropical podzols. The erosion cliff on the southern side of the island allows a thorough study of their lateral morphological variation. The profiles in the cliff are permanently exposed to air, marine spray and eventual contact with tides - a characteristic that could directly influence decomposition by microorganisms. Such exposure is not present further inland, where profiles may have retained their original drainage condition. At the south-western corner of the island (Ponta da Trincheira) and in the cliffs facing the Mar de Cananéia, thick cemented B horizons are found (Figure 1).

Figure 1 – Overview of Ponta da Trincheira. This is the oldest portion of the Holocene barrier island studied

To understand the relationships between OM deposition and formation of B-podzol horizons, it is essential to know the chemical composition of the OM, which can be studied in detail using pyrolysis in combination with gas chromatography/mass spectrometry (Py-GC/MS) (SCHULTEN; SCHNITZER, 1997; LEINWEBER; SCHULTEN, 1999; GONZÁLEZ-PÉREZ et al., 2012; BUURMAN; VIDAL-TORRADO; LOPES, 2013). Py-GC/MS allows a very detailed chemical characterization and may be used to distinguish, for example, the contribution of compounds derived directly from plants and microorganisms (BUURMAN et al., 2005; BUURMAN et al., 2007; BUURMAN; PETERSE; MARTIN, 2007).

Podzols show a large morphological variation, both within a landscape and between landscapes. A morphological analysis of the podzol sequence from Ilha Comprida was studied (Chapter 2) and allowed a subdivision into four distinct groups: poorly-drained profiles, profiles with well-drained B horizons, strongly rooted profiles and superposed profiles. This suggests, among others, varying contributions of dissolved organic matter (DOM) and root-derived organic matter (OM) in relation to drainage, decay of the upper B horizon by (biological and) microbial activity, precipitation of OM in bands within the E horizon and below the B horizon, and differentiation of OM within the B horizon. In order to understand these processes we decided to study in detail the molecular composition of the OM of the podzol chrono-hydrosequence on the southern side of Ilha Comprida (cliff of a Holocene forested barrier island) in SE-Brazil, and relate the results to the morphological differences.

3.2 Material and Methods

3.2.1 Soil Samples

The profile sequence is situated at Ilha Comprida and is described in detail in Chapter 2. Samples were taken from all horizons of the studied profiles, except the E horizons, which did not have sufficient OM for analysis. The morphological analysis allowed a subdivision into four distinct groups: poorly drained profiles (P01, P02, P04, P40); profiles with well-drained B horizons (P31, P32, P33); strongly rooted profiles (P11, P37, P38) and superposed profiles (P10).

3.2.2 Extraction and Purification of Organic Matter

Five grams of air-dried soil sample (< 2 mm) were mixed witch 25 mL of 0.1 M NaOH and shaken for 24 h. The suspension was centrifuged at 10,000 rpm for 1 hour and the extract decanted. The extracts were then acidified to pH 1 with concentrated HCl to protonate OM. One mL of concentrated HF was added to dissolve silicates and increase the content of organic C of the extracted fraction. The acid mixture was shaken for 48 h, after which it was dialyzed to neutral pH against distilled water to remove excess salt using a dialysis membrane with a pore diameter of 10,000 Da. Finally, the solution was freeze-dried. It should be noted that, in podzols, this procedure extracts virtually all non-particulate OM (BUURMAN et al., 2005). The residues after extraction always have the color of pure quartz sand. Litters and the dead bromeliad leaves were finely crushed and analyzed without further treatment.

3.2.3 Pyrolysis-Gas Chromatography/Mass Spectrometry

A Micro-furnace single shot PY-3030S pyrolyser coupled to a GCMS-QP2010 (Frontier Laboratories LTD.) was used. The pyrolysis time was set at 6 s, pyrolysis temperature at 600 ℃ ± 0.1 ℃. The injection T of the GC (split 1:20) and the GC-MS interface were set at 320 ℃. The GC oven was heated from 50 to 320 ℃ (held 10 min) at 15 ℃ min^{-1}. The GC instrument was equipped with a Column UltraAlloy-5 (Frontier Laboratories LTD.), length 30 m, thickness 0.25 μm, diameter 0.25 mm with He as carrier gas. The MS was scanning in the range of m/z 45–600.

Compounds were identified using the NIST '05 library and pyrolysis-GC/MS literature (e.g., POUWELS et al., 1989; RALPH; HATFIELD, 1991; BUURMAN et al., 2007). After elimination of silica peaks, minor unidentified compounds and compounds that occurred in only one sample, 196 compounds remained and were quantified. The pyrolysis products were grouped according to probable origin and chemical similarity into a number of source groups: (i) aliphatic hydrocarbons, that includes *n*-alkanes, *n*-alkenes and methyl ketones, (ii) aromatics and alkylbenzenes, (iii) polyaromatic hydrocarbons (PAHs) and benzofurans, (iv) fatty acids and esters, (v) lignins, (vi) N compounds, (vii) phenols, and (viii) polysaccharides. Quantification of the relative contributions of pyrolysis products was based on the peak area of two characteristic ions using Masslab software. All quantifications were checked manually. The combined peak area of all quantified pyrolysis products (total peak area, TPA) was set as 100% and the relative proportions of the pyrolysis products were expressed as percentage of the TPA. The resulting quantification allowed comparison of the abundance of the pyrolysis products within the data set.

3.2.4 Statistical Analysis

The data set contained 79 samples with 196 variables each, the quantified pyrolysis data were subjected to factor analysis using Statistica Version 8 (Statsoft, Tulsa OK, USA). Factor analysis is a statistical approach that can be used to analyze interrelationships among a large number of variables and to explain these variables in terms of their common underlying dimensions (factors). It is a prime method to explain the intercorrelations among input variables and to detect structures. Each variable is modeled as a linear combination of the factors plus error terms. Factors are selected by grouping related items and are independent (orthogonal). Consecutive factors account for less and less variance. Only the variability that variables have in common with other variables is used. The degree of correlation between the variables and the extracted factor is called the factor loading, while the values of samples for each factor are called the factor score. Factor loading diagrams of organic fragments can be interpreted in terms of different plant contributions, microbial contribution, degradation, etc. Projections of samples in factor space can be understood by examining the projection of factor loadings in the same space.

Factor analysis was carried out to reveal the covariance of various (groups of) pyrolysis products. It allows the distinction of patterns of behavior in large groups of

variables. A first factor analysis was applied to all quantified pyrolysis products ($n=196$) for litter samples and soil samples from a selection of profiles. A second factor analysis was applied to soil samples alone; because litter chemistry deviates considerably from that of soil OM, the litter samples were excluded here in order not to bias the factor analysis. The first factor analysis was used to check which compounds were associated with litter and to reduce the variables so that quantification of the other profiles can be reduced to the relevant pyrolysis products only.

3.3 Results and Discussion

3.3.1 General Chemistry

The quantified pyrolysis products and their characteristics are listed in Appendix B. The compounds were discussed according to chemical group.

3.3.1.1 *n*-Alkanes, *n*-alkenes and *n*-methyl ketones

Straight-chain alkanes and alkenes in pyrolysates of soil organic matter (SOM) may have several sources, including plant biopolymers, plant waxes and microbial material. The distribution of their chain lengths provides information on their source and can additionally be influenced by decomposition and burning. A dominance of odd-over-even chain-lengths *n*-alkanes are indicative of plant leaf waxes (EGLINTON; HAMILTON, 1967), while even-numbered mid-chain lengths (C_{20-28}) are indicative of cutan and suberan that are abundant in roots and bark (TEGELAAR et al., 1995; NIEROP, 1998). A large contribution from *n*-alkenes also points towards a biopolymer source. Decomposition and fire result in shortening of chain lengths and a loss of an odd or even predominance (ALMENDROS et al., 1988). The source of *n*-methyl ketones is not clear, some authors have attributed them to be a result of microbial oxidation of *n*-alkanes (JANSEN; NIEROP, 2009), but they have also been identified in pyrolysates from fresh plant material (SCHELLEKENS et al., 2013).

Seventy-one pyrolysis products from this group were quantified. The *n*-alkanes and *n*-alkenes showed chain-lengths between C_7 and C_{34}, the chain-length of *n*-methyl ketones varied between C_{17} and C_{31}. Most profiles showed a dominance of short-chain *n*-alkanes (C_{7-15}), a dominance of short chain *n*-alkenes (C_{7-15}; especially the C_{10}), no odd or even predominance, and no predominance of typical microbial chain lengths (C_{15} and C_{17}),

suggesting a major contribution from macromolecular structures and/or a generally strong degree of decomposition or a considerable contribution from burnt material. Exceptions were found for AE horizons from profiles P37, P38 and P40, that showed a dominance of longer chain lengths (C_{23-29}), and EB and EB2 horizons from profiles P31 and P2, respectively, that showed a dominance of the long chain *n*-alkanes (C_{28-33}). Litter samples showed a dominance of even numbered mid-chain *n*-alkanes and *n*-alkenes (C_{20-28}), suggesting a larger contribution from root than leaf material to the litter. The strongly rooted profiles P11, P37 and P38 showed the largest abundance of short-chain *n*-alkanes, *n*-alkenes and *n*-methyl-ketones; more specifically in the A horizon of profile P11 and the AE horizons of profiles P37 and P38. The hydromorphic profiles (P01, P02, P04 and P40) generally showed a low abundance of total *n*-alkanes, *n*-alkenes and *n*-methyl ketones, with the smallest abundance of short chain *n*-alkanes in B horizon samples. The well-drained profiles P31, P32 and P33 showed intermediate values between the previous groups.

3.3.1.2 Aromatics and alkylbenzenes

Aromatics in pyrolysates of SOM may originate from several sources, including lignin, carbohydrates, proteins and charcoal. The alkylbenzenes generally showed a decrease in alkyl chain length (except for the litter samples that showed an odd predominance with the highest abundance of the C_9 alkylbenzene), which may be related to chain-length shortening during to decay (BUURMAN; VIDAL-TORRADO; LOPES, 2013).

We quantified 28 different aromatic compounds that included nine alkylbenzenes. The latter made up about 1.5% of all quantified compounds. The chain length of the alkylbenzenes ranged from C_4 to C_{12}. Total aromatic compounds varied between 15 and 47% (samples P10A and P32Bh1, respectively). The SOM bands from profile P02 (P02EB2band) showed the largest abundance of aromatic compounds. Benzene and toluene were the dominant aromatic compounds; together they reached up to 28% of total quantified compounds.

3.3.1.3 Polyaromatic hydrocarbons

We quantified 18 different polyaromatic compounds. Most of the identified fragments were indene and naphthalene compounds, but 3-ring polyaromatics were also present. Polyaromatic pyrolysis products in SOM pyrolysates are usually derived of charred plant

material as a result of forest or grass fires (GONZALEZ-PEREZ et al., 2004; KAAL et al., 2008). Although polyaromatic pyrolysis products have been ascribed to pyrolysis of fatty acids (SAIZ-JIMENEZ, 1994), the general lack of PAHs in OM that is not influenced by burning indicates that this source can be neglected.

3.3.1.4 Fatty acids and methyl esters

The C_{16}-C_{22} fatty acids, especially the C_{16} and C_{18}, are common components of cutin and cutan in higher plants (ALMENDROS et al., 1996; TEGELAAR et al., 1989), while microbes may produce compounds of C_4-C_{26} chain length (SCHNITZER et al., 1986). Fatty acids (especially the shorter chain lengths) have been associated with roots compared to aerial parts in a pyrolysis study of plant material (SCHELLEKENS et al., 2013). We quantified ten fatty acid compounds. The most common was the C_{16} fatty acid. The Bh3-band from profile P32, the EB2-band from profile P02, and the gallery sample from profile P04 did not contain the C_{16} fatty acid. Only a few samples showed all chain lengths. The Bh1 band from profile P37 was the only sample that showed all ten fatty acids, confirming the root signal observed from the *n*-alkane distribution in this profile. Samples from profiles P10, P11, P33 and P38 contained shorter chain fatty acids.

Only one fatty acid methyl ester was identified, and its abundance was low in all samples. Methyl esters are found in the external protective wax of aerial plant tissue (KILLOPS; KILLOPS, 2005). Esters are rare in pyrolysates of SOM extracts because the ester bonds are easily degraded microbially, or upon alkaline extraction (KONDO et al., 1991).

3.3.1.5 Lignin phenols

Lignin is exclusively plant-derived and is composed of *p*-hydroxyphenyl, guaiacyl and syringyl units that are irregularly bound to each other. Lignin fragments produced during pyrolysis retain the substitution patterns of the lignin macromolecule (RALPH & HATFIELD, 1991). The contribution of each type differs between plant species and plant parts, which is frequently used to study SOM dynamics. The composition of lignin furthermore provides information on the degree of decomposition of plant material; syringyl lignin is preferentially degraded over guaiacyl lignin, C_3-alkyl side chains indicate intact

lignin, while oxidized alkyl side chains point towards decomposed material (THEVENOT et al., 2010).

Seventeen different lignin-derived products were quantified. The most common were guaiacol (Lg1), 4-vinylphenol (Lg3), 4-vinylguaiacol (Lg5) and 4-acetylguaiacol (Lg10). Generally, the lignin content was lower in B horizons and higher in A horizons and litter samples. Although some authors state that lignin is more easily degraded at less acidic pH (BRACEWELL; ROBERTSON, 1984), decay in mineral acidic soils is usually rapid (NIEROP; VERSTRATEN, 2003).

3.3.1.6 N compounds

Seventeen N compounds were quantified. The most abundant compounds were pyridines (N3, N5, N8 and N10) and pyrroles (N4, N6, N7, N9 and N15). The abundance of N containing compounds varied between 7 and 22 % (Table 1) which indicates a considerable contribution from microbial material. 4-Ethyl-2-methylpyrrole (N9) was the most abundant N compound in all samples. Imidazoles (N1, N12) were less abundant pyrolysis products, and may originate from histidine (amino acid essential for tissue growth) or from thermal degradation of microorganisms (SCHULTEN; SCHNITZER, 1998). Indoles (N13) may have a bacterial source. Benzonitrile (N11) and quinoline (N14) can be related to burning (ALCAÑIZ et al., 1994).

3.3.1.7 Phenols

Apart from the lignin group (methoxyphenols), nine phenolic compounds were quantified. Phenol (Ph1) was the most abundant compound, followed by C_1-phenol (Ph3). The presence of the marker of lichens (Ph10; SCHELLEKENS et al., 2009, 2011) is in agreement with their abundance on the island. The Bhm horizons showed the largest phenol content, while the AE, EB and BE horizons had the lowest abundance in general.

3.3.1.8 Polysaccharides and benzofurans

Fourteen polysaccharide compounds were quantified. Polysaccharides can be of both plant and microbial origin. The levosugars (Ps12, Ps13, Ps14) are usually attributed to

cellulose (STUCZYNSKI et al., 1997; POIRIER et al., 2005). Acetic acid, furans and furanones (Ps1, Ps2, Ps3, Ps6) in soils are commonly derived from microbial material or strongly degraded plant polysaccharides (BUURMAN et al., 2009; BUURMAN & ROSCOE, 2011). All profiles showed high concentrations of acetic acid in all samples; levoglucosan was the dominant polysaccharide compound in surface samples and EB samples. Benzofurans can be pyrolysis products of partially charred cellulose (KAAL et al., 2009).

3.3.2 Factor analysis with litter samples

Four extracted factors explained 71% of the variance. The projections of factor scores and factor loadings for the first two factors are given in Figure 2. The factor scores showed a clear differentiation of samples (Figure 2). All litter samples showed negative scores on both factor 1 (F1) and factor 2 (F2). All A horizons showed negative scores on F1 and low scores on F2; E and B horizons were separated into two groups with hydromorphic profiles showing positive scores on F1, while E and B horizons from other profiles were more scattered on F1. The factor loadings also showed a clear differentiation of chemical groups (Figure 2).

(a)

(b)
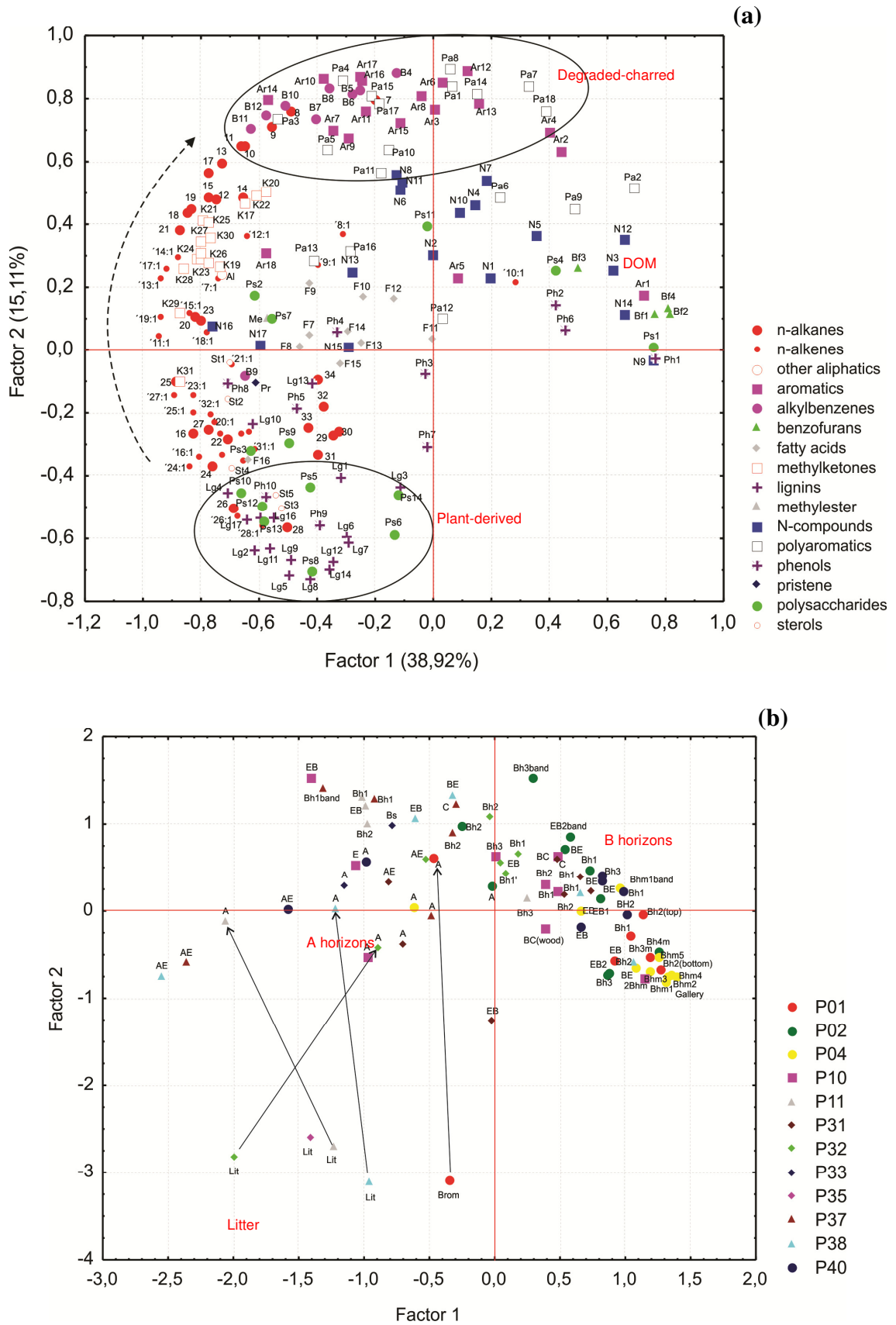
Figure 2 – (a) Projection of the factor scores with litter samples in F1-F2 space; (b) Projection of the factor loadings of the pyrolysis products with litter samples in F1-F2 space

Compounds with negative loadings on F2 all showed negative loadings on F1. These typically involved pyrolysis products indicative of relatively fresh plant material, and included all lignin fragments (KLOTZBÜCHER et al., 2011), catechols derived from tannin (Ph7, Ph9; GALLETTI; REEVES, 1992), and markers for lichens (Ar18; SCHELLEKENS et al., 2009, 2011), hemicellulose (Ps8; POUWELS et al., 1987) and cellulose (Ps14; POUWELS et al., 1989). Furthermore, the sterols (KILLOPS; KILLOPS, 2005) and long-chain n-alkanes (C$_{26–33}$; EGLINTON ; HAMILTON, 1967) are indicative of relatively intact plant material. Pristene (Al), being a pyrolysis product of chlorophyll (YASSIR; BUURMAN, 2012) is also indicative of plant material. Thus, these products reflect relatively fresh plant-derived OM, which is in agreement with the factor scores of the litter samples being negative on both factors. High negative loadings on F2 for pyrolysis products of which the source is less clear (Ps5–6, Ps10, Ps12–13), suggests a relation with plant material within this data set.

Compounds with high positive loadings on F2 included most aromatic, polyaromatic and alkylbenzene compounds, which points towards burnt or strongly decomposed material. This suggests that F2 reflects degradation, with high positive loadings reflecting most resistant SOM (black carbon; SCHMIDT et al., 2000), and negative loadings reflecting relatively intact plant material (see above). This interpretation of F2 is supported by: 1) the intermediate loadings of n-alkanes and n-alkenes, which are pyrolysis products from cutan and suberan (TEGELAAR et al., 1995) being more resistant against degradation than lignin (KLOTZBÜCHER et al., 2011); 2) chain length reduction of n-alkanes, n-alkenes, n-methyl ketones, and the alkyl side chain of alkylbenzenes, all showing more negative loadings for longer chain lengths; this chain-length shortening is generally interpreted as an effect of decomposition (BUURMAN et al., 2006; BUURMAN; VIDAL-TORRADO; LOPES, 2013, BUURMAN; PETERSE; MARTIN, 2007; BUGGLE et al., 2010); and 3) the factor scores of litter samples and samples from the corresponding A horizons, indicated by arrows in Figure 2b, will be explained in more detail below.

Only litter samples from profiles P11, P32, P35, P38 and P01 were analyzed. The litter of profile P35 was analyzed but not the A horizon, so that a litter-soil comparison cannot be made for this profile. All samples of A horizons plot closest to the litter samples. The arrows in Figure 2b connect litter samples and A horizon from the same profile, and clearly showed that the major shift is on F2. The largest distance on F2 is between litter and A horizon of profile P01. This may be due to the fact that the litter sample was a dead bromeliad leaf, which may have been less decomposed than the litter of the other profiles. The largest shifts on F1 are found between litters and A horizons from profiles P11 and P32.

Thus, according to the pyrolysis products with negative loadings on F1, we conclude that F2 reflects a degradation trend, from fresh (lignin and plant sugars) to more resistant (cutan/suberan: C_7-C_{24} *n*-alkanes and *n*-alkenes, *n*-methyl ketones) to very resistant (polyaromatics and aromatics) material. Considering that compounds with negative loadings on F1 were associated with macromolecular structures from plants, it is suggested that compounds with high positive loadings on F1 include low molecular weight (LMW) products. Indeed, benzofurans (Bf1–Bf4), phenol (Ph1), acetic acid (Ps1) and C_2 quinoline (N14) have been associated with DOM (BUURMAN et al., 2005). The fact that none of the compounds associated with DOM showed negative loadings on F2 confirms that DOM is more strongly degraded than the litter. This interpretation shows that litter and most A, AE and EB horizons were associated with (burnt) plant material, while hydromorphic profiles and Bh horizons generally had a higher contribution from DOM. The differences between the profiles and horizons will be discussed in more detail in Section 3.3.3.

3.3.2.1 Relating trends observed from factor analysis to the proportion of (groups of) pyrolysis product

The shifts on F2 involve a strong loss of compounds that characterize fresh plant OM. It appeared that the loss of lignins was most prominent. 4-Vinylguaiacol (Lg6) and 4-vinylphenol (Lg3) dominated the litter lignins, in agreement with rather undegraded lignin (RALPH; HATFIELD, 1991). P01 litter (dead bromeliad leave) had the highest abundance of lignin compounds. 4-Vinylphenol is also a major compound of grass lignin (SAIZ-JIMENEZ; de LEEUW, 1986). In the A horizons, guaiacol (Lg1) was usually the dominant product, accompanied by 4-vinylguaiacol (Lg5) and 4-acetylguaiacol (Lg10). This indicates, as expected, a generally more degraded lignin in the A samples (YASSIR; BUURMAN, 2012). Shifts on Factor 1 between litter and A-horizons are difficult to interpret, because they appear to happen in two directions and in two samples only.

The loss of lignins, plant polysaccharides, and long-chain alkanes upon litter-SOM conversion appears to be largely compensated (Table 1) by an increase in aromatics, PAHs (accumulation of recalcitrant compounds), and N-compounds (microbial contribution). Alkane and alkene contents in litters are rather low; the litter samples of profile P32 presented the highest abundance of short-chain alkanes and profile P01 the smallest (Table 1). The largest increases in A horizons were found in profiles P01, P11, and P38, while there was no

increase in P32. In all litters and A horizons, toluene (Ar2) was the dominant aromatic compound.

Individual N-compounds constitute up to 3% in litters and to 8% in A horizon. The 4-ethyl-2-methylpyrrole (N9) is the most abundant N-compound in both litters and soil samples. A large abundance of N-compounds in SOM is generally linked with a higher degree of decomposition and a significant contribution of microbial SOM (NIEROP et al., 2001). As expected the higher concentration of N-compounds is found in the soil samples. Litter sample P01 showed the smallest abundance of N-compounds, while P32 showed the largest.

Phenol (Ph1) and 3/4-methylphenol (Ph3) are the most abundant phenol compounds in both litter and A horizons, but more abundant in the soil samples. Phenol constituted 10-16% of the pyrolysis products in litters and 13-17% of the A horizons .

The polysaccharides in litter samples generally showed a predominance of levoglucosan (Ps14), a pyrolysis product of relatively fresh cellulose (POUWELS et al., 1989). The A horizon showed the same predominance, but with less levoglucosan (P14; 5-12%). The litter sample of profile P32 showed a lower abundance of levoglucosan (Ps14) than the A horizon. In general, profile P32 showed the lowest abundance of polysaccharide compounds in the litter sample and the highest abundance in the A horizon compared to the other profiles.

Table 1 - Proportion (%) of groups of compounds for each horizon and litter samples   (continues)

Profile sample	n-alka C7-25	n-alka C26-35	n-alke C7-25	n-alke C26-35	other aliph	arom	alkylb	benzof	fatty acids	mket	lignins	mest	N-comp	polyar	phenols	prist	polysac	sterols
P01																		
Brom	1.5	0.5	1.9	0.6	0.0	1.9	0.8	0.2	0.2	0.4	63.6	0.0	3.0	0.6	10.3	1.2	12.7	0.5
A	6.8	1.1	3.9	0.7	0.0	25.4	1.7	1.4	0.1	0.4	5.0	0.6	13.6	8.1	15.5	0.2	15.1	0.3
EB	2.0	0.2	1.8	0.1	0.0	32.6	0.8	1.4	0.0	0.1	0.3	0.0	13.3	3.7	13.7	0.0	29.8	0.1
Bh1	2.3	1.0	1.8	0.5	0.0	37.3	1.0	2.2	0.0	0.1	0.8	0.0	16.9	4.7	23.8	0.0	7.6	0.0
Bh2(top)	2.0	0.4	1.7	0.0	0.0	31.2	1.2	2.7	0.0	0.1	2.1	0.0	18.6	5.3	27.0	0.0	7.7	0.0
Bh2(bottom)	1.0	0.3	1.8	0.2	0.0	28.9	0.5	2.9	0.0	0.0	1.7	0.0	18.0	4.1	28.3	0.0	12.1	0.0
Bh3m	1.4	0.0	1.5	0.0	0.0	23.0	0.7	3.2	0.0	0.1	3.6	0.0	19.0	4.8	30.1	0.0	12.6	0.0
P02																		
A	4.1	0.4	2.6	0.3	0.0	28.8	1.6	1.1	0.9	0.3	4.7	0.5	17.0	5.3	16.9	0.1	15.4	0.1
EB1	3.1	0.4	3.3	0.2	0.0	43.8	1.4	1.3	0.1	0.0	0.3	0.0	15.4	5.6	9.1	0.1	15.9	0.1
EB2	1.8	4.9	2.4	1.1	0.0	40.6	0.9	1.4	0.1	0.0	0.3	0.0	17.7	4.1	12.4	0.0	12.2	0.0
EB2band	3.5	0.7	2.4	0.3	0.0	48.8	2.0	1.4	0.0	0.3	0.3	0.0	15.2	7.6	10.4	0.1	7.0	0.1
BE	4.7	0.5	2.8	0.2	0.0	40.8	1.9	1.5	0.1	0.3	0.6	0.0	12.6	7.4	13.1	0.1	13.4	0.1
Bh1	3.8	0.3	2.8	0.2	0.0	35.1	1.9	1.9	0.1	0.2	0.9	0.0	17.5	6.6	15.9	0.0	12.8	0.0
Bh2	7.1	0.9	5.2	0.5	0.0	32.1	2.1	1.7	0.1	0.8	1.3	0.1	16.3	6.5	15.6	0.1	9.6	0.1
Bh3	2.2	0.1	2.7	0.0	0.0	21.9	0.8	1.4	0.1	0.0	0.5	0.0	13.9	3.5	11.7	0.0	41.0	0.1
Bh3band	5.5	0.7	3.4	0.3	0.0	39.6	2.8	2.0	0.0	0.3	0.7	0.0	16.1	8.8	13.0	0.1	6.6	0.1
Bh4m	1.6	0.1	1.9	0.0	0.0	22.9	0.8	2.9	0.0	0.0	3.2	0.0	22.0	4.5	28.7	0.0	11.2	0.0
P04																		
A	6.4	1.1	4.2	0.9	0.0	23.4	1.9	1.0	0.5	0.4	6.4	0.5	12.6	5.3	17.9	0.2	17.0	0.2
EB	2.7	1.3	3.1	0.4	0.0	36.8	1.4	1.4	0.1	0.1	0.7	0.1	16.1	5.0	13.6	0.1	17.0	0.1
BE	1.4	1.4	2.1	0.3	0.0	36.8	0.8	1.5	0.1	0.1	0.5	0.0	19.3	3.9	19.4	0.0	12.5	0.0
Bhm1	1.0	0.1	1.8	0.1	0.0	25.8	0.7	2.3	0.0	0.0	2.0	0.0	20.7	3.9	30.0	0.0	11.6	0.0
Bhm1band	2.3	0.4	2.1	0.3	0.0	29.8	1.4	2.6	0.0	0.1	2.0	0.0	19.9	7.1	26.1	0.0	5.8	0.0
Bhm2	0.9	0.0	1.7	0.0	0.0	22.8	0.7	2.9	0.1	0.0	2.4	0.0	21.5	4.0	29.9	0.0	13.0	0.0
Bhm3	1.1	1.2	1.8	0.3	0.0	19.9	0.7	3.3	0.0	0.0	4.7	0.0	21.0	4.7	31.4	0.0	9.9	0.0
Bhm4	0.7	0.0	2.2	0.0	0.0	22.6	0.5	3.3	0.1	0.0	2.2	0.0	22.2	4.4	34.5	0.0	7.3	0.0

Table 1 - Proportion (%) of groups of compounds for each horizon and litter samples (continuation)

Profile sample	n-alka C7-25	n-alka C26-35	n-alke C7-25	n-alke C26-35	other aliph	arom	alkylb	benzof	fatty acids	mket	lignins	mest	N-comp	polyar	phenols	prist	polysac	sterols
Bhm5	1.3	0.1	2.1	0.0	0.0	23.9	0.6	3.2	0.1	0.0	2.8	0.0	21.3	5.0	32.6	0.0	7.0	0.0
Galerie	0.7	0.2	1.9	0.1	0.0	22.0	0.4	4.0	0.0	0.0	2.0	0.0	21.3	4.7	36.6	0.0	5.9	0.0
P10																		
A	6.4	1.9	5.2	1.1	0.1	15.4	1.6	0.9	0.5	0.5	12.0	0.4	12.0	5.4	22.9	0.6	12.8	0.3
E	8.8	1.8	7.1	1.2	0.1	24.7	1.9	0.9	0.5	0.8	3.7	0.2	11.9	5.3	20.3	1.5	8.7	0.5
EB	11.8	1.9	7.8	1.2	0.1	34.0	2.5	1.0	0.3	1.0	2.9	0.1	8.3	7.0	12.5	2.1	4.8	0.6
BH1	4.0	0.4	3.0	0.3	0.0	29.7	1.6	1.5	0.1	0.2	2.6	0.1	17.9	5.8	27.6	0.2	4.9	0.1
Bh2	3.9	0.4	3.6	0.2	0.0	29.2	1.4	1.8	0.1	0.3	2.1	0.1	18.1	6.0	24.2	0.4	8.0	0.2
Bh3	5.6	1.2	4.4	0.7	0.0	25.9	1.8	2.1	0.1	0.5	2.6	0.1	16.7	6.5	23.2	0.2	8.3	0.1
BC	3.9	0.9	3.1	0.5	0.0	36.4	1.5	2.2	0.1	0.4	1.3	0.1	17.1	7.0	17.6	0.2	7.9	0.1
BC(wood)	3.8	0.5	3.8	0.4	0.0	24.2	1.2	1.4	0.2	0.3	2.5	0.1	19.4	4.6	31.0	0.3	6.4	0.1
2Bhm	1.0	0.1	2.1	0.1	0.0	19.3	0.6	2.8	0.1	0.1	3.9	0.0	20.6	4.7	38.0	0.0	6.7	0.0
P11																		
Lit	5.2	8.2	8.1	5.3	0.0	6.9	0.6	0.5	0.4	0.4	16.3	0.0	6.4	1.3	16.1	1.2	22.1	0.9
A	10.8	4.1	9.6	2.5	0.1	18.3	1.6	0.7	0.8	1.0	9.6	0.5	7.8	4.2	13.3	1.2	12.8	1.1
EB	11.5	1.7	6.4	1.0	0.1	35.7	2.0	1.0	0.4	0.7	2.6	0.0	7.8	6.7	14.8	1.6	5.4	0.5
Bh1	10.8	1.8	6.9	1.3	0.1	31.9	2.5	1.4	0.2	0.9	2.9	0.1	10.9	6.9	15.7	0.6	5.0	0.2
Bh2	8.8	3.3	6.9	1.9	0.0	29.9	2.1	1.6	0.2	1.0	1.9	0.1	12.6	6.7	16.5	0.5	5.7	0.2
Bh3	4.5	1.0	3.8	0.6	0.0	26.7	1.3	1.9	0.1	0.4	2.4	0.1	16.7	5.6	26.8	0.1	7.8	0.0
P31																		
A	7.4	1.4	4.8	0.9	0.0	19.6	1.6	0.9	0.1	0.4	9.9	0.4	11.4	5.4	22.0	0.2	13.3	0.2
AE	8.0	1.6	5.6	1.3	0.0	25.3	1.6	0.9	0.1	0.6	4.4	0.5	12.3	5.4	19.5	0.5	11.8	0.5
EB	2.2	14.9	1.7	3.5	0.0	21.3	0.9	0.8	0.1	0.2	0.7	0.0	9.0	3.3	10.2	0.0	31.1	0.0
BE	2.9	0.5	2.4	0.3	0.0	36.9	1.4	1.9	0.0	0.2	1.2	0.0	18.4	5.7	20.4	0.1	7.7	0.1
Bh1	3.7	0.4	2.8	0.2	0.0	36.6	1.8	1.7	0.0	0.2	1.2	0.0	17.6	6.4	19.5	0.1	7.6	0.1
Bh2	3.6	0.5	3.0	0.3	0.0	27.5	1.5	2.1	0.0	0.3	2.4	0.0	19.5	5.6	24.3	0.0	9.1	0.1
C	4.3	1.6	3.1	0.6	0.0	35.5	1.6	2.1	0.1	0.2	1.0	0.1	17.4	6.5	18.2	0.1	7.8	0.0

Table 1 - Proportion (%) of groups of compounds for each horizon and litter samples (continuation)

Profile sample	n-alka C7-25	n-alka C26-35	n-alke C7-25	n-alke C26-35	other aliph	arom	alkylb	benzof	fatty acids	mket	lignins	mest	N-comp	polyar	phenols	prist	polysac	sterols
P32																		
Lit	6.4	6.5	10.6	4.8	0.0	7.9	1.0	0.4	0.4	0.7	16.5	0.0	7.2	2.0	13.7	0.8	17.6	3.7
A	6.3	1.6	4.6	0.9	0.0	18.1	1.6	0.8	0.2	0.5	8.7	0.8	10.8	5.3	16.4	0.3	22.2	0.7
AE	6.4	1.0	4.4	0.7	0.0	26.6	2.0	1.1	0.1	0.5	4.8	0.5	13.8	7.0	16.9	0.2	13.6	0.4
EB	4.7	0.9	4.3	0.7	0.0	32.3	2.0	1.2	0.1	0.5	1.1	0.1	13.7	6.2	11.1	0.0	20.9	0.3
Bh1	4.4	0.7	4.9	0.5	0.0	46.8	1.8	1.3	0.1	0.5	0.9	0.1	13.0	6.2	11.4	0.1	7.3	0.1
Bh1'	4.4	0.6	3.8	0.4	0.0	30.5	1.6	1.3	0.1	0.4	2.0	0.3	19.3	5.8	20.2	0.1	8.9	0.3
Bh2	6.1	0.7	3.8	0.5	0.0	35.6	2.0	1.7	0.1	0.5	1.1	0.1	16.6	6.8	15.9	0.1	8.4	0.1
P33																		
A	8.5	2.3	5.7	1.3	0.0	22.2	2.0	0.9	0.3	0.6	7.3	0.6	10.8	6.8	15.1	0.2	14.6	0.8
Bs	6.0	1.5	6.0	0.9	0.0	31.4	1.6	1.2	1.0	0.9	2.1	0.4	17.5	6.1	13.5	0.1	9.3	0.3
P37																		
A	6.7	1.0	3.7	0.6	0.0	25.2	1.5	1.0	0.1	0.3	9.6	0.4	11.2	5.8	19.8	0.2	12.8	0.1
AE	9.9	4.8	13.5	3.5	0.1	16.4	1.4	0.6	0.2	1.1	9.0	0.4	6.8	3.7	10.8	5.3	10.9	1.7
Bh1	8.5	3.5	6.6	1.9	0.0	30.2	2.4	1.7	0.1	1.1	1.3	0.0	13.5	7.3	16.0	0.3	5.3	0.1
Bh1band	9.5	2.4	6.7	1.6	0.1	30.3	2.5	1.5	0.5	1.1	2.0	0.1	11.5	7.4	14.7	1.8	5.8	0.6
Bh2	7.1	1.6	5.3	1.0	0.0	26.8	2.0	1.8	0.1	0.6	2.1	0.0	16.2	7.2	22.6	0.2	5.2	0.1
C	8.2	1.2	4.8	0.8	0.0	31.0	2.4	1.8	0.0	0.6	1.9	0.0	13.3	7.6	19.3	0.1	6.7	0.0
P38																		
Lit	4.5	4.7	5.8	3.7	0.0	6.2	0.4	0.4	0.1	0.3	16.5	0.0	6.3	1.1	13.1	0.3	34.4	2.0
A	10.1	2.0	6.4	1.2	0.0	19.8	1.6	0.8	0.1	0.6	9.3	0.6	9.1	5.4	16.9	0.6	15.2	0.3
AE	11.9	4.3	16.9	3.5	0.2	16.0	1.2	0.6	0.3	1.0	7.0	0.3	5.5	3.2	9.2	8.7	8.1	2.2
EB	9.4	1.2	6.6	0.8	0.1	32.3	2.2	1.1	0.1	0.6	1.9	0.1	10.9	6.8	18.0	0.8	7.0	0.2
BE	7.2	1.2	6.1	1.0	0.0	34.3	2.5	1.6	0.0	0.6	1.7	0.0	13.1	7.9	16.5	0.3	5.9	0.1
Bh1	3.1	0.5	3.5	0.4	0.0	23.4	1.3	2.3	0.0	0.3	1.6	0.0	20.9	6.1	28.6	0.1	7.8	0.0
Bh2	1.6	0.2	2.6	0.1	0.0	17.9	0.7	2.3	0.1	0.1	2.0	0.0	23.3	4.5	37.4	0.0	7.1	0.0
P40																		
A	8.5	1.6	6.1	1.1	0.0	23.8	2.0	0.9	0.1	0.7	4.1	0.6	12.4	6.1	18.6	0.3	12.3	0.7

Table 1 - Proportion (%) of groups of compounds for each horizon and litter samples (conclusion)

Profile sample	n-alka C7-25	n-alka C26-35	n-alke C7-25	n-alke C26-35	other aliph	arom	alkylb	benzof	fatty acids	mket	lignins	mest	N-comp	polyar	phenols	prist	polysac	sterols
AE	9.1	4.1	8.8	2.8	0.0	17.8	1.6	0.7	0.0	1.0	2.7	0.3	12.8	4.0	18.1	1.0	13.9	1.4
BE	2.6	1.0	2.7	0.6	0.0	35.4	1.5	2.2	0.0	0.3	0.7	0.0	19.6	7.0	16.8	0.0	9.5	0.0
EB	2.5	0.6	2.3	0.2	0.0	32.2	1.2	1.3	0.0	0.3	0.3	0.1	13.2	5.0	11.0	0.1	29.5	0.1
Bh1	2.3	0.5	2.3	0.2	0.0	30.5	1.3	2.6	0.0	0.2	0.6	0.0	19.6	6.9	26.0	0.0	6.8	0.0
Bh2	2.1	0.3	2.5	0.2	0.0	25.0	0.9	2.9	0.1	0.2	1.2	0.0	19.6	6.3	28.9	0.0	9.8	0.0
Bh3	2.7	0.7	2.8	0.4	0.0	27.6	1.2	3.5	0.0	0.3	1.6	0.0	18.2	7.6	22.9	0.0	10.6	0.0

n-alka = n-alkanes; n-alke = n-alkenes; other aliph = other aliphatics; arom = aromatics; alkylb = alkylbenzenes; mket = methylketones; mest = methylester; N-comp = N-compounds; polyar = polyaromatics; prist = pristine; polysac = polysaccharides

3.3.3 Factor analysis without litter samples

For the factor analysis without litter samples, all profiles were included. Four factors explained 71% of the variance. Factor loadings and factor scores for the F1–F2 and F3–F4 projection are given in Figures 3a,b and 4a,b respectively. The explained variance for all factors is given in Appendix C for each pyrolysis product separately. The exclusion of the litter samples did not cause major differences in factor analysis.

The distribution of compounds (Figures 2a and 3a) in the F1–F2 projection showed only slight differences. Pyrolysis products associated with DOM again formed a cluster with high positive loadings on F1. The lignin cluster in the lower left quadrant, along with a few phenolic compounds (Ph4, Ph5, Ph9), the marker of lichens (Ph10) and two levosugars (P12, P13), represented rather fresh ligno-cellulose. Lignins were better separated from the aliphatic compounds, which reflects the difference in degradation speed between the two groups. The spread out of phenols between the lignin cluster and the right hand cluster that represents DOM may indicate that these phenols are lignin degradation products that contribute to DOM, while in the litter the lignin was not yet enough degraded to contribute to DOM. Contrarily, aromatics and polyaromatics were more scattered compared to the factor analysis with litter samples, suggesting an absence of charred material in the litter samples.
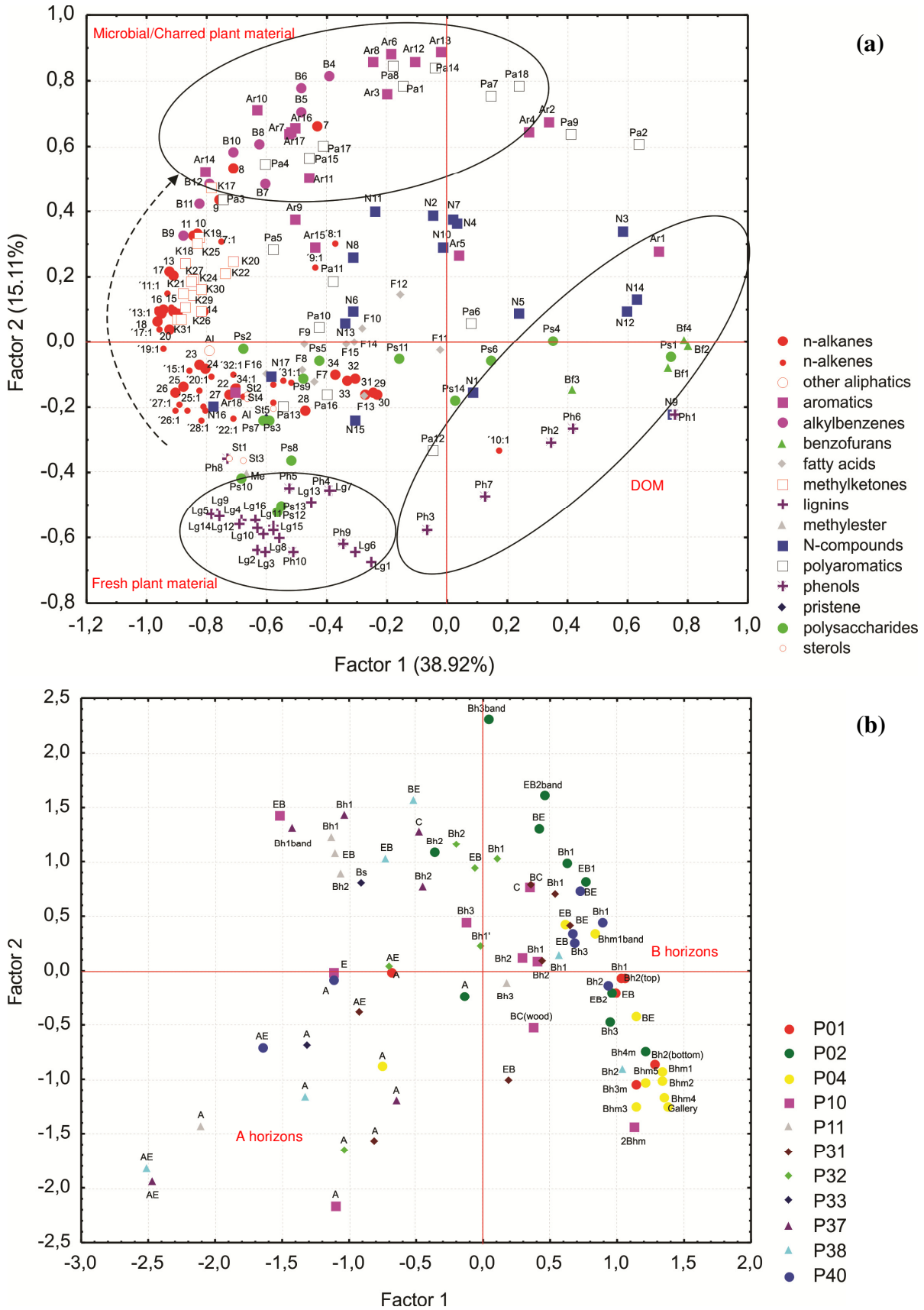
Figure 3 - (a) Projection of the factor loadings of the pyrolysis products without litter samples in F1-F2 space; (b) Projection of the factor scores without litters samples in F1-F2 space

All compounds with high positive loadings on F2 were aromatic or polyaromatic (Figure 3a). Contrarily to the projection with litter samples not all aromatics and polyaromatics showed high positive loadings (Figure 2a). Since F2 is again interpreted to reflect recalcitrance, this may suggest that (poly)aromatics with high positive loadings on F2 relatively accumulate during degradation; these compounds included toluene (Ar2), (C_1,C_2)benzenes (Ar2-Ar4, Ar6, Ar8, Ar12, Ar13), indene (Pa1), (C_1)naphthalenes (Pa2, Pa7, Pa8), biphenyl (Pa9), fluorene (Pa14) and phenanthrene (Pa18).

Combining these observations it is possible to divide the plot into distinct regions, which are identified in Figure 3a. These regions are related to source and transformations of SOM. The cluster with high positive loadings on F1 is characterized by LMW compounds associated to DOM, while straight chain aliphatics showed high negative loadings and reflect relatively degraded SOM. The top of the diagram reflects microbial and recalcitrant charred material, with high positive loadings on F2. The high negative loadings on F2 is related to compounds from relatively intact plant material. This distribution suggests that compounds that contribute DOM are mainly derived from two sources, being lignin and microbial and recalcitrant charred material (indicated by the arrows in Figure 3 a).

Both AE samples that project in the lower left corner of Figure 3b are from strongly rooted profiles and are in fact very similar to A horizon samples because the majority of their OM is derived from roots

In the F3–F4 projection (Figure 4a), long chain n-alkanes clearly formed a cluster with high positive loadings on F3. Long chain n-alkanes originate from leaf waxes (EGLINTON; HAMILTON, 1967), which indicates a high contribution from leaf waxes to the E horizons that all showed positive scores on F3 (except for the AE horizons from profiles P31 and P32; Figure 4 b).
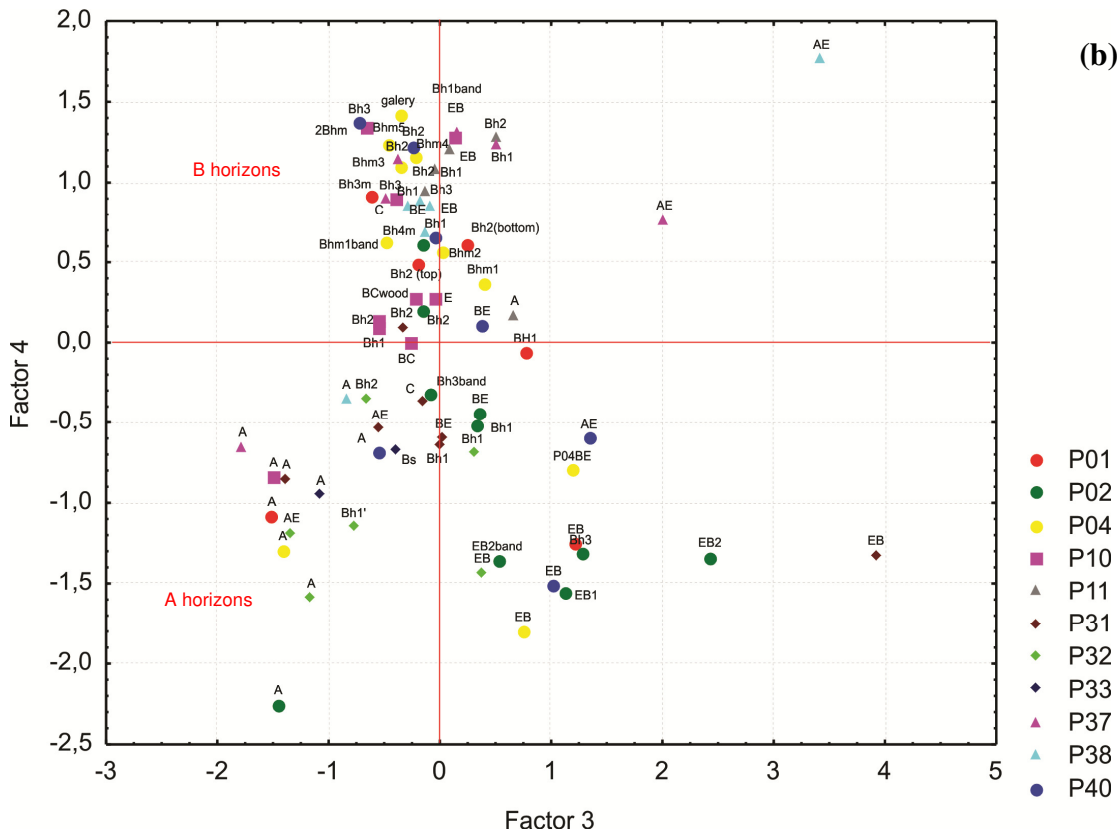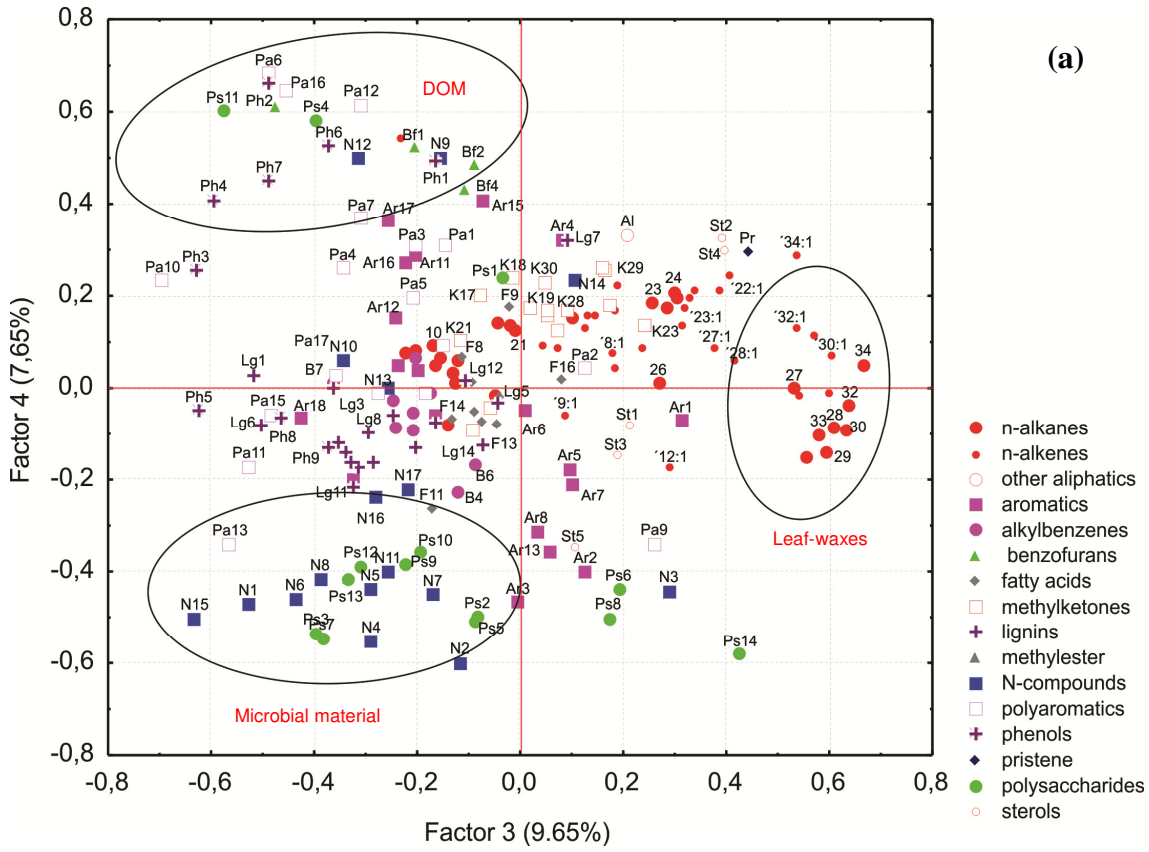
Figure 4 - (a) Projection of the factor loadings of the pyrolysis products without litter samples in F3-F4 space; (b) Projection of the factor scores without litters samples in F3-F4 space

F4 mainly separated two groups of compounds, both with negative loadings on F3. Compounds that showed (moderately) negative loadings on F4 included most N-compounds and most carbohydrates, pointing towards microbial material. The factor scores clearly showed that this corresponds to A (negative on F3) and EB (positive on F3) horizons. A high microbial activity in the A horizons is in line with continuous fresh plant input, while for the EB horizons it is associated with the decomposition of OM, leaving some whitish SOM-depleted mottles (See Chapter 4). The interpretation of levoglucosan is not straight-forward because many factors contributed to its explained variance (Appendix C), though F4 explained the major part. The association of levoglucosan with microbial matter is not in line with the literature but has been previously reported from loess palaeosols (VANCAMPENHOUT et al., 2009).

The cluster with positive loadings on F4 included polyaromatics with oxygen groups (Pa6, Pa12, Pa16), carbohydrates Ps4 and Ps11, phenols and benzofurans and N12, of which the carbohydrates, phenols and benzofurans were associated with DOM on F1. The scores show that all Bhm samples from profile P04, P02 and P40 showed positive scores on F4. This suggest either a second source/type of DOM or a selective degradation over time of all but the most recalcitrant compounds. The interpretation of the factor analysis is summarized in Table 2.

Table 2 - Summary of interpretation of loadings factor analysis

	Positive	Negative
F1	Phenolic DOM	Macromolecular structures
F2	Microbial/charred plant material	Fresh plant material
F3	Leaf waxes	-
F4	(Poly)aromatic DOM	Microbial material

3.3.3.1 Interpretation of the profiles: relation between morphology and chemical composition

3.3.3.1.1 Poorly-drained profiles

Profile P01

The P01 profile shows little chemical variation between the various horizons. All P01 B horizons have a contribution of phenolic DOM (F1F2), but the EB has a high contribution from microbial matter (F4), like all EB horizons. Samples of the lower B horizons, Bh2(bottom) and Bh3m, are both morphologically and chemically very similar (as described in Chapter 2). Scores on F4 indicated that these also have a high contribution from DOM with polyaromatics with oxygen functional groups, meanwhile the Bh1 and Bh2(top) have a some contribution of microbial material. Although profile P01 was formed under hydromorphic conditions, the upper part of the profile shows good drainage at present. Apart from some admixture of microbial material at the top of the B horizon, there is no clear overprint of recent processes on the older horizons.

Profile P02

This profile has morphological characteristics similar to those of P01, but the influence of processes that occur under well-drained conditions is clearer (see chapter 2). There is a clear breakdown of part of the former poorly-drained B horizon, accompanied by the accumulation of more recent SOM on the fringe of remnants of the older B (EB1, Bh1). In addition, there are black SOM bands in the E and B horizons that are clearly unrelated to the older morphology (Chapter 2). These bands have a high contribution from aromatic DOM (F3F4). The samples of the original poorly drained B horizon (Bh3, Bh4m) plot in the region influenced by phenolic DOM (F1F2) and the horizons affected by better-drained conditions (EB, BE and Bh1) had a influence of microbial material (F1F2). The two samples of recent SOM accumulation: EB2band and Bh3band represent a decomposed SOM with a strong influence of aromatic and polyaromatic material (F1F2) and microbial material (F3F4). The difference between the samples of the two SOM bands (the concentration of toluene (Ar2) is higher in the SOM band sample of EB2 horizon than in the Bh3 horizon) may indicate that the SOM band sample of EB2 horizon may be under greater influence of microbial material

and that in the Bh3 horizon has a larger proportion of charred material. This may be due to the position of the EB2 horizon surrounded by the E horizon.

Profile P04

This profile has a very-well developed and thick B horizon of about 3.5 m. It was formed under conditions of extreme hydromorphism and is still influenced by tides, although the upper portion of the profile is situated above mean high tide.

The cemented B horizon samples has a high contribution of both phenolic (F1F2) and polyaromatic (F3F4) DOM. The BE horizon plots nearly the B horizon samples (F1), while the EB present a high contribution from microbial material (F4), indicating an increase in microbial material toward the top due to improved drainage and microbial decomposition of the top of the B horizon. A single sample of SOM accumulation around a *Callichirus major* gallery (GA) plotted with the Bhm horizons of this profile. indicating that SOM has the same origin, but it showed especially high scores on F4, thus also a high contribution from 'degraded polyaromatics'.

Profile P40

The morphological features are very similar to those of profiles P04 and P01, but without a cemented B horizon. The A horizon had a low contribution from microbial matter according to F4, while the AE horizon has a more contribution of fresh plant material (F2). This implies that the AE has larger lignin contents than the A horizon, probably due to the presence of roots in the AE horizon.

The samples of the B horizons present a contribution of (poly)aromatic DOM (F4) and some contribution from microbial and charred plant material (F2). This suggests that, although the morphology of P40 indicates accumulation of OM in a wet environment, the present better drained position led to decay of OM throughout the B horizon and admixture of burnt material.

3.3.3.1.2 Profiles with well-drained B horizons

Profile P31

This is a well-drained profile that showed considerable decomposition at the top of the B horizon (Chapter 2). The morphology of the B horizon suggests that the OM is largely root-derived and that a local DOM fraction has stained the lower part of this horizon (Chapter 2). Similar to other profiles, the transformation of the A into the AE horizon involves a loss of lignins. The B and BC horizon samples has a high contribution from burnt material (charred plant material, F2). The EB showed particularly high positive scores on F3 indicating a high contribution from leaf wax *n*-alkanes and carbohydrates, particularly levoglucosan.

Profile P32

Profile P32 has well-drained morphology, but there appears to be a preferential drainage through inclined root channels OM accumulation in the B horizon is restricted to the periphery of these channels (Chapter 2).

The change from A to AE horizon is similar to that in profile P31. The EB and Bh1 and Bh2 horizons plot close together in the region with the high contribution from charred plant material (F2) and has low contribution from phenolic DOM (F1), also indicated by negative scores on F4 for all samples. The Bh1' horizon (located in a slightly higher and better drained position relative to the EB, Bh1 and Bh2 horizons, (Chapter 2)) showed lowest scores on F2, indicating less contribution from charred plant material and a high negative score on F4, indicating a influence from microbial material.

Profile P33

Profile P33 lies at the top of the beach ridge in the beach-ridge-swale transect of profile P31-33 (Chapter 2). Only the A and the Bs horizon were analyzed. In this well-drained profile, the composition of the B horizon OM indicates a high accumulation of charred plant material (F2).

3.3.3.1.3 Rooted Profiles

These profiles combine present good drainage with indications of (weak) former DOM accumulation through groundwater flow. They all have a high contribution from (ploy)aromatics DOM.

Profile P11

The A horizon sample contains an appreciable amount of lignin and primary polysaccharides (fresh plant material, F2), but a less content from microbial material (F4) than the P37 and P38 A horizons.

Profile P11 has many decaying roots throughout the E, EB and Bh1-2 horizons (Chapter 2). Samples of EB, Bh1 and Bh2 horizons has a relative accumulation of recalcitrant plant macromolecules (straight-chain aliphatics, F1) and a high contribution from burnt material (charred plant material, F2). Roots do not appear to influence the lignin content of these horizons. The Bh3 horizon sample plots nearly the cemented horizons, in the region with a contribution of phenolic DOM (F1).

Profile P37

The AE horizon present a high influence by leaf waxes (F3) and fresh plant material (F2), like the P38 AE horizon. All samples of the deeper horizons has a high contribution of charred plant material (F2) and some contribution from (poly)aromatic DOM (F4).

Profile P38

Profile P38 is very similar to the previous one, but is has more clear signs of B horizon decomposition (EB and BE horizons), while the rather homogeneous colors of the lower B horizon may indicate some accumulation of groundwater-derived DOM (Chapter 2). The lower Bh2 horizon plotted together with the cemented horizons of poorly-drained profiles, had a high contribution from phenolic DOM (F1). The EB and BE horizons present an accumulation of burnt material (F2), like the P11 EB, Bh1 and Bh2 horizons.

The combination of properties suggests that this was originally a hydromorphic profile with accumulation of groundwater-transported DOM. At present, drainage is better, which has led to significant decomposition in the top of the former B (EB and BE horizons).

3.3.3.1.4 Superposed profiles

Profile P10

This is a well-drained profile with a buried tree trunk near its base, and underneath a layer with eroded remnants of an earlier, cemented B horizon. The A horizon of this profile is strongly rooted, with a high contribution from fresh plant material (F2) and some content of microbial material (F4). The E and the EB horizon indicate progressive decomposition with a strong increase in both macromolecular structures (F1) and charred plant material (F2). The buried BC horizon (BCwood) and especially the remnants of the eroded Bhm horizon (2Bhm) indicate a strong influence of phenolic DOM (F1). These two horizons have a strong similarity to the B horizons of the poorly drained profiles described above, and it is likely that these remains are indeed remnants of the same old profile. The wood trunk was dated at 1,500 years which means that the eroded profile is considerably older than the superposed horizons (Chapter 2).

3.4 Conclusions

The B horizons of well-drained Podzols differ in characteristics from the poorly drained ones in composition, deposition and source of OM (some from phenolic DOM and some from (poly)aromatics DOM), as well as its decomposition, which is directly related to the activity of groups of microorganisms. They also differ in the relative contribution of OM-derived from roots (fresh plant material), DOM, microbial material and charred plant material.

The composition of DOM within one profile may depend on its location, and recent DOM frequently has a different composition from the DOM that is preserved in B-horizons.

The grouping of profiles not differ only in the soil morphology properties and features but in the OM chemical composition and their sources.

References

ALCAÑIZ, J.M.; GRANADA, E.; COMELLAS, L. Simulating the effects of burning on soil organic matter in a forest soil studied by pyrolysis gas chromatography. In: SENESI, N.; MIANO, T.M. (Ed.). **Humic substances in the global environment and implications on human health.** Amsterdam: Elsevier, 1994. p. 205-212.

ALMENDROS, G.; GUADALIX, M.E.; GONZÁLEZ-VILA, F.J.; MARTIN, F. Preservation of aliphatic macromolecules in soil humins. **Organic Geochemistry**, Oxford, v. 24, p. 651-659, 1996.

BRACEWELL, J.M.; ROBERTSON, G.W. Quantitative comparison of the nitrogen-containing pyrolysis products and amino acid composition of soil humic acids. **Journal of Analytical & Applied Pyrolysis**, Amsterdam, v. 6, p. 19–29, 1984

BUGGLE, B.; WIESENBERG, G.L.B.; GLASER, B. Is there a possibility to correct fossil n-alkane data for post-sedimentary alteration effects? **Applied Geochemistry,** Oxford, v. 25, p. 947–957, 2010.

BUURMAN, P.; ROSCOE, R. Different chemistry of free light and occluded light and extractable SOM fractions in soils of Cerrado. tilled and untilled fields. Minas Gerais Brazil: a pyrolysis-GC/MS study. **European Journal of Soil Science**, Oxford, v. 62, p. 253-266, 2011.

BUURMAN, P.; PETERSE, F.; MARTIN, G.A. Soil organic matter chemistry in allophonic soils: a pyrolysis-GC/MS study of a Costa Rican Andosol catena. **European Journal of Soil Science**. Oxford, v. 58, p. 1330-1347, 2007.

BUURMAN, P.; VIDAL-TORRADO, P.; LOPES, J.M. The podzol hydrosequence of Itaguaré. São Paulo. Brazil. 2. Soil organic matter chemistry by Pyrolysis-GC/MS. **Soil Science Society of America Journal,** Madison, v. 77, n.4, p. 1307-1318, 2013.

BUURMAN, P.; VIDAL-TORRADO, P.; MARTINS, V.M. The podzol hydrosequence of Itaguaré (Sao Paolo, Brazil). 1. Geomorphology and interpretation of profile morphology. **Soil Science Society of America Journal, Madison**, v. 77, n. 4, p. 1294-1306, 2013.

BUURMAN, P.; NIEROP, K.G.J.; KAAL, J.; SENESI, N. Analytical pyrolysis-GC/MS and thermally assisted hydrolysis and methylation of EUROSOIL humic acid samples. **Geoderma**, Amsterdam, v. 150, p. 10–22, 2009.

BUURMAN, P.; NIEROP, K.G.J.; PONTEVEDRA-POMBAL, X.; MARTINEZ-CORTIZAS, A. Molecular chemistry by pyrolysis-GC/MS of selected samples of the Penido Vello peat deposit. Galicia. NW Spain. In: MARTINI, I.P.; MARTINEZ-CORTIZAS, A.; CESWORTH, W. **Peatlands:** evolution and records of environmental and climate change. Amsterdam: Elsevier, 2006. chap. 10, p. 217-240.

BUURMAN, P.; SCHELLEKENS, J.; FRITZE, H.; NIEROP, K.G.J. Selective depletion of organic matter in mottled podzol horizons. **Soil Biology and Biochemistry,** Oxford. v. 39. p. 607-621, 2007.

BUURMAN, P.; VAN BERGEN, P.F.; JONGMANS, A.G.; MEIJER, E.L.; DURAN. B.; VAN LAGEN, B. Spatial and temporal variation in podzol organic matter studied by pyrolysis-gas chromatography/mass spectrometry and micromorphology. **European Journal of Soil Science**, Oxford, v. 56, p. 253–270, 2005.

DAVID, M.B.; ZECH, W. Adsorption of dissolved organic carbon and sulfate by acid forest soils in the Fichtelgebirge FRG. **Journal of Plant Nutrition and Science**, Weinheim, v. 153, p. 379-384, 1990.

EGLINTON, G.; HAMILTON, R.J. Leaf epicuticular waxes. **Science**, Washington, v. 156, p. 1322-1325, 1967.

GALLETTI, G.C.; REEVES, J.B. Pyrolysis/gas chromatography/ion trap detection of polyphenols (vegetable tannins): preliminary results. **Organic Mass Spectromety**, Chichester, v. 27, p. 226-230, 1992.

GONZÁLEZ-PÉREZ, J.A.; GONZÁLEZ-VILA, F.J.; ALMENDROS, G.; KNICKER, H. The effect of fire on soil organic matter: a review. **Environment International**, Oxford, v. 30, p. 855–870, 2004.

GONZÁLEZ-PÉREZ, M.; BUURMAN, P.; VIDAL-TORRADO, P.; MARTIN-NETO, L. Pyrolysis-gas chromatography/ mass spectrometry characterization of humic acids in Spodosols under Atlantic forest in Southeastern Brazil. **Soil Science Society of America Journal**. Madison, v. 76, p. 961-971, 2012.

JANSEN, B.; NIEROP, K.G.J. Methyl ketones in high altitude Ecuadorian Andosols confirm excellent conservation of plant-specific n-alkane patterns. **Organic Geochemistry**, Oxford, v. 40, p. 61-69, 2009.

KAAL, J.; MARTÍNEZ-CORTIZAS, A.; NIEROP, K.G.J. Characterisation of aged charcoal using a coil probe pyrolysis-GC/MS method optimised for black carbon. **Journal of Analytical and Applied Pyrolysis**, Amsterdam, v. 85, p. 408-416, 2009.

KAAL, J.; MARTÍNEZ-CORTIZAS, A.; NIEROP, K.G.J.; BUURMAN, P. A detailed pyrolysis-GC/MS analysis of a black carbon-rich acidic colluvial soil (Atlantic ranker) from NW Spain. **Applied Geochemistry**, Oxford, v. 23, p. 2395-2405, 2008.

KACZOREK, D.; SOMMER, M.; ANDRUSCHKEWITSCH, L.; OKTABA, L.; CZERWINSKI, Z.; STAHR, K. A comparative micromorphological and chemical study of "Raseneisenstein" (bog iron ore) and "Orstein". **Geoderma**. Amsterdam, v. 121, p. 83-94, 2004.

KILLOPS, S.; KILLOPS, V. **Introduction to organic geochemistry**. Malden: Blackwell, 2005. 408 p.

KINDEL, A.;GARAY, I. Humus form in ecossystems of the Atlantic Forest. Brazil. **Geoderma**, Amsterdam, v. 108, p. 101-118, 2002.

KLOTZBUCHER, T.; KAISER, K.; GUGGENBERGER, G.; GATZEK, C.; KALBITZ, K. A new conceptual model for the fate of lignin in decomposing plant litter. **Ecology**, Washington, v. 92, p. 1052–1062, 2011.

KONDO, T.; OHSHITA, T.; KYUMA, T. Ester- and ether-linked phenolic acids in orchardgrass (*Dactylis glomerata* L.) and their digestion from cell walls when fed to sheep. **Canadian Journal of Botany**, Ottawa, v. 71, p. 1179-1182, 1991.

LEINWEBER, P.; SCHULTEN, H.R. Advances in analytical pyrolysis of soil organic matter. **Journal of Analytical and Applied Pyrolysis**, Amsterdam, v. 49, p. 359-383, 1999.

NIEROP, K.G.J. Origin of aliphatic compounds in a forest soil. **Organic Geochemistry**, Oxford, v. 29, p. 1009-1016, 1998.

NIEROP, K.G.J.;VERSTRATEN, J.M. Organic matter formationin sandy subsurface horizons of Dutch coastal dunes in relation to soil acidification**. Organic Geochemistry**, Oxford, v. 34, p. 499 -513, 2003.

NIEROP, K.G.J.; PULLEMAN, M.M.; MARINISSEN, J.C.Y. Management induced organic matter differentiation in grassland and arable soil: a study using pyrolysis techniques. **Soil Biology and Biochemistry**, Oxford, v. 33, p. 755-764, 2001.

POIRIER, N.; SOHI, S.P.; GAUNT, J.L.; MAHIEU, N.; RANDALL, E.W.; POWLSON, D.S. The chemical composition of measurable soil organic matter pools. **Organic Geochemistry**, Oxford, v. 36, p. 136-151, 2005.

POUWELS, A.D.; EIJKEL, G.B.; BOON, J.J. Curie-point pyrolysis-capillary gas chromatography-high-resolution mass spectrometry of microcrystalline cellulose. **Journal of Analytical and Applied Pyrolysis**, Amsterdam, v. 14, p. 237-280, 1989.

POUWELS, A.D.; TOM, A.; EIJKEL, G.B.; BOON, J.J. Characterisation of beech wood and its holocellulose and xylan fractions by pyrolysis-gas chromatographymass spectrometry. **Journal of Analytical and Applied Pyrolysis**, Amsterdam, v. 11, p. 417-436, 1987.

RALPH, J.; HATFIELD, R.D. Pyrolysis-GC/MS characterization of forage materials. **Journal of Agricultural and Food Chemistry**, Washington, v. 39, p. 1426-1437, 1991.

SÁIZ-JIMÉNEZ, C. Production of alkylbenzenes and alkylnaphthalenes upon pyrolysis of unsaturated fatty acids. A model reaction to understand the origin of some pyrolysis products from humic substances? **Naturwissenschafte**n, Berlin, v. 81, p. 451-453, 1994.

SÁIZ-JIMÉNEZ, C.; de LEEUW, J.W. Chemical characterization of soil organic matter fractions by analytical pyrolysis-gas chromatography-mass spectrometry. **Journal of Analytical and Applied Pyrolysis**, Amsterdam, v. 9, p. 99-119, 1986.

SCHELLEKENS, J.; BARBERÁ, G.; BUURMAN, P. Potential vegetation markers – analytical pyrolysis of modern plant species representative of Neolithic SE Spain. **Journal of Archaeological Science**, Amsterdam, v. 40, p. 365–379, 2013.

SCHELLEKENS, J.; BUURMAN, P.; PONTEVEDRA-POMBAL, X. Selecting parameters for the environmental interpretation of peat molecular chemistry - A pyrolysis-GC/MS study. **Organic Geochemistry**, Oxford, v. 40, p. 678-691, 2009.

SCHELLEKENS, J.; BUURMAN, P.; FRAGA, I.; MARTÍNEZ-CORTIZAS, A. Holocene vegetation and hydrologic changes inferred from molecular vegetation markers in peat, Penido Vello, (Galicia, Spain). **Palaeogeography, Palaeoclimatology, Palaeoecology**, Amsterdam, v. 299, p. 56–69, 2011.

SCHMIDT, M.W.I.; NOACK, A.G. Black carbon in soils and sediments: analysis, distribution, implications, and current challenges. **Global Biogeochemical Cycles**, Washington, v. 14, p. 777–793, 2000.

SCHULTEN. H.R.; SCHNITZER. M. The chemistry of soil organic nitrogen: a review. **Biology and Fertility of Soils**. Berlin, v. 26, n. 1, p. 1-15, 1997.

SCHWARTZ, D. Some podzols on bateke sands and their origins. people's republic of Congo. **Geoderma**, Amsterdam, v. 43, p. 229-247, 1988.

STUCZYNSKI, T.I.; MCCARTHY, G.W.; REEVES, J.B.; WRIGHT, R.J. Use of pyrolysis GC/MS for assessing changes in soil organic matter quality. **Soil Science**, Baltimore, v. 162, p. 97-105, 1997.

TEGELAAR, E.W.; de LEEUW, J.W.; SÁIZ-JIMÉNEZ, C. Possible origin of aliphatic moieties in humic substances. **Science of the Total Environment**, Amsterdam, v. 81/82, p. 1-17, 1989.

TEGELAAR, E.W.; HOLLMAN, G.; VANDERVEGT, P.; de LEEUW, J.W.; HOLLOWAY, P.J. Chemical characterization of the periderm tissue of some angiosperm species -recognition of an insoluble. nonhydrolyzable. aliphatic biomacromolecule (suberan). **Organic Geochemistry**, Oxford, v. 23, p. 239-251, 1995.

THEVENOT, M.; DIGNAC, M.F.; RUMPEL, C. The fate of lignin in soils: A review. **Soil Biology and Biochemistry**, Oxford, v. 42, p. 1200–1211, 2010.

VANCAMPENHOUT, K.; WOUTERS, K.; De VOS, B.; BUURMAN, P.; SWENNEN, R.; DECKERS, J. Differences in chemical composition of soil organic matter in natural ecosystems from different climatic regions: a pyrolysis–GC/MS study. **Soil Biology and Biochemistry**, Oxford, v. 41, p. 568–579, 2009.

YASSIR, I.; BUURMAN, P. Soil organic matter chemistry changes upon secondary succession in Imperata grasslands, Indonesia; a pyrolysis-GC/MS study. **Geoderma**, Amsterdam, v. 173/174, p. 94–103, 2012.

4 MOLECULAR CHEMISTRY OF SOM-DEPLETED MOTTLES OF SOME TROPICAL COASTAL PLAIN PODZOL PROFILES (SE- BRAZIL)

Abstract

Some podzols shows organic matter-depleted light-colored mottles in various horizons. Such mottles are evidence of microbial activity. A change of hydrological position and improvement of drainage and aeration with time can result in strong changes, especially in the originally very poorly drained soils. Such morphological alterations include greater friability in subsurface horizons, accelerated decomposition of roots present in subsurface horizons that were protected by the anaerobic environment in depth; thickening of the E horizon with consequent thinning of the B horizon; introduction of mesofauna that can rework the OM by burrowing; and microbial degradation of OM. To understand the effect of depletion in these mottles, it is essential to know the chemical composition of the OM, and its differences with the surrounding soil. The chemical composition of SOM can be studied in detail using pyrolysis in combination with gas chromatography/mass spectrometry (Py-GC/MS). Samples were taken both from the center of the mottle (M) and from the direct surroundings (S) from distinct horizons of the studied profiles at Ilha Comprida. Of the seventeen profiles studied in this thesis, thirteen had depletion mottles scattered along the profile. Most of these mottles are whitish and are located preferentially at the transition of the E and B horizons, particularly in conditions of good drainage. Most of the mottles are related to OM decomposition by microorganisms, leaving whitish (or with a color slightly lighter than the soil matrix) mottles of many different shapes and sizes. Four extracted factors explained 63% of the variation in all pyrolysis products; Factors 1 and 2 together explained 44%. The interpretation from factor analysis is summarized: (a) F1 positive – DOM (Bh horizons), F1 negative – degraded SOM (E horizons); (b) F2 positive – microbial material, F2 negative – burnt material. Detailed comparison of microbial and chemical data will be done in a future study, but these similar trends suggest that the chemical differences obtained with pyrolysis are clearly related to the microbial community. There is a wide variation in the characteristics of decomposition by microorganisms between the profiles of Podzols permanently exposed to air and marine spray (the cliffs) on Ilha Comprida and those more inland. There are therefore two main processes that change the morphology of Podzols (OM and composition): (a) change in drainage and rooting, and (b) exposure to air.

Keywords: Py-GC/MS; Tropical podzol; OM-depleted mottles by microorganisms; Improve drainage

4.1 Introduction

Some podzols have organic matter-depleted light-colored mottles in various horizons. Such mottles are evidence of microbial activity (BUURMAN et al., 2007). According to Buurman et al. (2007), some well-drained podzols have OM-depleted mottles mainly associated with root channels. The phenomenon is widespread in the Netherlands, Belgium

and Germany, and such depletion mottles have even been observed in recently exposed fossil podzols of Tertiary age.

Drainage is the factor that directly influences the formation of B-podzol horizons (SCHWARTZ, 1988; BUURMAN et al., 2006). A change of hydrological position and improvement of drainage and aeration can result in strong changes, especially in originally very poorly drained soils. Such morphological alterations include greater friability in subsurface horizons, accelerated decomposition of roots present in subsurface horizons that were protected by the anaerobic environment in depth; thickening of the E horizon with consequent thinning of the B horizon; introduction of mesofauna that can rework the OM by burrowing, and microbial degradation of OM (BUURMAN et al., 2005, 2013).

A previous joint research with Silva et al. (2014) evaluated the community structure and diversity of *Bacteria* and *Archaea* in well-drained Podzols and OM-depleted mottles from Bertioga and Ilha Comprida, State of São Paulo. Significant differences were observed in the community structures of *Bacteria* and *Archaea* between depleted mottles and the adjacent soil. There was less diversity in bacterial groups in the depleted mottles than in the adjacent soil, suggesting a special community in the depleted areas that was responsible for the depletion. In the podzols of Bertioga, *Pseudomonas* strains were prevalent, whereas in depleted patches of the Ilha Comprida profiles, *Acidobacteria* were dominant, suggesting the involvement of these groups in the selective degradation of OM in these spots.

To understand the effect of depletion in these mottles, it is essential to know the chemical composition of the OM, and its differences with the surrounding soil. The chemical composition of SOM can be studied in detail using pyrolysis in combination with gas chromatography/mass spectrometry (Py-GC/MS) (SCHULTEN; SCHNITZER, 1997; LEINWEBER; SCHULTEN, 1999; GONZÁLEZ-PÉREZ et al., 2012; BUURMAN et al., 2013).

4.2 Material and Methods

4.2.1 Samples

Samples were taken from distinct horizons of the studied profiles at Ilha Comprida, which are described in detail in Chapter 2. Samples were taken both from the center of the mottle (M) and from the direct surroundings (S). An example of the sampling is given in Figure 1; photographs of all sampled mottles are given in Appendix D. All analyzed samples

are mentioned in Table 1. The soil morphological analysis allowed a subdivision into three distinct groups: poorly-drained profile (P02, P04, P40); profiles with well-drained B horizons (P30, P31, P32, P34, P35); and strongly rooted profiles (P11, P37, P38).
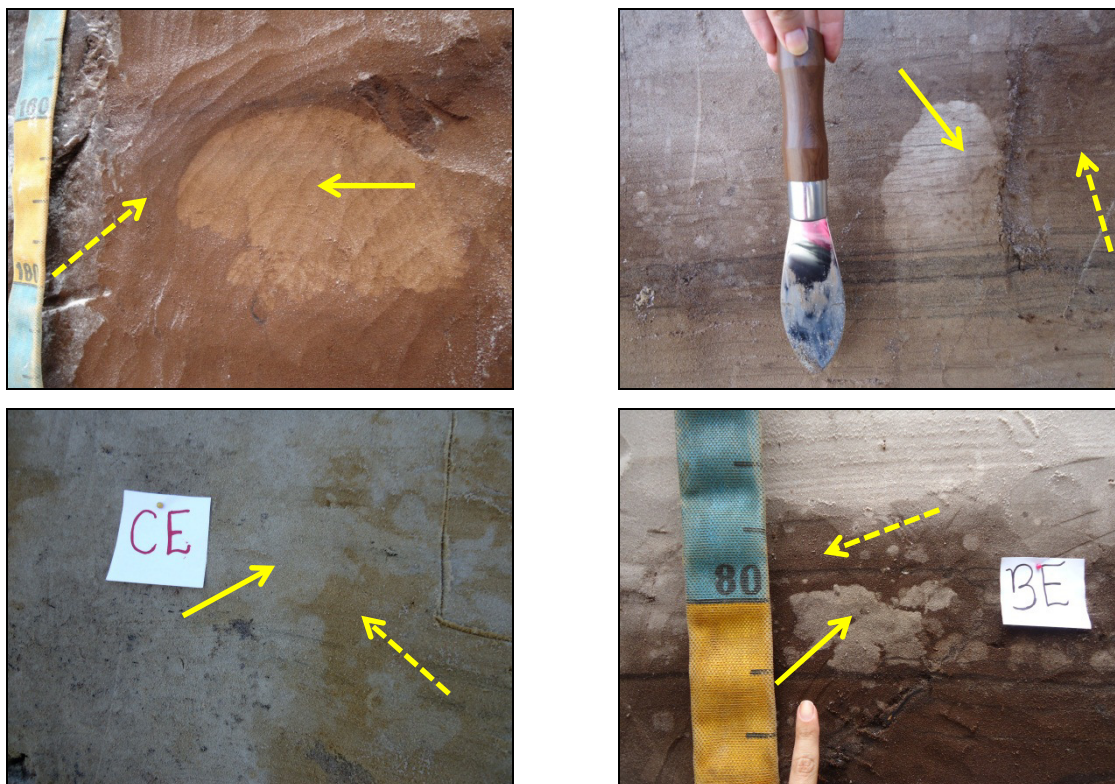
Figure 1 – Samples of mottles (arrow) and adjacent soil (dashed arrow). (a) Profile P04. Concentric OM-depleted mottles with color slightly lighter than the matrix; (b) Profile P31. Ghost OM-depleted mottle in the Bh2 horizon; (c) Profile 32. Irregular OM-depleted mottle in the CE horizon; (d) Profile 38. Irregular OM-depleted mottle in the BE horizon

4.2.2 Extraction and Purification of Organic Matter

Five grams of air-dried soil sample (< 2 mm) were mixed witch 25 mL of 0.1 M NaOH and shaken for 24 h. The suspension was centrifuged at 10,000 rpm for 1 hour and the extract was decanted. The extracts were then acidified to pH 1 with concentrated HCl to protonate OM. One mL of concentrated HF was added to dissolve silicates and increase the organic C content of the extracted fraction. The acid mixture was shaken for 48 h, after which it was dialyzed to neutral pH against distilled water to remove excess salt, using a dialysis membrane with a pore diameter of 10,000 Da. Finally, the solution was freeze-dried. In podzols, this procedure extracts virtually all non-particulate OM (BUURMAN et al., 2005). After extraction all residues showed the color of pure quartz sand.

4.2.3 Pyrolysis-Gas Chromatography/Mass Spectrometry

A micro-furnace single shot PY-3030S pyrolyser coupled to a GCMS-QP2010 (Frontier Laboratories LTD.) was used. The pyrolysis temperature was set at 600 ºC ± 0.1 ºC. The injection temperature of the GC (split 1:20) and the GC-MS interface were set at 320 ºC. The GC oven was heated from 50 to 320 ºC (held 10 min) at 15 ºC min^{-1}. The GC instrument was equipped with a Column UltraAlloy-5 (Frontier Laboratories LTD.), length 30 m, thickness 0.25 µm, diameter 0.25 mm with He as carrier gas. The MS was scanning in the range of m/z 45–600.

Compounds were identified using the NIST '05 library and pyrolysis-GC/MS literature (e.g., POUWELS et al., 1989; RALPH; HATFIELD, 1991; BUURMAN; PETERSE; MARTIN., 2007). After elimination of silica peaks, minor unidentified compounds and compounds that occurred in only one sample, 118 compounds remained and were quantified. The pyrolysis products were grouped according to probable origin and chemical similarity into a number of source groups: (i) aliphatic hydrocarbons, that includes n-alkanes, n-alkenes and n-methyl ketones, (ii) aromatics, (iii) polyaromatic hydrocarbons (PAHs) and benzofurans, (iv) n-fatty acids and esters, (v) lignin phenols, (vi) N containing compounds, (vii) phenols, and (viii) polysaccharides. Quantification of the relative contributions of pyrolysis products was based on the peak area of two characteristic ions using Masslab software. All quantifications were checked manually. The combined peak area of all quantified pyrolysis products (total peak area, TPA) was set at 100% and the relative proportions of the pyrolysis products were expressed as percentage of the TPA. The resulting quantification allows comparison of the abundance of the pyrolysis products within a data set.

4.2.4 Statistical Analysis

The quantified data set of 46 samples with 118 pyrolysis products each, was subjected to factor analysis using Statistica Version 8 (Statsoft, Tulsa OK, USA). Factor analysis is a statistical approach that can be used to analyze interrelationships among a large number of variables and to explain these variables in terms of their common underlying dimensions (factors). This method was mentioned earlier in this thesis on the Chapter 3.

4.3 Results and Discussion

4.3.1 Sampled podzol profiles

Of the seventeen profiles studied in this thesis, thirteen had depletion mottles scattered along the profile. Most of these mottles are whitish and are located preferentially at the transition of the E and B horizons, particularly in conditions of good drainage. Most of the mottles described in Chapter 2 are related to OM decomposition by microorganisms, leaving whitish (or with a color slightly lighter than the soil matrix) mottles of many different shapes and sizes.

4.3.1.1 General Chemistry

All quantified pyrolysis products and their mean abundance are listed in Appendix E. The possible origin of the compounds was discussed according to chemical group in Chapter 3.

Table 1 - Proportion (%) of groups of compounds for mottle (M) and adjacent soil samples (S)   (continues)

Profile sample	n-alka C_{13-25}	n-alka C_{25-31}	n-alke C_{13-25}	n-alke C_{25-31}	other	arom	benzof	fatty acids	methylk	lignins	mest	N-comp	polyar	phenols	polysac[a]
						Poorly-drained profiles									
P02Bh3-M	3.3	2.9	2.6	0.1	0.0	29.0	1.7	0.6	1.1	1.8	0.1	13.6	7.6	18.9	16.9
P02EB1-M	1.7	0.2	1.0	0.0	0.0	22.1	2.3	0.2	0.2	11.3	0.0	9.0	5.3	25.8	20.9
P04Bhm2-M	2.3	1.0	2.2	0.6	0.0	18.8	1.9	0.4	0.5	2.8	0.3	7.6	5.1	21.2	35.4
P04Bhm2-S	2.6	1.8	1.9	0.1	0.1	45.2	1.3	0.1	0.8	1.0	0.0	6.1	9.3	16.1	13.7
P04Bh2-M	0.8	0.1	0.8	0.0	0.0	20.0	2.6	0.2	0.1	5.9	0.1	10.0	4.4	26.3	28.7
P04Bh-S	1.2	0.5	0.9	0.0	0.0	18.1	3.0	0.4	0.0	7.7	0.1	14.5	5.1	20.4	28.0
P40BE/Bh1-M	3.1	0.9	2.0	0.0	0.1	24.5	1.6	0.3	0.1	1.9	0.1	15.1	6.7	20.6	23.0
P40BE/Bh1-S	3.1	1.0	2.2	0.6	0.1	23.7	1.9	0.5	0.2	4.5	0.1	15.4	7.3	22.8	16.5
P40Bh1-M	2.5	0.7	2.3	0.5	0.1	28.2	1.4	1.0	0.2	1.2	0.1	19.6	7.2	15.9	19.2
P40Bh1-S	2.1	0.5	1.7	0.0	0.1	21.5	2.0	1.1	0.1	4.4	0.1	15.0	5.9	23.1	22.3
P40Bh2-M	2.0	0.6	1.5	0.0	0.0	24.5	2.6	0.2	0.1	1.7	0.0	14.5	6.2	17.4	28.6
P40Bh2-S	2.3	1.7	0.7	0.0	0.2	20.6	3.0	0.5	0.0	7.7	0.1	13.6	6.1	17.7	26.0
						Profiles with well-drained B horizons									
P30Bh2-M	1.9	1.0	1.5	0.1	0.0	19.4	2.1	1.4	0.3	5.7	0.1	14.5	5.0	22.1	25.0
P30Bh2-S	2.0	0.5	1.1	0.1	0.0	16.8	2.2	0.5	0.3	11.2	0.1	13.8	5.1	25.4	21.0
P30EB-M	3.8	1.6	5.1	0.3	0.1	20.2	0.6	0.6	0.4	1.9	0.3	31.4	3.4	9.0	21.4
P30EB-S	5.1	1.3	5.9	1.0	0.1	28.6	1.3	0.8	0.6	4.2	0.3	13.7	7.0	13.1	16.7
P31Bh2-M	4.2	0.7	4.2	0.1	0.1	17.8	0.9	1.3	0.2	1.3	1.0	15.4	4.7	11.3	36.6
P31Bh2-S	2.3	1.3	1.8	0.0	0.1	18.4	2.2	0.5	0.1	7.4	0.3	16.6	5.0	21.1	23.0

Table 1 - Proportion (%) of groups of compounds for mottle (M) and adjacent soil samples (S) (continuation)

Profile sample	n-alka C_{13-25}	n-alka C_{25-31}	n-alke C_{13-25}	n-alke C_{25-31}	other	arom	benzof	fatty acids	methylk	lignins	mest	N-comp	polyar	phenols	polysac[a]
P31Bh1/Bh2-M	1.7	1.3	1.3	0.6	0.0	17.0	0.8	0.3	0.1	1.2	0.2	16.9	3.0	9.0	46.6
P31Bh1/Bh2-S	2.5	0.7	1.8	0.1	0.1	20.3	1.6	0.7	0.1	3.6	0.2	18.5	5.3	21.2	23.3
P32Bh1-M	3.3	1.8	2.9	0.3	0.1	15.9	1.3	0.4	0.1	7.1	0.4	14.3	4.0	11.1	37.2
P32Bh1-S	2.7	0.7	1.9	0.1	0.1	20.3	1.5	1.2	0.4	4.7	0.3	16.3	5.3	15.8	28.7
P32BE-M	2.5	0.8	1.6	0.0	0.0	19.6	1.0	0.3	0.2	1.4	0.3	16.6	4.7	11.8	39.2
P32BE-S	3.3	1.8	1.7	0.0	0.1	22.5	1.9	1.1	0.2	4.0	0.2	20.5	6.0	18.5	18.2
P32CE-M	5.6	2.3	4.5	2.0	0.3	19.8	1.2	0.7	1.1	2.4	0.4	18.8	5.2	15.3	20.6
P32CE-S	1.9	0.4	0.9	0.0	0.0	11.9	0.7	0.5	0.1	0.8	0.3	10.0	2.4	6.8	63.3
P34Bh2-M	2.9	0.7	2.8	0.5	0.1	21.0	1.5	0.8	0.2	4.9	0.6	19.7	5.3	16.3	22.7
P34Bh2-S	1.4	0.3	0.7	0.0	0.1	18.7	1.5	0.6	0.1	3.0	0.1	17.8	3.7	15.7	36.2
P34Bs-M	2.5	0.5	1.1	0.0	0.0	17.8	1.3	0.6	0.1	5.0	0.5	17.8	3.8	15.0	33.9
P34Bs-S	1.9	0.5	1.1	0.0	0.0	20.3	1.3	0.7	0.1	3.0	0.5	23.5	3.8	9.5	33.9
P35Bh1-M	2.6	0.6	2.3	0.2	0.1	16.3	0.7	0.5	0.1	2.8	0.6	21.0	3.3	8.7	40.2
P35Bh1-S	5.0	1.5	3.6	1.2	0.2	24.0	1.2	0.5	0.1	3.4	0.7	20.8	5.9	13.6	18.2
P35Bh2-M	2.9	2.1	1.4	0.0	0.4	23.3	1.4	0.6	0.2	2.7	0.3	18.4	5.9	13.9	26.7
P35Bh2-S	4.5	0.6	2.0	0.0	0.1	17.7	1.2	0.7	0.1	4.0	0.5	16.2	4.5	13.8	34.0
Strongly rooted profiles															
P11Bh2-M	1.0	0.6	0.5	0.0	0.0	17.8	3.0	0.1	0.1	10.9	0.0	11.8	5.3	23.5	25.3
P11Bh2-S	2.8	1.2	2.1	0.8	0.1	18.6	2.1	0.8	0.5	5.6	0.1	12.6	5.4	18.7	28.7

Table 1 - Proportion (%) of groups of compounds for mottle (M) and adjacent soil samples (S) (conclusion)

Profile sample	n-alka C_{13-25}	n-alka C_{25-31}	n-alke C_{13-25}	n-alke C_{25-31}	other	arom	benzof	fatty acids	methylk	lignins	mest	N-comp	polyar	phenols	polysac[a]
P11Bh1-M	1.8	1.0	1.3	0.0	0.1	18.2	2.3	0.2	0.2	13.0	0.1	12.9	4.6	22.2	22.0
P11Bh1-S	4.7	1.2	3.4	1.4	0.1	22.7	1.5	0.5	0.3	4.8	0.1	15.1	6.5	18.9	18.9
P37E-M	5.5	1.3	9.9	0.0	0.0	14.7	0.4	0.9	0.0	4.9	0.3	14.4	1.9	2.7	43.2
P37E-S	6.8	1.7	7.6	0.0	0.1	20.7	0.7	0.6	0.1	6.7	0.4	15.1	3.4	5.5	30.7
P38EB-M	8.6	2.3	10.8	2.3	0.1	24.0	1.0	0.8	0.1	6.8	0.2	17.7	5.2	7.3	12.7
P38EB-S	8.9	2.2	8.0	1.7	0.1	25.9	1.3	0.8	0.2	6.2	0.2	12.0	7.3	9.3	15.7
P38BE-M	6.7	1.0	5.9	0.8	0.1	26.0	1.5	0.7	0.2	5.3	0.2	13.1	7.7	10.7	20.0
P38BE-S	6.2	1.4	3.7	0.9	0.1	30.9	1.8	0.4	0.2	6.6	0.1	11.3	9.4	12.7	14.4
P38Bh2-M	1.9	0.8	1.4	0.0	0.1	16.6	1.9	0.4	0.2	6.7	0.1	12.8	4.2	18.1	34.7
P38Bh2-S	1.3	0.3	0.8	0.0	0.0	19.6	2.5	1.2	0.0	10.1	0.1	12.7	4.2	27.1	20.3

[a] *n*-alka = *n*-alkanes; *n*-alke = *n*-alkenes; other = other aliphatics; arom = aromatics; benzof = benzofurans; mket = methylketones; mest = methylester; N-comp = N-compounds; polyar = polyaromatics; polysac = polysaccharides

4.3.1.2 Factor analysis

Four extracted factors explained 63% of the variation in all pyrolysis products; Factors 1 and 2 together explained 44%. The projections of factor loadings and factor scores for the first two factors are given in Figure 2 and 3.
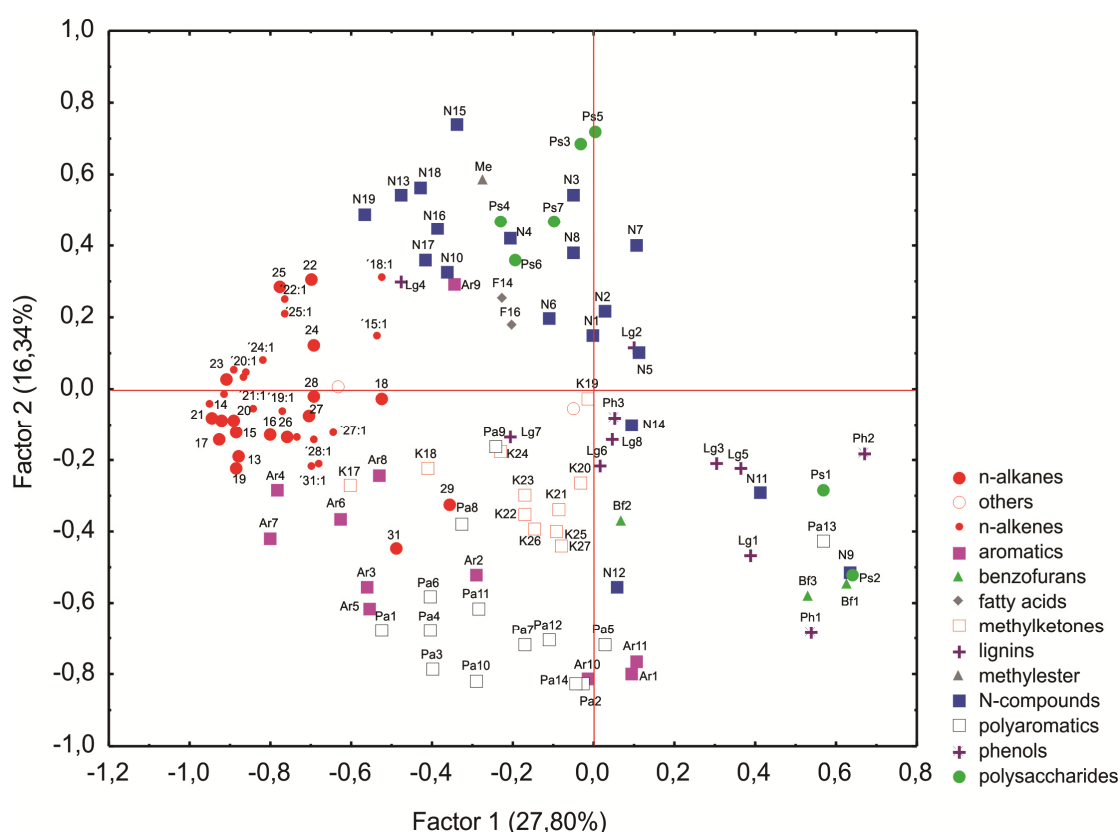
Figure 2 - Projection of the factor loadings in F1-F2 space

Compounds with positive loadings on F1 have been associated with DOM, and included phenols (Ph1-Ph3), benzofurans (Bf1-Bf3), acetic acid (Ps2), C_2 quinoline (N9; BUURMAN et al., 2005). On the other hand, the aliphatic compounds (*n*-alkanes and *n*-alkenes) presented high negatives loadings on F1. The projection of factor scores in F1-F2 space (Figure 3) showed that most E horizons (including EB and BE) were associated with aliphatic material (negative on F1), while Bh horizons generally had a higher contribution from DOM (positive on F1). All PAHs and aromatics presented negative loadings on F2. A high abundance of PAHs and aromatics points

towards burnt material. Compounds that presented high positive loadings on F2 included most N-compounds and some polysaccharides, including furaldehydes (Ps4, Ps6), butenoic acid (Ps3, Ps5) and levoglucosan (Ps7). A large abundance of N-compounds in SOM is generally linked with a higher degree of decomposition and a significant contribution from microbial material (NIEROP et al., 2001). The separation of microbial material and (poly)aromatics on F2 suggests that black carbon relatively accumulates during degradation (SCHMIDT et al., 2000). Combining these observations it is possible to relate to source and transformations of SOM. Bh horizons were characterized by DOM (positive on F1), while E horizons reflect relatively degraded SOM with relative accumulation of recalcitrant compounds (straight chain aliphatics, negative on F1). F2 reflects microbial *vs.* burnt material, represented by N-compounds and polysaccharides (positive on F2), and (poly)aromatics (negative), respectively. The interpretation from factor analysis is summarized in Table 2.

Table 2 - Summary of interpretation of factor analysis

	Positive	**Negative**
F1	DOM (Bh horizons)	Degraded SOM (E horizons)
F2	Microbial material	Burnt material

4.3.1.3 Relation between mottles and soil adjacent samples and chemical composition

Using the interpretation of factors (Table 2) it is now possible to identify trends from mottles to adjacent samples; the arrows in Figure 3 connect mottle (open symbol) samples with their corresponding soil adjacent samples (filled symbol). The arrows generally showed a shift from more negative to positive scores on F2 (except for samples from P32), indicating a loss of PAHs and an increase in microbial material in the mottles, suggesting that PAHs are degraded. Probably these microorganisms are consuming polyaromatic and aromatic compounds in the soil and leave microbial products characterized by N-compounds and sugars. In summary, the transformation of the soil adjacent into the mottles samples involves a loss of polyaromatics and aromatics and increase of N-compounds.

The largest shift are found in the E horizons (BE, EB and CE), while the shifts in the B horizon samples are generally minor, reflecting that the B horizons OM is less degraded yet (complexes with Al and Fe).

The large shift between adjacent soil and mottle of P32CE sample and their inversion of the tendency (arrow towards more negative scores on F2) may be due to the fact that this sample was different from the others (Appendix D). These samples were collected in a transition between the E and the C horizon, about 100 cm in depth, with more characteristics of C than E horizon, while all other samples were collected at the transition of B and E horizon. A chemical explanation for the deviating trend in this CE horizon is that the adjacent sample is already depleted in PAHs and further degradation causes a loss of secondary microbial products with aliphatics remaining.

The sequence of the E horizons on F2, from BE, EB, to E (from negative to positive scores) and then the CE pointing into the other direction, can be interpreted as a degradation gradient, and supports the interpretation of Buurman et al. (2007), that the E horizons expand due to microbial decomposition of SOM from the B horizon. The fact that the poorly drained profiles showed the smallest difference between mottle and adjacent soil, P40 (Bh2, BE) and P4 (Bhm2) also support this interpretation.
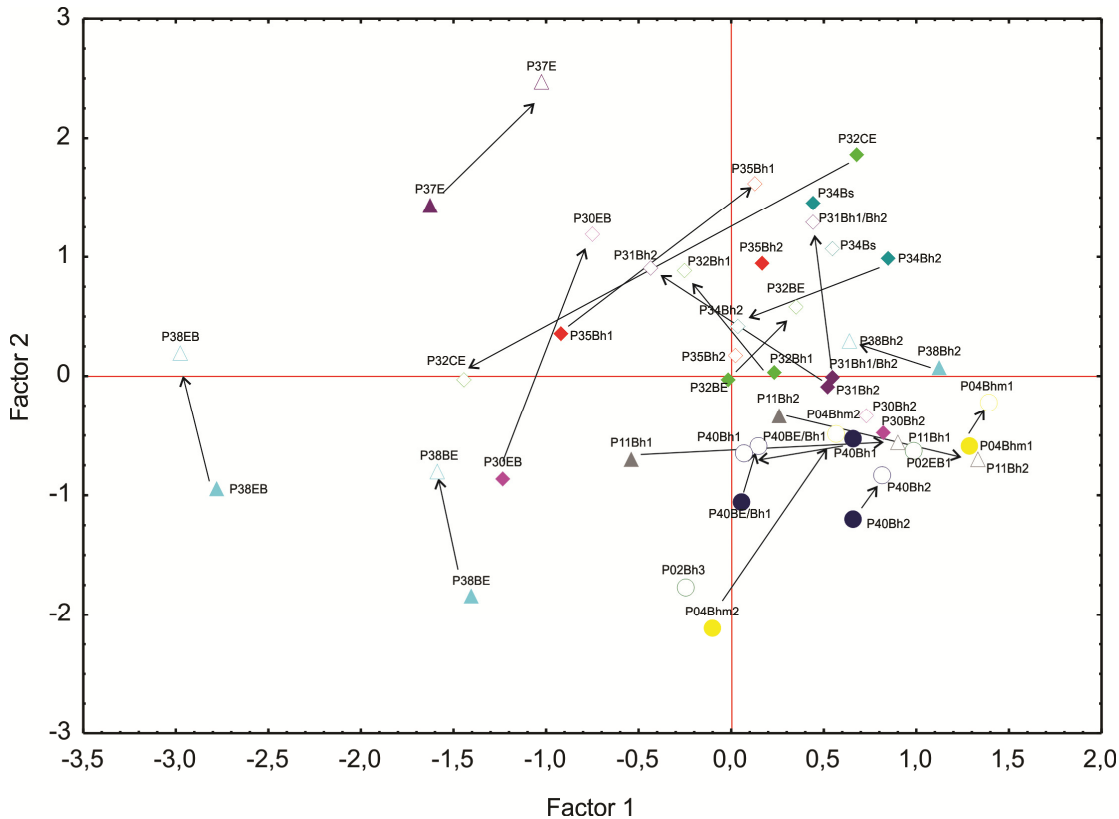
Figure 3 - Projection of the samples in F1-F2 space. The filled symbols represent the adjacent soil samples and the open symbols represent the mottle samples

The B horizons of poorly-drained profiles (P02, P04, P40) formed a cluster negative on F2 and positive F1 (Figure 3). These profiles have a very-well developed and thick B horizon and were formed under conditions of strong hydromorphism. This provides further support for the interpretation of F1, reflecting DOM with positive values.

The well-drained profiles (P30, P31, P32, P33, P34, P35), that showed considerable decomposition at the top of the B horizon (see Chapter 2), formed a cluster with mostly positive scores on both F1 and F2. These profiles showed particularly high positive scores on F2 indicating a high contribution from microbial material.

The strongly rooted profiles (P11, P37, P38) presented preferentially negative scores on F1. However, the fact that most of them were samples from the E, EB or BE horizons (except the Bh samples from profiles P37 and P38), makes it difficult to connect the chemical difference to the presence of roots. These profiles combine present good drainage with indications of (weak) former DOM accumulation through groundwater flow on the Bh horizons (see Chapter 3).

Well-drained profiles were those with greater amounts of depletion mottles, as well as the top of the Bh horizon from poorly-drained profiles. These SOM-mottles mainly indicate the presence of microorganisms that are consuming the OM present in the soil leaving almost only the mineral material, mostly quartz with some occurrence of heavy minerals such as ilmenite (MARTINEZ, 2015).

The mottle samples of Bh2 horizons contain less benzofurans than adjacent soil samples, i.e. P04-Bh2 (2.6% in mottles and 3.0% in adjacent soil); P31-Bh2 (0.9% in mottles and 2.2% in adjacent soil); P38-Bh2 (1.9% in mottles and 2.5% in adjacent soil). It is likely that microorganisms are consuming the benzofuran compounds, because benzofurans are probably more easily degradable than PAHs. The P11 samples not present the same tendency, the mottles samples have more benzofurans compounds than adjacent soil.

4.4 Conclusions

There are different groups of SOM-depleted mottles (see Chapter 2) which may be related to different groups of microorganisms. According to Matos (2015), there is a differentiation of the types of microorganisms present in these podzols, grouped into podzols with good, intermediate and poor drainage. Applying a factor analysis on the identified microbes using the same data set, showed similar trends: i) separation of the E and B horizons by F1, ii) a shift on F2 from mottle to adjacent sample into the same direction, iii) major shifts between mottle and corresponding adjacent sample in the E horizons, and iv) similar sequence of well drained, and poorly drained profiles on F2 (data not shown). A detailed comparison of microbial and chemical data will be done in a future study, but these similar trends suggest that the chemical differences obtained with pyrolysis are clearly related to the microbial community.

References

BUURMAN, P.; PETERSE, F.; MARTIN, G.A. Soil organic matter chemistry in allophonic soils: a pyrolysis-GC/MS study of a Costa Rican Andosol catena. **European Journal of Soil Science**, Oxford, v. 58, p. 1330-1347, 2007.

BUURMAN, P.; VIDAL-TORRADO, P.; LOPES, J.M. The podzol hydrosequence of Itaguaré, São Paulo, Brazil. 2. Soil organic matter chemistry by Pyrolysis-GC/MS. **Soil Science Society of America Journal**, Madison, v. 77, n. 4, p. 1307-1318, 2013.

BUURMAN. P.; NIEROP. K.G.J.; PONTEVEDRA-POMBAL. X.; MARTINEZ-CORTIZAS. A. Molecular chemistry by pyrolysis-GC/MS of selected samples of the Penido Vello peat deposit. Galicia. NW Spain. In: MARTINI, I.P.; MARTINEZ-CORTIZAS, A.; CESWORTH, W. **Peatlands:** evolution and records of environmental and climate change. Amsterdam: Elsevier. 2006. chap. 10, p. 217-240.

BUURMAN, P.; SCHELLEKENS, J.; FRITZE, H.; NIEROP, K.G.J. Selective depletion of organic matter in mottled podzol horizons. **Soil Biology and Biochemistry**, Oxford, v. 39, p. 607-621, 2007.

BUURMAN, P.; VAN BERGEN, P.F.; JONGMANS, A.G.; MEIJER, E.L.; DURAN, B.; VAN LAGEN, B. Spatial and temporal variation in podzol organic matter studied by pyrolysis-gas chromatography/mass spectrometry and micromorphology. **European Journal of Soil Science**, Oxford, v. 56, p. 253–270, 2005.

GONZÁLEZ PÉREZ, M.; BUURMAN, P.; VIDAL-TORRADO, P.; MARTIN-NETO, L. Pyrolysis-gas chromatography/ mass spectrometry characterization of humic acids in Spodosols under Atlantic forest in Southeastern Brazil. **Soil Science Society of America Journal**, Madison, v. 76, p. 961-971, 2012.

LEINWEBER, P.; SCHULTEN, H.R. Advances in analytical pyrolysis of soil organic matter. **Journal of Analytical and Applied Pyrolysis**, Amsterdam, v. 49, p. 359-383, 1999.

MARTINEZ, P.H.R.M. **Relações sedimentologia-geomorfologia-hidrologia e seus efeitos na gênese de Espodossolos sob Restinga na Ilha Comprida-SP**. 2015. 157 p. Dissertação (Mestrado em Solos e Nutrição de Plantas) - Escola Superior de Agricultura "Luiz de Queiroz", Universidade de São Paulo, Piracicaba, 2015

MATOS, E.R. **Variações das estruturas das comunidades de bactérias e fungos em Espodossolos sob diferentes regimes de drenagem**. 2015. 153 p. Tese (Doutorado em Microbiologia Agrícola) - Escola Superior de Agricultura "Luiz de Queiroz", Universidade de São Paulo, Piracicaba, 2015.

NIEROP, K.G.J.; PULLEMAN, M.M.; MARINISSEN, J.C.Y. Management induced organic matter differentiation in grassland and arable soil: a study using pyrolysis techniques. **Soil Biology and Biochemistry**, Oxford, v. 33, p. 755-764, 2001.

POUWELS, A.D.; EIJKEL, G.B.; BOON, J.J. Curie-point pyrolysis-capillary gas chromatography-high-resolution mass spectrometry of microcrystalline cellulose. **Journal of Analytical and Applied Pyrolysis**, Amsterdam, v. 14, p. 237-280, 1989.

RALPH, J.; HATFIELD, R.D. Pyrolysis-GC/MS characterization of forage materials. **Journal of Agricultural and Food Chemistry**, Washington, v. 39, p. 1426-1437 1991.

SCHMIDT, M.W.I.; NOACK, A.G. Black carbon in soils and sediments: analysis, distribution, implications, and current challenges. **Global Biogeochemical Cycles**, Washington, v. 14, p. 777–793, 2000.

SCHULTEN, H.R.; SCHNITZER, M. The chemistry of soil organic nitrogen: a review. **Biology and Fertility of Soils**, Berlin, v. 26, n. 1, p. 1-15, 1997.

SCHWARTZ. D. Some podzols on bateke sands and their origins. people's republic of Congo. **Geoderma**. Amsterdam. v. 43, p. 229-247, 1988.

SILVA, K.J.; VIDAL-TORRADO, P.; LAMBAIS, M.R. Bacterial and Archaeal communities in Bleached Mottles of Tropical Podzols. **Microbial Ecology**, New York, v. 69, p. 372-382, 2014.

5   FINAL CONSIDERATIONS

The study area was chosen because to present a chronosequence of Podzols, with easy access, with very distinct evidence of formation and soil degradation. It was possible to describe morphologically the details of these soils along almost the entire cliff, grouping them by similarities in four key groups and establish identification parameters for each group, such as: drainage variation; presence and abundance of roots; presence and morphology OM-depleted mottles, etc. This chronosequence of Podzols located along 3 km long may, in a way, represent the all kind of Podzols found around the São Paulo coast. A detailed description of the morphology, as shown in this work, it is essential to better understand the formation and degradation of these soils and the possibles way to its maintenance.

The study of OM chemistry was essential for a better understanding of the possible sources of this OM and how it is distributed throughout the profile, and throughout the Podozlos sequence of the cliff. It was possible to establish that the chemistry of the OM is directly related to the morphogenetic classification of horizons and profiles of these soils.

The detailed morphological description of OM-depleted mottles and its chemical characterization allowed to relate the possible differences between the mottles and types of Podzols profiles studied. Almost all kinds of OM-depleted mottles have been identified both in the cliff profiles, as in the pit, in the latter in smallest numbers. There were also differences in the type of OM-depleted mottles and its location in profile, showing that each distinct group of mottles may be the result of a summation of different features present in each part of the profile, as different groups of organisms (microrganisms and fauna); difference in drainage over the profile and between them (being the top of the B horizon well drained); different sources of OM; presence of roots; and others.

APPENDICES

Appendix A – General chemistry of all sample   (continues)

Horizon	Depth	pH (H₂O)	Ca	Mg	Na	K	Al	P	H+Al	MO	Corgᵃ	Fe	Al
	cm		...........................cmol$_c$ kg^{-1}...........................							..................g kg^{-1}..............			
						P01								
A	0-30	5.21	0.20	0.20	0.83	0.26	0.16	0.00	1.76	10.11	5.88	0.026	0.107
E1	30-70	5.14	0.15	0.07	0.22	0.05	0.02	0.00	0.20	0.00	0.00	0.016	0.095
E2	70-145	5.06	0.13	0.07	0.22	0.05	0.03	0.00	0.92	0.72	0.42	0.009	0.071
EB	145-165	4.73	0.13	0.07	0.17	0.08	0.08	0.00	0.86	1.08	0.63	0.018	0.088
Bh1	165-185	4.59	0.12	0.09	0.22	0.05	0.24	0.00	2.00	3.61	2.10	0.029	0.170
Bh2	185-315 (Top)	4.19	0.14	0.10	0.39	0.08	0.50	0.00	2.64	7.58	4.41	0.017	0.231
Bh2	185-315 (bottom)	4.16	0.22	0.36	5.22	2.30	0.02	0.00	3.26	10.11	5.88	0.005	0.303
Bh3m	315-345+	3.45	0.52	1.85	1.04	0.26	1.42	0.00	6.22	23.83	13.85	0.080	0.752
						P02								
A	0-20	4.32	0.26	0.17	0.78	0.33	0.19	0.75	1.98	9.03	5.25	0.029	0.111
E1	20-65	5.15	0.18	0.07	0.17	0.08	0.03	0.00	0.92	0.00	0.00	0.006	0.077
BE	65-73	4.91	0.19	0.09	0.17	0.05	0.47	16.33	3.68	8.66	5.04	0.015	0.557
EB1	73-95	5.23	0.22	0.10	0.09	0.05	0.07	1.94	1.30	0.72	0.42	0.000	0.141
E2	100-130	4.98	0.14	0.07	0.17	0.05	0.06	0.00	0.74	0.00	0.00	0.012	0.099
Bh1	75-90	4.89	0.25	0.14	0.17	0.08	1.00	25.95	4.88	16.25	9.44	0.089	1.483
Bh2	90-115	5.21	0.19	0.11	0.22	0.10	0.86	5.12	5.42	14.44	8.40	0.056	1.643
EB2	115-150	5.22	0.18	0.27	0.09	0.08	0.23	2.44	1.48	2.89	1.68	0.020	0.359
Bh3	135-180	4.78	0.19	2.26	0.13	0.08	0.53	19.80	3.14	9.75	5.67	0.041	0.635
Bh4m	180-240+	4.40	0.22	3.50	1.78	0.20	1.39	16.63	9.00	29.24	17.00	0.065	2.085
						P04								
A	0-40	5.34	0.22	0.14	0.57	0.26	0.16	0.95	1.98	10.47	6.09	0.015	0.031
E	40-110	5.59	0.12	0.06	0.09	0.05	0.02	0.00	1.16	0.00	0.00	0.001	0.000
EB	110-130	4.61	0.15	0.07	0.17	0.08	0.12	0.00	1.54	1.08	0.63	0.000	0.055

Appendix A – General chemistry of all sample   (continuation)

Horizon	Depth	pH (H₂O)	Ca	Mg	Na	K	Al	P	H+Al	MO	Corg[a]	Fe	Al
	cm		..........................cmol$_c$ kg^{-1}..........................							................g kg^{-1}..............			
						P04							
BE	130-140	4.67	0.13	0.06	0.26	0.08	0.14	0.00	1.52	1.44	0.84	0.000	0.065
Bhm1	140-155	4.83	0.24	0.20	0.21	0.28	1.14	0.00	5.62	20.22	11.75	0.000	0.422
Bhm2	155-250	4.24	0.17	0.18	0.17	1.28	0.99	0.85	5.58	18.77	10.91	0.000	0.647
Bhm3	250-262	4.20	0.39	1.29	1.22	1.28	0.98	2.14	6.60	23.47	13.64	0.055	1.137
Bhm4	262-360	6.60	0.94	1.88	1.04	2.56	0.03	4.23	0.82	13.36	7.77	0.015	0.411
Bh5m	360-460+	6.57	1.36	2.63	1.65	3.84	0.03	6.61	0.82	162.45	94.45	0.057	0.461
						P09							
A	0-20	4.38	0.15	2.63	1.00	0.38	0.46	0.46	3.10	45.13	26.24	0.017	0.075
AE	20-25	4.50	0.13	0.10	0.44	0.10	0.10	0.00	1.42	2.89	1.68	0.003	0.070
E	25-50	4.89	0.11	0.06	0.22	0.05	0.08	0.00	1.42	0.00	0.00	0.000	0.073
EB	50-55	4.69	0.14	0.11	0.48	0.20	0.25	0.00	2.52	12.27	7.14	0.001	0.086
Bh1	55-63	4.24	0.20	0.25	1.09	0.51	1.13	2.84	6.58	71.12	41.35	0.033	0.286
Bh2	63-80	4.15	0.12	0.10	0.39	0.13	1.34	0.00	5.68	23.10	13.43	0.002	0.592
Bh3	80-92	4.29	0.12	0.07	0.26	0.10	0.95	0.00	4.18	11.55	6.72	0.000	0.510
BC	92-150	4.55	0.10	0.06	0.26	0.10	0.40	0.00	2.56	5.05	2.94	0.000	0.280
C	150-165	4.85	0.11	0.08	0.26	0.10	0.30	0.26	1.70	1.81	1.05	0.000	0.206
2Bh	165+	4.70	0.17	0.22	2.65	0.28	0.53	10.38	3.30	9.03	5.25	0.000	0.387
						P10							
A	0-15	4.32	0.37	0.51	1.57	0.61	0.83	2.64	5.78	134.65	78.29	0.032	0.153
E	15-23	4.61	0.13	0.11	0.35	0.15	0.35	0.00	2.74	15.88	9.23	0.007	0.130
EB	23-35	4.31	0.16	0.11	0.26	0.13	0.41	0.00	2.22	9.39	5.46	0.018	0.200
Bh1	25-36	4.17	0.20	0.14	0.39	0.15	1.46	0.00	4.82	18.05	10.49	0.053	0.737
Bh2	36-43	4.28	0.13	0.11	0.57	0.23	1.81	0.00	7.28	25.63	14.90	0.029	1.291
Bh3	55-65	4.54	0.13	0.08	0.35	0.13	0.94	0.00	5.56	15.88	9.23	0.028	1.034
BC	45-63	4.62	0.13	0.07	0.17	0.33	0.55	0.00	2.98	5.05	2.94	0.028	0.605

Appendix A – General chemistry of all sample   (continuation)

Horizon	Depth	pH (H₂O)	Ca	Mg	Na	K	Al	P	H+Al	MO	Corgᵃ	Fe	Al
	cm		...........................cmol_c kg⁻¹...........................								................g kg⁻¹..............		
						P10							
BC (wood)	45-63	4.48	0.12	0.08	0.30	0.13	0.90	0.00	5.52	13.36	7.77	0.026	0.845
C	63-160	4.83	0.13	0.07	0.17	0.13	0.44	2.04	1.98	1.81	1.05	0.012	0.350
2Bhm	160+	5.13	0.29	0.33	0.57	0.13	0.89	4.23	3.96	20.58	11.96	0.025	1.343
						P11							
A	0-15	4.25	0.61	0.26	2.05	0.38	0.43	1.65	4.50	61.01	35.47	0.004	0.165
E	15-35	4.50	0.13	0.08	0.30	0.31	0.14	0.00	1.02	6.86	3.99	0.000	0.149
EB	35-45	4.05	0.14	0.09	0.35	0.15	0.41	0.00	2.18	9.75	5.67	0.007	0.294
Bh1	45-55	3.97	0.15	0.11	0.91	0.18	1.32	0.00	5.62	16.25	9.44	0.015	0.706
Bh2	55-90	4.09	0.12	0.07	0.35	0.13	1.25	0.00	4.76	16.25	9.44	0.000	0.871
Bh3	90-145	4.70	0.12	0.07	0.39	0.10	0.88	0.00	4.12	9.03	5.25	0.014	0.730
Bhm	145+												
						P30							
A	0-20	4.95	0.17	0.20	0.44	0.31	0.36	0.00	3.58	20.58	11.96	0.021	0.143
AE	20-34	5.05	0.13	0.10	0.17	0.13	0.13	0.00	1.52	3.61	2.10	0.016	0.126
E	34-58	5.29	0.14	0.08	0.17	0.08	0.06	0.00	0.96	0.72	0.42	0.010	0.135
EB	58-70	4.67	0.16	0.10	0.13	0.08	0.31	0.00	1.74	2.53	1.47	0.019	0.255
BE	70-92	4.55	0.12	0.10	0.35	0.10	0.80	0.00	3.68	10.11	5.88	0.041	0.642
Bh1	70-90	4.52	0.10	0.09	0.48	0.10	1.43	0.00	6.52	20.58	11.96	0.003	1.294
Bh2	90-135	4.40	0.15	0.11	0.52	0.13	1.22	0.00	5.68	16.25	9.44	0.012	1.047
C	135+	4.65	0.10	0.07	0.30	0.10	0.37	0.85	1.76	2.53	1.47	0.044	0.426
						P31							
A	0-22	4.16	0.15	0.30	0.44	0.33	0.61	1.75	3.21	56.32	32.74	0.007	0.155
AE	22-30	4.82	0.10	0.09	0.17	0.15	0.11	0.00	1.78	3.61	2.10	0.000	0.121
E	30-63	4.98	0.11	0.07	0.09	0.08	0.10	0.00	0.92	1.44	0.84	0.000	0.144
EB	63-100	4.48	0.13	0.09	0.26	0.10	0.22	0.00	2.05	1.08	0.63	0.021	0.258

Appendix A – General chemistry of all sample   (continuation)

Horizon	Depth	pH (H₂O)	Ca	Mg	Na	K	Al	P	H+Al	MO	Corg[a]	Fe	Al
	cm		.........................cmol$_c$ kg^{-1}.........................							.................g kg^{-1}..............			
							P31							
Bh2	100-125	4.51	0.10	0.08	0.35	0.13	0.89	0.00	5.68	8.66	5.04	0.007	0.652
C	125+	4.56	0.11	0.07	0.30	0.13	0.51	0.00	1.32	2.89	1.68	0.012	0.431
BE		4.32	0.11	0.08	0.13	0.08	0.57	0.00	2.54	5.42	3.15	0.025	0.426
Bh1		4.26	0.16	0.07	0.26	0.10	0.97	0.00	6.22	11.55	6.72	0.060	0.605
							P32							
A	0-20	4.56	0.13	0.19	0.96	0.23	0.30	0.00	3.68	18.77	10.91	0.017	0.208
AE	20-34	4.93	0.12	0.18	0.22	0.13	0.17	0.00	1.30	6.14	3.57	0.000	0.199
E	34-100	4.86	0.09	0.09	0.30	0.08	0.08	0.00	0.74	0.72	0.42	0.000	0.209
EB	60-85	4.65	0.10	0.07	0.13	0.10	0.29	0.00	0.92	1.08	0.63	0.042	0.337
BE	100-115	4.67	0.11	0.08	0.22	0.10	0.42	0.00	2.56	3.25	1.89	0.056	0.379
Bh1	110-140	4.55	0.08	0.08	0.26	0.13	0.73	0.06	5.42	8.66	5.04	0.027	0.564
Bh2	130-145	4.93	0.10	0.08	0.44	0.15	0.58	0.26	6.43	5.42	3.15	0.027	0.588
Bh1'	45-80	4.70	0.13	0.08	0.57	0.23	0.82	0.00	3.14	11.91	6.93	0.947	0.566
Bs	60-75	4.98	0.12	0.08	0.22	0.13	0.36	0.00	3.05	4.33	2.52	0.421	0.476
CE	80-140	5.17	0.11	0.07	0.13	0.10	0.19	0.00	1.98	0.00	0.00	0.054	0.278
Cg	120-150	5.14	0.10	0.07	0.22	0.13	0.24	0.00	1.16	0.36	0.21	0.482	0.499
C	160-210+	5.06	0.11	0.09	0.39	0.13	0.32	0.00	1.54	1.08	0.63	0.063	0.297
							P33							
A	0-20	4.78	0.17	0.21	0.30	0.20	0.29	0.00	3.62	14.44	8.40	0.050	0.144
E	20-44	4.66	0.12	0.11	0.17	0.36	0.16	0.00	0.78	2.53	1.47	0.053	0.175
Bh1'	40-62	4.66	0.11	0.12	0.30	0.33	0.99	0.00	3.56	14.08	8.19	1.400	0.532
Bs	62-75	5.14	0.07	0.07	0.26	0.15	0.46	0.00	3.18	5.42	3.15	0.944	0.509
C1	75-150	5.24	0.10	0.07	0.17	0.13	0.31	0.00	0.82	2.53	1.47	0.344	0.476
C2	150-210+	5.17	0.12	0.08	0.13	0.13	0.35	3.53	0.82	1.08	0.63	0.031	0.349

Appendix A – General chemistry of all sample   (continuation)

Horizon	Depth	pH (H$_2$O)	Ca	Mg	Na	K	Al	P	H+Al	MO	Corg[a]	Fe	Al
	cm		...........................cmol$_c$ kg^{-1}...........................							..................g kg^{-1}..............			
			P34											
A	0-20	4.73	0.15	0.14	0.52	0.20	0.26	0.00	3.10	8.66	5.04	0.036	0.209
AE	20-32	4.24	0.12	0.14	2.09	0.20	0.18	0.00	1.42	2.89	1.68	0.044	0.212
E	32-50	4.57	0.10	0.08	0.17	0.15	0.27	0.00	1.09	0.00	0.00	0.085	0.223
EB	50-65	4.58	0.13	0.09	0.35	0.13	0.33	0.00	2.52	1.81	1.05	0.087	0.217
BE	60-85	4.69	0.11	0.08	0.35	0.13	0.31	0.00	2.78	2.17	1.26	0.117	0.228
Bh1	65-75	4.37	0.16	0.08	0.35	0.15	0.51	0.00	5.68	2.89	1.68	0.101	0.209
Bh1'	75-95	4.67	0.10	0.10	0.35	0.18	0.87	0.00	4.18	8.30	4.83	0.393	0.446
C	95-155	4.82	0.16	0.08	0.39	0.13	0.20	0.00	1.65	0.00	0.00	0.170	0.203
Bh2	90-110	4.67	0.10	0.08	0.30	0.15	0.83	0.00	6.87	7.22	4.20	0.099	0.414
Bs		4.70	0.10	0.07	0.30	0.13	0.43	0.00	3.30	3.25	1.89	0.492	0.345
			P35											
A	0-25	4.90	0.14	0.16	0.35	0.20	0.17	0.00	3.78	10.83	6.30	0.038	0.078
E	20-50	4.81	0.11	0.07	0.17	0.10	0.11	0.00	0.74	4.33	2.52	0.033	0.095
EB	50-72	4.74	0.13	0.10	0.22	0.13	0.31	0.00	2.22	1.08	0.63	0.136	0.171
Bh1	50-60 e 70-85	4.40	0.11	0.09	0.52	0.18	0.61	0.00	4.82	6.86	3.99	1.020	0.265
Bh1'	60-82	4.71	0.12	0.07	0.26	0.10	0.59	0.00	7.28	6.86	3.99	0.610	0.498
Bs	70-80	4.79	0.11	0.07	0.26	0.08	0.39	0.00	3.05	3.97	2.31	1.274	0.469
Bh2	85-110	4.99	0.13	0.09	0.17	0.10	0.46	0.00	5.52	4.33	2.52	0.147	0.273
C	85-150+	5.11	0.12	0.09	0.26	0.10	0.28	0.00	1.67	0.00	0.00	0.385	0.165
			P37											
A	0-20	4.33	0.91	0.31	0.74	0.26	0.41	0.00	4.50	42.96	24.98	0.035	0.123
AE	20-32	4.39	0.21	0.09	0.17	0.08	0.10	0.00	3.96	11.19	6.51	0.011	0.093
E	32-50	4.90	0.17	0.07	0.09	0.08	0.03	0.00	1.02	0.00	0.00	0.014	0.090
Bh1	50-65	4.24	0.16	0.08	0.13	0.10	1.49	0.00	6.87	15.16	8.82	0.042	0.687
Bh2	65-90	4.47	0.14	0.07	0.13	0.10	0.88	0.00	5.32	9.03	5.25	0.028	0.589

Appendix A – General chemistry of all sample   (continuation)

Horizon	Depth	pH (H₂O)	Ca	Mg	Na	K	Al	P	H+Al	MO	Corg[a]	Fe	Al
	cm		..........................cmol$_c$ kg^{-1}..........................							...................g kg^{-1}...............			
			P37										
C	90-130+	4.54	0.13	0.06	0.13	0.08	0.51	2.64	2.01	3.25	1.89	0.034	0.369
			P38										
A	0-20	4.01	0.17	0.24	1.22	0.36	0.68	1.25	4.76	79.78	46.38	0.034	0.145
AE	20-26	4.44	0.16	0.09	0.17	0.08	0.20	0.00	2.12	6.86	3.99	0.017	0.080
E	26-40	4.74	0.11	0.08	0.09	0.05	0.06	0.00	0.96	1.08	0.63	0.015	0.101
EB	40-57	4.44	0.14	0.07	0.13	0.05	0.16	0.00	1.52	1.08	0.63	0.028	0.124
BE	57-75	4.32	0.14	0.09	0.13	0.08	0.38	0.00	1.74	3.25	1.89	0.045	0.235
Bh1	75-100	4.09	0.15	0.09	0.22	0.08	1.15	0.00	6.52	9.39	5.46	0.064	0.335
Bh2	100-135	4.10	0.16	0.08	0.17	0.08	1.32	0.00	3.68	13.00	7.56	0.029	0.450
C	135-145+	4.23	0.16	0.07	0.26	0.10	0.66	1.05	1.23	5.78	3.36	0.021	0.285
			P39										
A	0-25	5.29	0.30	0.27	0.26	0.33	0.11	0.26	2.12	2.89	1.68	0.124	0.098
C1	25-75	5.68	0.63	0.36	0.48	0.36	0.08	0.95	0.87	0.00	0.00	0.047	0.069
2C2	75-86	5.48	0.26	0.60	1.09	0.56	0.13	1.75	0.20	0.00	0.00	0.131	0.128
C2	86-110	5.54	0.24	0.51	1.87	0.59	0.06	3.43	0.92	0.00	0.00	0.041	0.116
C3	110-170+	5.42	0.29	0.90	0.22	1.28	0.05	3.73	0.86	0.00	0.00	0.025	0.076
			P40										
A	0-15	5.20	0.14	0.15	0.30	0.26	0.23	0.00	2.64	12.27	7.14	0.030	0.093
AE	15-32	5.14	0.13	0.08	0.09	0.10	0.07	0.00	2.00	1.08	0.63	0.009	0.056
E	32-65	5.42	0.09	0.07	0.09	0.05	0.05	0.00	0.92	0.00	0.00	0.004	0.018
EB	65-76	4.87	0.10	0.07	0.09	0.08	0.19	0.00	1.98	1.44	0.84	0.013	0.050
BE	76-80	4.85	0.09	0.06	0.26	0.10	0.54	1.75	3.68	7.94	4.62	0.023	0.114
Bh1	80-97	4.46	0.11	0.06	0.17	0.08	0.87	1.94	6.23	10.83	6.30	0.010	0.242
Bh2	97-110	4.56	0.10	0.06	0.09	0.08	1.10	0.00	5.30	16.25	9.44	0.000	0.513
Bh3	110-155+	4.90	0.55	0.07	0.09	0.08	0.61	0.00	3.20	10.11	5.88	0.008	0.345

Appendix A – General chemistry of all sample   (conclusion)

Horizon	Depth	pH (H$_2$O)	Ca	Mg	Na	K	Al	P	H+Al	MO	Corg[a]	Fe	Al
	cm		...........................cmol$_c$ kg^{-1}...........................								..................g kg^{-1}..............		
						P41								
A	0-30	4.65	0.14	0.14	0.17	0.18	0.33	0.00	2.74	10.47	6.09	0.006	0.000
E1	30-80	5.25	0.12	0.07	0.09	0.05	0.02	0.00	0.20	0.00	0.00	0.004	0.000
E2	80-125	5.31	0.11	0.07	0.09	0.05	0.03	0.00	0.30	0.00	0.00	0.004	0.000
Bh1	125-135	4.14	0.15	0.14	0.17	0.05	0.03	8.10	3.48	11.55	6.72	0.029	0.000
Bh2	135-1558	4.01	0.12	0.14	0.22	0.05	0.69	0.00	3.14	12.27	7.14	0.020	0.000
2C1	155-165	4.14	0.11	0.09	0.13	0.08	0.37	0.00	0.70	2.53	1.47	0.082	0.015
2C2	165-180	4.44	0.10	0.08	0.17	0.10	0.24	0.00	0.98	1.08	0.63	0.056	0.043
2C3	180-190	4.61	0.12	0.07	0.09	0.08	0.06	0.00	1.16	0.00	0.00	0.010	0.037
2C4	190-220	4.88	0.15	0.07	0.17	0.13	0.07	0.00	1.54	0.00	0.00	0.004	0.016
3EB	220-223	4.48	0.14	0.08	0.26	0.08	0.72	0.00	1.52	8.30	4.83	0.000	0.204
3Bh1	223+	4.20	0.19	0.41	1.13	0.26	0.60	0.00	3.61	9.03	5.25	0.003	0.209

[a] – organic carbon

Appendix B - Identified pyrolysis products grouped according to origin and there after retention time

(continues)

Code	Name	m/z^a	M^{+b}	RT^c
7-34	C_7-C_{34} n-alkanes	57+71	-	0.47–4.62
10:1-34:1	C_7-C_{34} alkenes	55+69	-	1.00–4.62
Al	Branched unsaturated C_{19} alkene	109	264	2.57
Ar1	Benzene	77+78	78	0.44
Ar2	Toluene	91+92	92	0.56
Ar3	Ethylbenzene	91+106	106	0.73
Ar4	Dimethylbenzene	91+106	106	0.74
Ar5	Styrene	78+104	104	0.79
Ar6	Dimethylbenzene	91+106	106	0.79
Ar7	Unsaturated C_3 benzene	117+118	118	0.91
Ar8	Propylbenzene	91+120	120	0.92
Ar9	C_3 benzene	105+120	120	0.95
Ar10	C_3 benzene	105+120	120	0.98
Ar11	Ethylmethyl-benzene	105+120	120	1.02
Ar12	Ethylmethyl-benzene	105+120	120	1.09
Ar13	Unsaturated C_3 benzene	117+118	118	1.09
Ar14	Unsaturated C_3 benzene	117+118	118	1.12
Ar15	Benzoic acid	77+105	120	1.19
Ar16	C_4 benzene	119+134	134	1.31
Ar17	Unsaturated C_4 benzene compound	115+130	130	1.39
Ar18	Branched C_7 benzene	118+174	174	1.80
B4-B12	C_4-C_{12} alkylbenzenes	91+92	134-246	1.16 - 2.75
Bf1	C_1 benzofuran	131+132	132	1.28
Bf2	C_1 benzofuran	131+132	132	1.29
Bf3	Dimethylbenzofuran	145+146	146	1.53
Bf4	Dibenzofuran	139+168	168	2.15
F7-F16	C_7-C_{16} fatty acids	60+73	-	1.23 - 2.87
K17-K31	C_{17}-C_{31} methyl ketones	58+59	-	2.77 - 4.51
Lg1	Guaiacol	109+124	124	1.24
Lg2	4-methylguaiacol	123+138	138	1.47
Lg3	4-vinylphenol	91+120	120	1.55
Lg4	4-ethylguaiacol	137+152	152	1.66
Lg5	4-vinylguaiacol	135+150	150	1.74
Lg6	Syringol	139+154	154	1.81
Lg7	4-formylguaiacol	151+152	152	1.93
Lg8	4-methylsyringol	153+168	168	2.00
Lg9	4-(prop-1-enyl)guaiacol, *trans*	164	164	2.01
Lg10	4-acetylguaiacol	151+166	166	2.10
Lg11	4-ethylsyringol	167+182	182	2.15

Appendix B - Identified pyrolysis products grouped according to origin and there after retention time

(continuation)

Code	Name	m/z^a	M^{+b}	RT^c
Lg12	4-(propan-2-one)guaiacol	137+180	180	2.21
Lg13	Vanillic acid	153+168	168	2.28
Lg14	4-(prop-1-enyl)syringol, *trans*	194	194	2.47
Lg15	4-acetylsyringol	181+196	196	2.53
Lg16	4-(propan-2-one)syringol	167+210	210	2.59
Lg17	4-(propan-3-one)syringol	181+210	210	2.67
Me	Methyl ester	74+87	-	1.91
N1	1H-imidazole, 2,4-dimethyl	95+96	96	0.48
N2	C_1-cyclohexene-1-acetronitrile	80+81	81	0.52
N3	Pyridine	52+79	79	0.53
N4	Pyrrole	67	67	0.54
N5	C_1 pyridine	66+93	93	0.65
N6	C_1 pyrrole	80+81	81	0.68
N7	C_1 pyrrole	80+81	81	0.70
N8	C_2 pyridine	106+107	107	0.88
N9	pyrrole, 4-ethyl-2-methyl	109	109	1.00
N10	Acetoxypyridine	95	137	1.30
N11	Benzeneacetonitrile	90+117	117	1.35
N12	1H-imidazole compound	121+136	136	1.41
N13	1H-indole-3-ethanamine	130+131	131	1.90
N14	C_2 quinoline	157	157	2.02
N15	Diketodipyrrole	93+186	186	2.50
N16	Diketopiperazine derivative	70+154	194	2.69
N17	Diketopiperazine derivative	70+194	194	2.72
Pa1	Indene	115+116	116	1.14
Pa2	Naphthalene	128	128	1.47
Pa3	1H-indene, 1,1-dimethyl	129+144	144	1.62
Pa4	1H-indene, 1,1-dimethyl	129+144	144	1.64
Pa5	1H-indene, 1,1-dimethyl	129+144	144	1.65
Pa6	1H-inden-1-one, 2,3-dihydro	104+132	132	1.68
Pa7	C_1 naphthalene	141+142	142	1.71
Pa8	C_1 naphthalene	141+142	142	1.75
Pa9	Biphenyl	153+154	154	1.88
Pa10	C_2-naphthalene	141+156	156	1.94
Pa11	C_2-naphthalene	141+156	156	1.98
Pa12	2-naphthalenol	115+144	144	2.16
Pa13	C_3-naphthalene	155+170	170	2.24
Pa14	Fluorene	165+166	166	2.28
Pa15	C_3-naphthalene	155+170	170	2.29

Appendix B - Identified pyrolysis products grouped according to origin and there after retention time

(conclusion)

Code	Name	m/z[a]	M[+b]	RT[c]
Pa16	2-methyl-1-naphthalenol	129+158	158	2.34
Pa17	C_4-naphthalene	169+184	184	2.54
Pa18	Anthracene / phenantrene	178	178	2.63
Ph1	Phenol	66+94	94	1.00
Ph2	C_1 phenol	107+108	108	1.17
Ph3	C_1 phenol	107+108	108	1.22
Ph4	C_2 phenol	107+122	122	1.38
Ph5	C_2 phenol	107+122	122	1.43
Ph6	C_2 phenol	107+122	122	1.49
Ph7	catechol	64+110	110	1.58
Ph8	Ethylmethylphenol	121+136	136	1.58
Ph9	Methoxycatecol	97+140	140	1.65
Ph10	3-methoxy-5-methylphenol	109+138	138	1.76
Al	Pristene	55+56	-	2.49
Ps1	Acetic acid	60	60	0.41
Ps2	(2H)-furan-3-one	55+84	84	0.61
Ps3	3-furaldehyde	95+96	96	0.67
Ps4	2-cyclopenten-1-one, 2-methyl	53+67	96	0.82
Ps5	2,5-furandione, 3-methyl	68+98	110	0.86
Ps6	2,3-dihydro-5-methylfuran-2-one	55+98	98	0.87
Ps7	5-methyl-2-furaldehyde	109+110	110	0.94
Ps8	4-hydroxy-5,6-dihydro-(2H)-pyran-2-one	58+114	114	1.03
Ps9	3-hydroxy-2-methyl-2-cyclopenten-1-one	55+112	112	1.10
Ps10	Dianhydrorhamnose	113+128	128	1.13
Ps11	2.3-dimethylcyclopent-2-en-1-one	67+110	110	1.13
Ps12	Levogalactosan	60+73	-	2.15
Ps13	Levomannosan	60+73	-	2.17
Ps14	Levoglucosan	60+73	-	2.21
St1	?	163+190	-	4.09
St2	Gamma tocopherol	151+416	-	4.21
St3	?	163+190	-	4.26
St4	?	165+430	-	4.31
St5	?	163+190	-	4.34

[a] fragment ions used for quantification
[b] molecular weight
[c] retention time relative to phenol

Appendix C - The explained variance for all factors for each pyrolysis product separately (Horizons pyrolysis) (continues)

Compound	Factor 1	Factor 2	Factor 3	Factor 4
7	-0.19922	0.79688	0.16266	-0.08089
8	-0.49429	0.76328	0.04445	-0.15462
9	-0.55693	0.71085	-0.04042	-0.04181
10	-0.65112	0.65219	-0.09591	0.01421
11	-0.66217	0.65484	-0.14102	-0.01026
12	-0.75350	0.48233	-0.15836	0.03564
13	-0.72842	0.59886	-0.19206	0.01818
14	-0.65745	0.48504	-0.16790	-0.00159
15	-0.77611	0.48849	-0.20616	0.05078
16	-0.82918	-0.26409	-0.02544	-0.12608
17	-0.77374	0.56775	-0.14073	0.00926
18	-0.84742	0.43736	-0.08812	0.13266
19	-0.83566	0.45116	-0.11006	0.12906
20	-0.82092	0.10659	0.07032	0.15173
21	-0.87862	0.38665	-0.07297	0.12384
22	-0.71201	-0.27846	0.16131	0.22138
23	-0.80560	0.09969	0.12310	0.26131
24	-0.76093	-0.36883	0.19362	0.13568
25	-0.88632	-0.10056	0.14848	0.26961
26	-0.69252	-0.49896	0.16471	0.01576
27	-0.77979	-0.25157	0.34693	0.17912
28	-0.50383	-0.56415	0.32031	0.06046
29	-0.35012	-0.27027	0.44239	0.10626
30	-0.32823	-0.25788	0.46268	0.16462
31	-0.39890	-0.32937	0.41552	0.08530
32	-0.37901	-0.17869	0.47647	0.20591
33	-0.43421	-0.24712	0.43798	0.13044
34	-0.39972	-0.08927	0.47045	0.29394
´10:1	0.27917	0.21743	-0.43255	0.51191
´11:1	-0.94599	0.04979	0.08657	0.07872
´12:1	-0.64360	0.36854	0.32521	-0.09553
´13:1	-0.94491	0.23378	0.01947	0.08613
´14:1	-0.88359	0.29636	0.06963	0.17395
´15:1	-0.84567	0.12025	0.09174	0.23238
´16:1	-0.80827	-0.33516	0.15941	0.00815
´17:1	-0.92093	0.26398	0.04252	0.16677
´18:1	-0.78565	0.06262	0.16411	0.31532
´19:1	-0.94018	0.10815	0.07985	0.21618
´20:1	-0.75970	-0.22674	0.17168	0.19753

Appendix C - The explained variance for all factors for each pyrolysis product separately (Horizons pyrolysis) (continuation)

Compound	Factor 1	Factor 2	Factor 3	Factor 4
´21:1	-0.69607	-0.04470	0.20538	0.36503
´22:1	-0.73356	-0.33177	0.19238	0.26593
´23:1	-0.82998	-0.14280	0.14142	0.23712
´24:1	-0.84099	-0.36615	0.12967	0.10308
´25:1	-0.83131	-0.19756	0.15054	0.27188
´26:1	-0.67542	-0.52730	0.11894	0.01275
´27:1	-0.89547	-0.14165	0.17695	0.21325
´28:1	-0.59483	-0.55797	0.19588	0.05927
´29:1	-0.63615	-0.25797	0.42226	0.19254
´30:1	-0.65562	-0.35035	0.37692	0.24625
´31:1	-0.62001	-0.31073	0.37744	0.15703
´32:1	-0.77010	-0.19963	0.35671	0.27974
´33:1	-0.66679	-0.26515	0.37848	0.27690
´34:1	-0.73452	-0.26412	0.30643	0.34594
´7:1	-0.74438	0.23208	0.25584	0.19442
´8:1	-0.31152	0.36941	0.24553	0.09705
´9:1	-0.40123	0.27583	0.16457	-0.06405
Al	-0.73271	0.24188	0.04564	0.37595
Ar1	0.72256	0.17633	0.42016	0.01164
Ar2	0.44015	0.63686	0.36290	-0.29307
Ar3	0.00238	0.76678	0.30863	-0.43852
Ar4	0.39826	0.69749	0.21002	0.22988
Ar5	0.08152	0.23453	0.22741	-0.17184
Ar6	0.02806	0.85569	0.31465	-0.13115
Ar7	-0.34705	0.70164	0.34063	-0.21974
Ar8	-0.04391	0.81319	0.37140	-0.34467
Ar9	-0.29500	0.67552	-0.11491	-0.02352
Ar10	-0.38110	0.86388	0.09887	-0.16430
Ar11	-0.23233	0.76152	-0.06155	0.17008
Ar12	0.11234	0.88947	0.09451	-0.01519
Ar13	0.15771	0.78558	0.41369	-0.35944
Ar14	-0.57074	0.79601	-0.02688	-0.05527
Ar15	-0.11943	0.72517	-0.06639	0.32048
Ar16	-0.24844	0.86092	-0.01645	0.11328
Ar17	-0.25296	0.87388	-0.05645	0.18731
Ar18	-0.57828	-0.46547	-0.53834	-0.08068
Ar19	-0.58089	0.30908	-0.38339	-0.18644
B10	-0.51284	0.78336	0.00361	-0.05877
B11	-0.62990	0.70881	-0.08740	-0.12055

Appendix C - The explained variance for all factors for each pyrolysis product separately (Horizons pyrolysis) (continuation)

Compound	Factor 1	Factor 2	Factor 3	Factor 4
B12	-0.57996	0.75305	-0.04043	-0.14339
B4	-0.12677	0.88489	0.19496	-0.27552
B5	-0.25691	0.82857	0.10921	-0.12747
B6	-0.27920	0.81612	0.23755	-0.27075
B7	-0.40660	0.73745	-0.14377	-0.11431
B8	-0.36370	0.83317	0.00327	-0.17621
B9	-0.65220	-0.07971	-0.02369	-0.25849
Bf1	0.76279	0.11756	-0.25477	0.46307
Bf2	0.81782	0.11285	-0.12522	0.44625
Bf3	0.49949	0.26007	-0.52716	0.48927
Bf4	0.80797	0.13639	-0.11435	0.38938
F7	-0.42860	0.04702	-0.15666	0.03007
F8	-0.46021	0.01483	-0.13301	0.05088
F9	-0.42360	0.21408	-0.09926	0.17423
F10	-0.24497	0.16873	-0.08398	-0.06550
F11	-0.00641	0.03656	-0.14028	-0.26757
F12	-0.13672	0.16182	0.00752	-0.03168
F13	-0.24986	0.02465	-0.14077	-0.02585
F14	-0.29456	0.06317	-0.11050	-0.04274
F15	-0.32256	-0.04266	-0.04404	0.00051
F16	-0.63627	-0.34950	0.06071	0.01583
K17	-0.65147	0.46653	0.02422	0.00896
K18	-0.81417	0.29133	0.02924	0.16322
K19	-0.73946	0.26710	0.05129	0.02534
K20	-0.57890	0.50451	-0.01611	-0.12234
K21	-0.79776	0.41359	-0.11299	0.06233
K22	-0.61173	0.49369	-0.05640	-0.04766
K23	-0.80566	0.29301	0.18948	0.17746
K24	-0.80645	0.31117	0.15966	0.18327
K25	-0.77564	0.40967	0.10484	0.11789
K26	-0.77962	0.27811	0.02392	0.14181
K27	-0.80518	0.34520	0.07076	0.16781
K28	-0.86401	0.26275	-0.01178	0.17704
K29	-0.87811	0.12018	0.11784	0.25426
K30	-0.76772	0.36039	0.00401	0.21613
K31	-0.87366	-0.09550	0.13291	0.21654
Lg1	-0.31808	-0.40254	-0.68708	0.01122
Lg2	-0.61643	-0.63566	-0.20757	-0.06411
Lg3	-0.11448	-0.43252	-0.06649	-0.20144

Appendix C - The explained variance for all factors for each pyrolysis product separately (Horizons pyrolysis) (continuation)

Compound	Factor 1	Factor 2	Factor 3	Factor 4
Lg4	-0.71365	-0.45327	-0.39818	-0.17589
Lg5	-0.50145	-0.71383	-0.03732	-0.15177
Lg6	-0.29903	-0.59505	-0.41562	-0.23085
Lg7	-0.29444	-0.60994	-0.03912	-0.08128
Lg8	-0.42855	-0.72700	-0.10641	-0.20319
Lg9	-0.49195	-0.66560	0.02812	-0.08387
Lg10	-0.62405	-0.23053	-0.54338	-0.08987
Lg11	-0.56566	-0.62786	-0.27969	-0.25076
Lg12	-0.34639	-0.67271	-0.04999	-0.20550
Lg13	-0.41738	-0.10154	-0.39622	-0.06266
Lg14	-0.36296	-0.69384	0.01305	-0.20279
Lg15	-0.59832	-0.52982	-0.40333	-0.19779
Lg16	-0.55267	-0.53325	-0.30441	-0.22364
Lg17	-0.64646	-0.53716	-0.33556	-0.18603
Me	-0.57197	0.10183	-0.47912	-0.33581
N1	0.19249	0.23229	-0.45162	-0.40951
N2	-0.00699	0.30528	0.17721	-0.59577
N3	0.61989	0.25873	0.44734	-0.29377
N4	0.14135	0.46551	-0.01947	-0.51766
N5	0.35164	0.36427	-0.14229	-0.35272
N6	-0.11325	0.51094	-0.32776	-0.40337
N7	0.18141	0.54502	0.02861	-0.38896
N8	-0.13185	0.56395	-0.21877	-0.39983
N9	0.75842	-0.02914	-0.27555	0.47806
N10	0.09051	0.44168	-0.20554	-0.04857
N11	-0.10689	0.53682	-0.04099	-0.42444
N12	0.65559	0.35066	-0.27499	0.37119
N13	-0.28404	0.25266	-0.24660	-0.05131
N14	0.65810	0.11443	0.14669	0.23987
N15	-0.29544	0.01291	-0.55283	-0.51426
N16	-0.76445	0.07945	-0.34931	-0.22055
N17	-0.60069	0.01807	-0.22853	-0.20772
Pa1	0.06114	0.84246	0.12048	0.14376
Pa2	0.68772	0.51679	0.33839	0.02234
Pa3	-0.53749	0.73743	-0.10086	0.17583
Pa4	-0.31265	0.86276	-0.15954	0.10655
Pa5	-0.36773	0.63738	-0.14692	0.12723
Pa6	0.22974	0.48823	-0.47732	0.50045
Pa7	0.32921	0.84270	-0.02104	0.16208

Appendix C - The explained variance for all factors for each pyrolysis product separately (Horizons pyrolysis) (continuation)
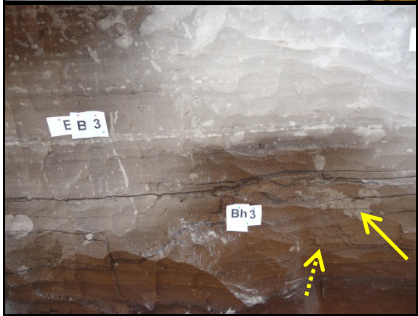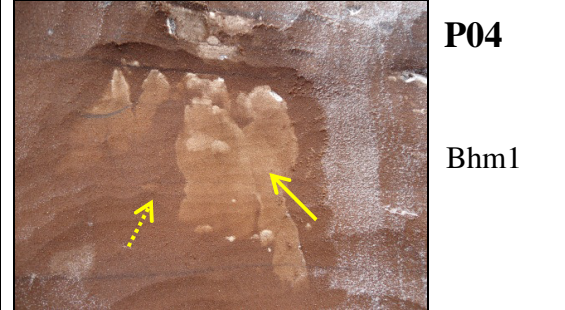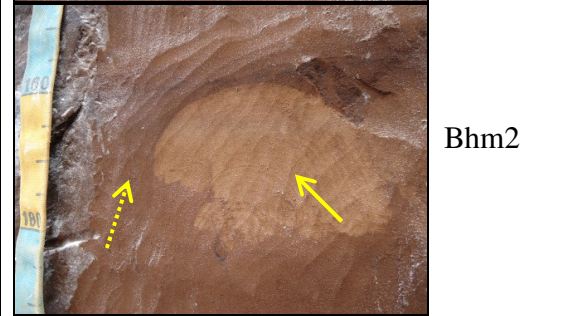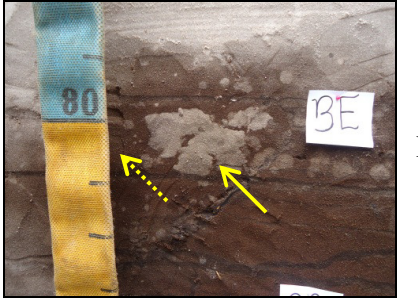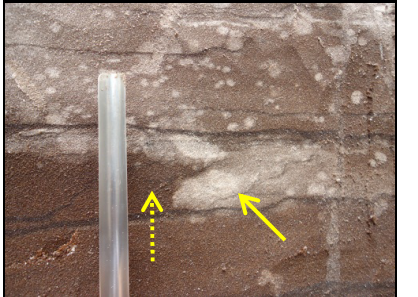
Compound	Factor 1	Factor 2	Factor 3	Factor 4
Pa8	0.05754	0.89462	0.08962	-0.13955
Pa9	0.48308	0.45227	0.54434	-0.29845
Pa10	-0.15438	0.63824	-0.59250	0.10401
Pa11	-0.18265	0.56868	-0.37367	-0.24155
Pa12	0.03040	0.10126	-0.52012	0.58366
Pa13	-0.41678	0.28401	-0.56923	-0.36171
Pa14	0.14716	0.81830	0.18395	-0.14339
Pa15	-0.21419	0.81078	-0.19845	-0.21250
Pa16	-0.28795	0.31897	-0.60327	0.53937
Pa17	-0.18845	0.78770	-0.07783	-0.13012
Pa18	0.38321	0.76490	0.16733	-0.02210
Ph1	0.76427	-0.02445	-0.28364	0.46922
Ph2	0.41927	0.14639	-0.63703	0.56244
Ph3	-0.03118	-0.07594	-0.85675	0.22076
Ph4	-0.33731	0.05858	-0.81102	0.34109
Ph5	-0.47181	-0.18361	-0.72098	-0.18373
Ph6	0.45429	0.06564	-0.48200	0.47486
Ph7	-0.02050	-0.30375	-0.35611	0.28570
Ph8	-0.71155	-0.10298	-0.57333	-0.16289
Ph9	-0.39400	-0.55583	-0.44927	-0.19578
Pr	-0.61065	-0.10211	0.18870	0.41718
Ps1	0.75347	0.01224	-0.04636	0.24191
Ps2	-0.61592	0.17565	-0.07023	-0.45605
Ps3	-0.63058	-0.31974	-0.29667	-0.52839
Ps4	0.42095	0.25300	-0.41404	0.46187
Ps5	-0.42688	-0.43546	-0.00413	-0.43726
Ps6	-0.13610	-0.58335	0.18493	-0.33609
Ps7	-0.56094	0.10630	-0.40921	-0.50888
Ps8	-0.42187	-0.70458	0.06858	-0.28869
Ps9	-0.50228	-0.29474	-0.18350	-0.42511
Ps10	-0.66309	-0.45019	-0.16932	-0.25089
Ps11	-0.02481	0.39581	-0.62629	0.44567
Ps12	-0.59423	-0.49618	-0.28660	-0.30529
Ps13	-0.58298	-0.54358	-0.21224	-0.27171
Ps14	-0.11950	-0.46037	0.36680	-0.36364
St1	-0.70246	-0.03924	-0.03246	0.08597
St2	-0.70776	-0.15065	0.18513	0.38771
St3	-0.52364	-0.50218	0.09049	-0.05908
St4	-0.69863	-0.37521	0.19754	0.27571

Appendix C - The explained variance for all factors for each pyrolysis product separately (Horizons pyrolysis) (conclusion)

Compound	Factor 1	Factor 2	Factor 3	Factor 4
St5	-0.54668	-0.45934	0.10316	-0.16692
Expl.Var	63.09042	44.12797	15.93112	12.76620

Appendix D – Pictures of sampled mottles (arrow) and adjacent soil (dashed arrow)
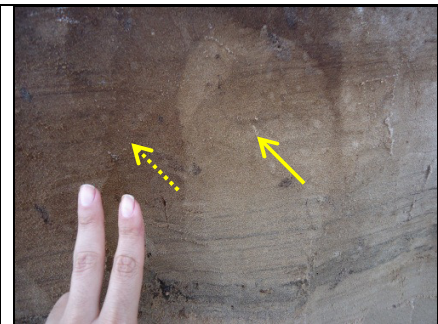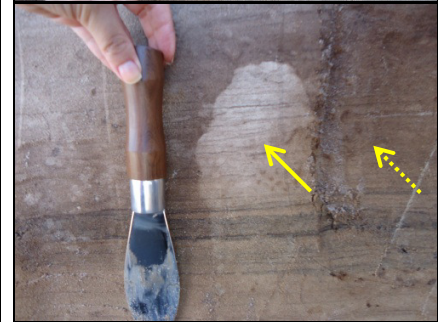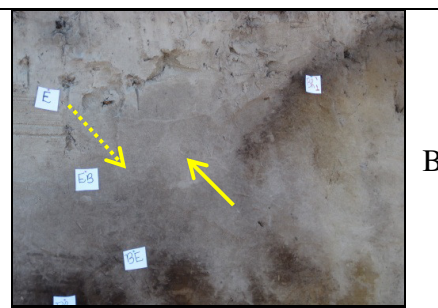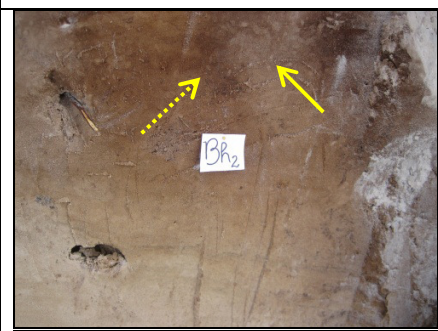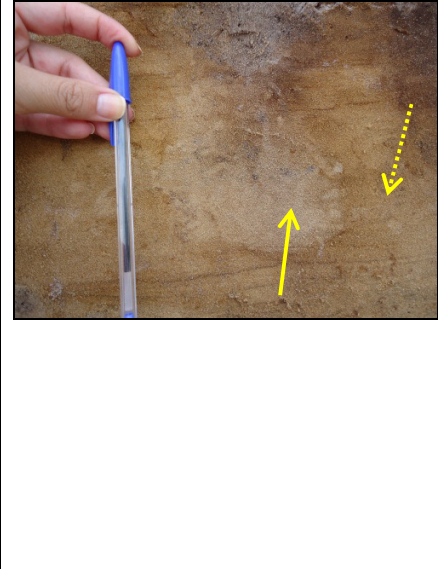
Profiles with poorly drainage

P02 EB1 Bh3	**P04** Bhm1 Bhm2
P40 BE/Bh1 Bh1 Bh2	

Strongly rooted profiles

Profiles with well-drained B horizons

	P30
	EB
	Bh2

	P31
	Bh1/Bh2
	Bh2

	P32
	BE
	Bh1
	CE
	80 – 140 cm

	P34
	Bh2
	Bs

Well-drained B podzol horizons

	P35 Bh1	
	Bh2	

Appendix E – List of pyrolysis products with *m/z* values used for quantification. molecular weight (M$^+$) and relative retention time to phenol (RT) (continues)

Code	Name	*m/z*[a]	M^{+}[b]	Relative RT[c]
13-31	C$_{13}$-C$_{31}$ *n*-alkanes	57+71	-	1.67 - 4.22
13:1 - 31:1	C$_{13}$-C$_{31}$ *n*-alkenes	57+71	-	1.66 - 4.22
Ar1	Benzene	77+78	78	0.42
Ar2	Toluene	91+92	92	0.54
Ar3	Dimethylbenzene	91+106	106	0.72
Ar4	Ethylmethylbenzene	105+120	-	0.92
Ar5	Ethylmethylbenzene	105+120	120	1.00
Ar6	Unsaturated C$_3$ benzene	117+118	118	1.08
Ar7	Unsaturated C$_3$ benzene	117+118	118	1.10
Ar8	Benzoic acid	77+105	120	1.17
Ar9	1-methylepthylbenzoate	70+105	-	2.48
Ar10	Fluoranthene	202	-	3.12
Ar11	Pyrene	202	-	3.20
Bf1	2/7-methylbenzofuran	131+132	-	1.27
Bf2	Dimethylbenzofuran	145+146	-	1.52
Bf3	Dibenzofuran	139+168	-	2.16
F14	*n*-Fatty acid, C$_{14}$	129	-	2.56
F16	*n*-Fatty acid, C$_{16}$	60+73	-	2.88
K17 - K27	C$_{17}$-C$_{27}$ *n*-methyl ketones	58+59	-	2.79 - 4.02
Lg1	Guaiacol	109+124	124	1.24
Lg2	4-Vinylphenol	91+120	-	1.55
Lg3	Catechol	110	-	1.58
Lg4	4-Vinylguaiacol	135+ 150	-	1.74
Lg5	Syringol	139+ 154	-	1.81
Lg6	4-Acetylguaiacol	151+ 166	-	2.10
Lg7	4-Vinylsyringol	151	-	2.23
Lg8	4-Acetylsyringol	181+196	-	2.55
Me	Methylester	74+ 87	-	1.89
N1	Pyridine	52+79	79	0.52
N2	Pyrrole	67	67	0.53
N3	Acetamide	59	-	0.66
N4	C$_1$-pyrrole	80+81	81	0.68
N5	C$_1$-pyrrole	80+81	81	0.69
N6	Benzeneacetonitrile	90+117	-	1.34
N7	Indole	90+117	-	1.73
N8	1*H*-indole-3-ethanamine	130+131	-	1.90
N9	C$_2$-quinoline	157	157	2.01
N10	C$_{14}$ alkylamine	58	-	2.12
N11	3-methyl-N, N-diethylbenzamide	119+190+91	-	2.26

Appendix E – List of pyrolysis products with m/z values used for quantification. molecular weight (M^+) and relative retention time to phenol (RT)   (conclusion)

Code	Name	m/z^a	M^{+b}	Relative RT^c
N12	Pyrimidine, 5-hidroxy-4-phenyl-	170+171	-	2.36
N13	C_{14} alkylamine	58	-	2.47
N14	Diketodipyrrole	93+186	-	2.53
N15	Diketopiperazine	70+154	-	2.68
N16	Diketopiperazine	70+194	-	2.89
N17	1-benzylpiperazine	91+134	160	3.12
N18	?	86+114	-	3.29
N19	1-benzylpiperazine	91+134	178	3.41
Pa1	Indene	115+116	116	1.12
Pa2	Naphthalene	128	-	1.45
Pa3	C_1 - naphthalene	141+142	142	1.70
Pa4	C_1 - naphthalene	141+142	142	1.73
Pa5	Biphenyl	153+154	154	1.87
Pa6	C_2 - naphthalene	141+156	-	1.95
Pa7	C_2 - naphthalene	141+156	-	1.97
Pa8	Indene	173	188	2.15
Pa9	C_3 - naphthalene	155+170	-	2.24
Pa10	Fluorene	165+166	-	2.28
Pa11	C_3-naphthalene	155+170	-	2.29
Pa12	C_4-naphthalene	169+184	184	2.55
Pa13	1H-Indole, 2-(1,1-dimethylethyl)	158+174	174	2.57
Pa14	Phenanthrene	178	-	2.65
Ph1	Phenol	66+94	94	1.00
Ph2	3/4-methyl-phenol	107+108	108	1.23
Ph3	Phenol, 2,4-Bis (1,1-dimethylethyl)	191	206	2.11
Ps1	2-methylfuran	53+82	-	0.38
Ps2	Acetic acid	45+60	60	0.38
Ps3	2-butenoic acid	68+86	-	0.65
Ps4	2-furaldehyde	95+96	-	0.68
Ps5	2-butenoic acid	68+86	-	0.73
Ps6	2-furaldehyde	109+ 110	-	0.94
Ps7	Levoglucosan	60+73	-	2.11

[a] fragment ions used for quantification
[b] molecular weight
[c] retention time relative to phenol